Numerical study of a family of dissipative KdV equations

Jean-Paul Chehab, Georges Sadaka

Numerical study of a family of dissipative KdV equations

J-P. Chehab*& G. Sadaka†

February 21, 2011

Abstract

The weak damped and forced KdV equation on the 1d Torus on $[0, L]$ have been analyzed by Ghidaglia[12, 13] Goubet[14, 15], Rosa and Cabral [4] and asymptotic regularization effects have been proven and observed numerically. In this work, we consider a family of dampings that can be even weaker, particularly it can dissipate very few the high frequencies. We give here numerical evidences that point out dissipation of energy, regularization effect, and presence of special solutions that characterize a non trivial dynamics.

1 Introduction

The modeling of the damping of asymptotic models for water wave is a very important challenge. In [23], Ott and Sudan have proposed a damped KdV equation as a model of Landau damping for ion acoustic wave, the (linear) damping being nonlocal, and in [24] they have presented different models of damping with the operator L as

$$u_t + \alpha_1 u_x + \alpha_2 u_{xxx} + \alpha_3 L[u] = 0, x \in \Omega, t > 0,$$

where $\Omega \subset \mathbb{R}$ and where L is the linear damping operator which satisfies

$$\int_\Omega uL[u]dx \geq 0,$$

and the L^2 norm of the solution is damped as

$$\frac{1}{2}\frac{d}{dt}\int_\Omega u^2 dx + \alpha_3 \int_\Omega uL[u]dx = 0.$$

Several authors have studied damped KdV equation, but anyway the literature is not so extensive and particularly relatively very few works have been done on the numerical simulation of these models.

The damping model that have been considered are mainly of the form

$$L[u] = |D|^\alpha u,$$

where $|D| = \sqrt{-\Delta}$, leading to the dissipative KdV equation

$$u_t + u_{xxx} + |D|^\alpha u + uu_x = 0; x \in \Omega, t > 0, \tag{1}$$

$$u(x, 0) = u_0(x), \tag{2}$$

with $\alpha \in [0, 2]$. A mathematical analysis have been done by S. Vento [29, 30] when $\Omega = \mathbb{R}$, particularly asymptotic estimates of norm decreasing for large time and, recently, in [22] when $\Omega = \mathbb{T}(0, L)$, the torus

*LAMFA, UMR 6140, Université de Picardie Jules Verne, Amiens, France (jean-paul.chehab@u-picardie.fr) and SIMPAF Project, INRIA Nord-Europe

†LAMFA, UMR 6140, Université de Picardie Jules Verne, Amiens, France (georges.sadaka@u-picardie.fr)

on $[0, L]$; D. Dutykh [11] has considered the case $\alpha = 2$ as a model of dissipative Tsunami wave (with the addition of an nonlocal damping in time). Many questions are open, particularly the long time behavior in the periodic case. We here propose to explore numerically some questions related to the time regularization, the asymptotic speed of norm-decreasing and also numerical implementation feature, particularly when using spectral Fourier or highly accurate finite differences for the spatial discretization. For that purpose, we restrict ourselves to the periodic case and consider the family of nonlocal dampings

$$L_\gamma[u] = \sum_{k\in\mathbb{Z}} \gamma_k \hat{u}_k e^{\frac{2i\pi kx}{L}}.$$

Here γ_k are positive real numbers in such a way we have

$$\int_\Omega L_\gamma[u] u dx \geq 0.$$

This expression of the damping allows to recover number of situations that have been studied, e.g, the choice $\gamma_k = \left|\frac{2\pi k}{L}\right|^\alpha$ corresponds to $L_\gamma[u] = |D|^\alpha u$. However, more general cases can be considered and the sequence γ_k can be chosen in such a way to vary the damping by band of frequencies.

When $\lim_{k\to+\infty} \gamma_k = +\infty$, (e.g. $\gamma_k = k^2$ for a parabolic damping [11]), the equation is regularizing at finite time. When γ_k is constant, say $L[u] = \gamma u$, the damping is said to be "weak" and is not regularizing at finite time but, as proved by Ghidaglia [12, 13] and Goubet [14, 15], it allows the equation to have a finite dimensional attractor which is in a more regular space than the initial data: this is the asymptotic regularization property. Rosa and Cabral in [4] pointed out a non trivial long time dynamics for mild values of γ, they computed numerically time periodic solutions of various cycle length.

Let $\mathbb{T}$ be the torus built on $[0, L]$. Let f be a function depending only of the space variable x. The aim of the present work is to investigate numerically the long time behavior of the forced damped KdV equation

$$u_t + u_{xxx} + L_\gamma[u] + uu_x = f,\ x \in \mathbb{T}, t > 0, \tag{3}$$

$$u(x, 0) = u_0(x), \tag{4}$$

for different type of sequences γ_k with a special focus when $\lim_{k\to+\infty} \gamma_k = 0$: this gives rise to a damping which is more weak than those mentioned before. Since the analysis seems very tricky, we first look on the numerical side. We address in particular the following points

- computation of the damping rates for different sequences γ_k
- numerical measure of the Sobolev regularity
- computation of steady state solution

Finally, in the appendix, we consider also KdV equations with nonlocal damping in time,

$$a_0 u_t + a_1 u_x + a_2 u_{xxx} + \sqrt{\nu} \cdot \frac{1}{\sqrt{\pi}} \int_0^t \frac{u_t(s)}{\sqrt{t-s}} ds + a_3 uu_x - a_4 u_{xx} = 0$$

and

$$a_0 u_t + a_1 u_x + a_2 u_{xxx} - \sqrt{\frac{\nu g}{h}} \cdot \frac{1}{\sqrt{\pi}} \int_0^t \frac{u_x(s)}{\sqrt{t-s}} ds + a_3 uu_x - a_4 u_{xx} = 0,$$

as proposed in [6, 11] respectively and for which we study numerically the rate of damping.

The paper is organized as follows: in Section 2, we give some properties of the equation for general damping operators L_γ. Then, in Section 3, we present the discretization schemes and establish some of their properties. Finally, in Section 4 we present number of numerical results with a special focus on the rate of damping, the Sobolev regularization and the computation of special solutions (steady states, time periodic solutions).

2 A model of Damped KdV Equations

2.1 Problem setting

When $u \in L^2(\mathbb{T})$, we can consider its Fourier expansion and write

$$u(x,t) = \sum_{k\in\mathbb{Z}} \hat{u}_k(t) e^{\frac{2i\pi kx}{L}}.$$

We define the nonlocal damping (or dissipative) term as

$$L_\gamma u = \sum_{k\in\mathbb{Z}} \gamma_k \hat{u}_k(t) e^{\frac{2i\pi kx}{L}}.$$

For obvious symmetry arguments, we will assume in the sequel of the paper that $\gamma_k \in \mathbb{R}$ and that the relations $\gamma_k = \gamma_{-k}$ are satisfied for each k in $\mathbb{Z}$.
The damped KdV equation we consider here is then

$$u_t + u_{xxx} + L_\gamma u + uu_x = f, x \in \mathbb{T}, t > 0, \tag{5}$$

$$u(x,0) = u_0(x). \tag{6}$$

As stated in the introduction, we do not address here to the study of the Cauchy problem. The presence of the damping enforces the regularity properties of the solutions and we will have at least the same properties of the Cauchy problem for the non damped KdV problem. The main problem will be the study of the gain of regularity carried by the damping according to the asymptotic behavior of the sequence γ_k.

Due to the particular form of the damping, we need to use some adapted energy space family, we introduce the following notations

Notations:

- $H_\gamma = \{u \in L^2 / \sum_{k\in\mathbb{Z}} \gamma_k |\hat{u}_k|^2 < +\infty\}$.
- $\dot{H}_\gamma = \{u \in H_\gamma / \int_0^L u dx = 0\} = \{u \in H_\gamma / \hat{u}_0 = 0\}$.
- Let $(\gamma)_k$ and $(\delta)_k$ be two sequences of positive real numbers. We will note $\gamma \leq \delta$ when $\gamma_k \leq \delta_k,\ \forall k$.

The associated norm is $|u|_\gamma = \sqrt{\sum_{k\in\mathbb{Z}} \gamma_k |\hat{u}_k|^2}$.

Finally, we will denote by $< .,. >$ the standard L^2 product.

Remark 1. *Let γ_k be a sequence of strictly positive real numbers. It is easy to prove that H_γ is a Hilbert space endowed with the scalar product $(u,v)_\gamma = \sum_{k\in\mathbb{Z}} \gamma_k \hat{u}_k \overline{\hat{v}_k}$ and of induced norm $|.|_\gamma = \sqrt{(.,.)_\gamma}$.*

Let $\alpha \geq \beta$ then $H_\alpha \hookrightarrow H_\beta$, with continuous injection.
We have also the inequality

$$< u, v > \leq |u|_\gamma |v|_{\frac{1}{\gamma}},\ \forall u \in H_\gamma, \forall v \in H_{\frac{1}{\gamma}}$$

where we have set for convention $(\frac{1}{\gamma})_k = \begin{cases} \frac{1}{\gamma_k} & \text{if } \gamma_k > 0 \\ 0 & \text{else} \end{cases}$.

Remark 2. *When* $u \in L^2(\mathbb{T})$ *and when the sequence* γ_k *is in* ℓ^2 *the term* $L_\gamma u$ *can be identified to the Fourier serie of the convolution product*

$$L_\gamma u(x) = \Lambda * u,$$

with $\Lambda(x) = \sum_{k\in\mathbb{Z}} \gamma_k e^{\frac{2i\pi x}{L}}$.

2.2 Damping properties

When the KdV equation is nor forced nor damped, it possesses an infinite number of invariants, the first ones being

- The mass : $I_0(u) = \int_0^L u(x,t)dx = \int_0^L u_0(x)dx.$
- The L^2 norm : $I_1(u) = \int_0^L (u(x,t))^2 dx = \int_0^L (u_0(x))^2 dx.$
- The Energy : $I_2(u) = \int_0^L \left(\frac{\partial u(x,t)}{\partial x}\right)^2 dx - \frac{1}{6}\int_0^L (u(x,t))^3 dx.$

It is then natural to study the effect of the damping on these quantities (the two first in practice). We begin with the mean $I_0(u)$. We have the

Lemma 3. *For every sufficiently regular function* v *(e.g.* v *is* $H^3(\mathbb{T})$ *in space), we set* $\bar{v}(t) = \frac{1}{L}\int_0^L v(x,t)dx$.
Assume that $\bar{f}(t) = 0$ *then* $\bar{u}(t) = e^{-\gamma_0 t}\bar{u}(0)$

Proof. We have

$$\int_0^L u_{xxx}(x,t)dx = 0 \text{ and } \int_0^L uu_x(x,t)dx = \frac{1}{2}\int_0^L \frac{\partial}{\partial x}u^2(x,t)dx = 0.$$

Hence integrating each term of the equation on space on the interval $[0, L]$, we get

$$\int_0^L \left(\frac{\partial u}{\partial t} + L_\gamma u\right) dx = 0.$$

But $\int_0^L L_\gamma u(x,t)dx = \int_0^L \sum_{k\in\mathbb{Z}} \gamma_k \hat{u}_k e^{\frac{2i\pi x}{L}} dx = L\gamma_0\hat{u}_0 = \gamma_0 \int_0^L u dx.$

$$\text{Therefore } \frac{d}{dt}\frac{1}{L}\int_0^L u(x,t)dx + \frac{1}{L}\int_0^L L_\gamma u(x,t)dx = 0,$$

so

$$\frac{d\bar{u}}{dt} + \gamma_0\bar{u} = 0,$$

Hence the result. In particular, if $\bar{u}(0) = 0$ then $\bar{u}(t) = 0,\ \forall t \geq 0$. □

2.2.1 The linear homogeneous equation

To derive estimates of the propagator associated to the damping, we first consider the linear equation

$$u_t + L_\gamma[u] + u_{xxx} = 0; x \in \Omega, t > 0, \tag{7}$$

$$u(x,0) = u_0(x). \tag{8}$$

Assume that $u(x,t) \in L^2(\mathbb{T}) \forall t > 0$. Expanding it in Fourier serie, we get

$$\sum_{k\in\mathbb{Z}} \frac{d\hat{u}_k(t)}{dt} e^{\frac{2i\pi kx}{L}} + \sum_{k\in\mathbb{Z}} (\gamma_k + \left(\frac{2ik\pi}{L}\right)^3)\hat{u}_k(t) e^{\frac{2i\pi kx}{L}} = 0. \tag{9}$$

By orthogonality of the trigonometric polynomial, we obtain directly

$$\hat{u}_k(t) = e^{-(\gamma_k + (\frac{2ik\pi}{L})^3)t}\hat{u}_k(0). \tag{10}$$

Hence

$$|u|^2_{L^2} = \sum_{k\in\mathbb{Z}} |\hat{u}_k(t)|^2 = \sum_{k\in\mathbb{Z}} e^{-2\gamma_k t}|\hat{u}_k(0)|^2. \tag{11}$$

We can now derive bounds.

Proposition 4. *Assume that $\gamma_k > 0, \forall k \in \mathbb{Z}$ and that $u_0 \in H_{\frac{1}{\gamma}}$. Then*

$$|u|^2_{L^2} \leq \text{Min}\left(\frac{e^{-1}}{2t}|u_0|^2_{\frac{1}{\gamma}}, |u_0|^2_{L^2}\right), \forall t > 0.$$

More generally, if $u_0 \in H_{\beta/\gamma}$ then

$$|u|^2_\beta \leq \frac{e^{-1}}{2t}|u_0|^2_{\frac{\beta}{\gamma}}.$$

Proof. On one hand we have, taking the scalar product of the equation (7) with u in L^2

$$\frac{d|u|^2_{L^2}}{dt} + \sum_{k\in\mathbb{Z}} \gamma_k |\hat{u}_k(t)|^2 = 0.$$

Hence

$$\frac{d|u|^2_{L^2}}{dt} \leq 0,$$

therefore $|u|^2_{L^2} \leq |u_0|^2_{L^2}$. On the other hand we have, solving directly the equation (7), mode by mode,

$$|u|^2_{L^2} = \sum_{k\in\mathbb{Z}} e^{-2\gamma_k t}|\hat{u}_k(0)|^2 = \sum_{k\in\mathbb{Z}} (\gamma_k e^{-2\gamma_k t})(\frac{1}{\gamma_k}|\hat{u}_k(0)|^2)$$

The function

$$\gamma \to \gamma e^{-2\gamma t}$$

is uniformly bounded by $\frac{e^{-1}}{2t}$ on $\mathbb{R}^{+*}$. Hence

$$|u|^2_{L^2} \leq \frac{e^{-1}}{2t} \sum_{k\in\mathbb{Z}} \frac{1}{\gamma_k}|\hat{u}_k(0)|^2.$$

The second inequality is obtained similarly starting from

$$\beta_k|\hat{u}_k(t)|^2 = \beta_k e^{-2\gamma_k t}|\hat{u}_k(0)|^2 = \gamma_k e^{-2\gamma_k t}\left(\frac{\beta_k}{\gamma_k}|\hat{u}_k(0)|^2\right).$$

Hence the result. □

More generally, using the same elementary proof, we can establish

Proposition 5. *Assume that $\gamma_k \in [0,1], \forall k \in \mathbb{Z}$ and that $u_0 \in H_{\frac{1}{\gamma^s}}$. Then, for every $s > 0$*

$$|u|_{L^2}^2 \leq \text{Min}\left(e^{-s}\left(\frac{s}{2t}\right)^s |u_0|^2_{\frac{1}{\gamma^s}}, |u_0|^2_{L^2}\right), \forall t > 0.$$

Proof. By bounding uniformly the function $\gamma \to \gamma^s e^{-2\gamma t}$. □

This simple result means that a better decay in time is obtained with higher regularity of the initial data.

2.2.2 The nonlinear homogeneous equation

We take the scalar product in L^2 of the equation

$$u_t + L_\gamma[u] + u_{xxx} + uu_x = 0;$$

and we obtain

$$\frac{1}{2}\frac{d|u|^2_{L^2}}{dt} + \sum_{k\in\mathbb{Z}} \gamma_k |\hat{u}_k(t)|^2 = 0. \tag{12}$$

We have $|u|^2_\gamma = \sum_{k\in\mathbb{Z}} \gamma_k |\hat{u}_k(t)|^2$. We can prove the

Proposition 6. *Assume that $\gamma_k > 0, \forall k \in \mathbb{Z}$ and that $u_0 \in L^2(\mathbb{T})$ with $\int_0^L u_0(x)dx = 0$. Assume that $u \in L^2(\mathbb{T}) \cap H_\gamma(\mathbb{T})$ for all $t > 0$. Then $u = 0$ is the only one critical point of the system and is asymptotically stable. More precisely*

i. $\lim_{t\to+\infty} |u|_{L^2} = 0.$

ii. In addition, if $\exists c > 0$ such that $\gamma_k \geq c > 0, \forall k \in \mathbb{Z}$ then $|u|_{L^2} \leq e^{-ct}|u|^2_L$.

Proof. For the first assertion, we note that

$$\frac{d|u|^2_{L^2}}{dt} \leq 0,$$

hence $|u(t)|_{L^2} \leq |u_0|_{L^2}, \forall t \geq 0$ and $t \to |u(t)|_{L^2}$ is decreasing in time, consequently $\lim_{t\to\infty} |u(t)|^2_{L^2} = C$. Assuming a sufficient regularity, we infer $\lim_{t\to\infty} |u(t)|^2_\gamma = 0$. Now, since $\gamma_k > 0$ then $\lim_{t\to\infty} \hat{u}_k = 0$ and $u = 0$ *a.e.* This implies $C = 0$.

Estimates [*ii.*] are obtained by a simple application of a Gronwall lemma: $\gamma_k \geq c > 0$, then $|u|_\gamma \geq c|u|^2_{L^2}$ and we have

$$\frac{1}{2}\frac{d|u|^2_{L^2}}{dt} + c|u|^2_{L^2} \leq 0,$$

so, by integration, we get directly

$$|u|^2_{L^2} \leq e^{-2ct}|u_0|^2_{L^2} \text{ therefore } \lim_{t\to+\infty} |u|_{L^2} = 0.$$

□

Corollary 7. *Assume that* $\gamma_k > 0, \forall k \in \mathbb{Z}^*$, $\gamma_0 = 0$ *and* $u_0 \in L^2$. *Then*

$$\lim_{t\to+\infty} u(t) = \hat{u}_0 = \frac{1}{L}\int_0^L u_0(x)dx.$$

Proof. It suffices to introduce $v = u - \hat{u}_0$ and to combine Lemma 3 and proposition **??**. □

When the γ_k are not bounded from below, the orbit converge to 0 in L^2 norm, but it can be at an arbitrary slow velocity, it depends on how γ_k converge to 0 as k goes to infinity.

The main difficulty comes out from the fact that, when γ_k converge toward 0 as $|k|$ goes to infinity, there is no injection from H_γ to L^2. So, the ratio of the two associated norm of the solution plays an important role as pointed out hereafter. We introduce the function

$$G \ : \ (u,t) \mapsto G(u,t) = \frac{|u|_\gamma}{|u|_{L^2}} = \sqrt{\frac{\sum_{k\in\mathbb{Z}} \gamma_k |\hat{u}_k|^2}{\sum_{k\in\mathbb{Z}} |\hat{u}_k|^2}},$$

and in practice we shall use $G(t)$ for $G(u,t)$ when there will be no ambiguity.

Proposition 8. *Let* $u(x,t)$ *be a regular solution of the homogeneous equation (5). We assume that* $G(u,t)$ *is* $\mathcal{C}^1$ *in* t. *Then we have the estimates*

- $|u(t)|^2_{L^2} = e^{-\int_0^t G^2(s)ds} |u_0|^2_{L^2}$
- $|u(t)|^2_\gamma = G^2(t) e^{-\int_0^t G^2(s)ds} |u_0|^2_{L^2}$

In particular, $\lim_{t\to+\infty} |u|_{L^2} = 0$ *iff* $t \mapsto G(t) \notin L^2_t(0,+\infty)$.

Proof. As above, taking the scalar product of the equation (5) in L^2 with u, we get

$$\frac{1}{2}\frac{d|u|^2_{L^2}}{dt} + |u|^2_\gamma = 0.$$

We have by definition of G : $|u|^2_\gamma = G^2(t)|u|^2_{L^2}$. Hence

$$\frac{1}{2}\frac{d|u|^2_{L^2}}{dt} + G^2(t)|u|^2_{L^2} = 0,$$

from that we infer directly

$$|u(t)|^2_{L^2} = e^{-2\int_0^t G^2(s)ds} |u_0|^2_{L^2}. \tag{13}$$

So $\lim_{t\to\infty} |u|_{L^2} = 0$ iff $t \mapsto G(t) \notin L^2_t(0,+\infty)$. Estimate in H_γ norm follows directly with the definition of G. We have

$$|u(t)|^2_\gamma = G^2(t) e^{-2\int_0^t G^2(s)ds} |u_0|^2_{L^2}. \tag{14}$$

We deduce from the proposition 11 that, since $\lim_{t\to\infty} |u|_\gamma = 0$, then $\lim_{t\to\infty} G^2(t) e^{-\int_0^t G^2(s)ds} = 0$. □

The condition $G(t) \notin L^2_t(0,+\infty)$ is of course automatically satisfied when $H_\gamma \subset L^2$ with continuous injection or, equivalently when γ_k are uniformly bounded by below by a strictly nonnegative constant. In such a case, $G(t)$ is bounded from below and $|u|_{L^2}$ converges to zero at an exponential rate as t tends to infinity. In the opposite case, say when $\lim_{k\to\infty} \gamma_k = 0$, according to the previous proposition, we still have $G(t) \notin L^2_t(0,+\infty)$ but we can not obtain a rate of convergence of $|u|_{L^2}$ to 0. These points are crucial for proving the existence of bounded absorbing sets, see [27].

2.2.3 The nonlinear forced equation

Our goal here is to explore numerically the long time behavior of the solutions of the forced and damped equation, and particularly to look to the possible nontrivial dynamics in that case.

First, and as before, we derive estimates in L^2 and H_γ norms:

Proposition 9. *Assume that f belongs to $H_{\frac{1}{\gamma}}$ and that $u_0 \in L^2 \bigcap H_\gamma$. Then*

$$|u(t)|_{L^2}^2 \leq e^{-\int_0^t G^2(s)ds} |u_0|_{L^2}^2 + \int_0^t e^{-\int_s^t G^2(\tau)d\tau} |f|_{\frac{1}{\gamma}}^2 ds.$$

Proof. Taking the scalar product of the equation (5) in L^2 with u, we get

$$\frac{1}{2}\frac{d|u|_{L^2}^2}{dt} + |u|_\gamma^2 = < f, u > .$$

Now,

$$| < f, u > | \leq |f|_{\frac{1}{\gamma}} |u|_\gamma.$$

Hence, introducing $G(t)$ and using Young's inequality,

$$\frac{1}{2}\frac{d|u|_{L^2}^2}{dt} + G^2(t)|u|_{L^2}^2 \leq \frac{1}{2\varepsilon}|f|_{\frac{1}{\gamma}}^2 + \frac{\varepsilon}{2}|u|_\gamma^2 = \frac{1}{2\varepsilon}|f|_{\frac{1}{\gamma}}^2 + \frac{\varepsilon}{2}G^2(t)|u|_{L^2}^2,$$

for any $\varepsilon > 0$. With $\varepsilon = 1$ we obtain, by Gronwall's lemma

$$|u(t)|_{L^2}^2 \leq e^{-\int_0^t G^2(s)ds} |u_0|_{L^2}^2 + \int_0^t e^{-\int_s^t G^2(\tau)d\tau} |f|_{\frac{1}{\gamma}}^2 ds. \tag{15}$$

In a same way, we derive estimates in H_γ, by multiplying each term by $G^2(t)$

$$|u(t)|_\gamma^2 \leq G^2(t) e^{-\int_0^t G^2(s)ds} |u_0|_{L^2}^2 + \int_0^t e^{-\int_s^t G^2(\tau)d\tau} G^2(t)|f|_{\frac{1}{\gamma}}^2 ds. \tag{16}$$

□

We deduce immediately the following result:

Corollary 10. *We make the assumptions of the previous proposition. In addition, we assume that the function*

$$F : t \mapsto \int_0^t e^{-\int_s^t G^2(\tau)d\tau} ds$$

is uniformly bounded in t. Then the equation possesses a bounded absorbing set in L^2.

Notice that it is difficult to obtain bounds on γ that garanties the existence of steady state, as proposed in [4] for the case $\gamma = cste$. Indeed, assume that the equation possesses a stationary solution v, we set $w = u - v$ and we find that

$$w_t + L_\gamma w + w_{xxx} + uu_x - vv_x = 0.$$

Hence, by taking the scalar product in L^2 with w

$$\frac{1}{2}\frac{d|w|_2^2}{dt} + |w|_\gamma^2 + \frac{1}{2}\int_0^L v_x w^2 dx = 0.$$

When $\gamma_k = cste$ or $\gamma_k \geq c > 0$, the equation is (at least) weakly damped and Rosa and Cabral [4] have pointed out non trivial dynamics (multiple stationary solutions, periodic solutions). In such a case,

$$|w|_\gamma^2 \geq c|w|_{L^2}^2,$$

hence, if there exists a strictly positive constant κ such that

$$c + \frac{v_x}{2} \geq \kappa > 0, a.e. \text{ in } [0, L],$$

then

$$|w|_{L^2} \leq e^{-\kappa t}|w_0|_{L^2},$$

so v is the only one steady state and it is asymptotically stable.

When γ_k converge towards 0 it is not possible to proceed as above because, $|.|_\gamma$ and $|.|$ are not equivalent norms. However, when f is constant, $u = \frac{f}{\gamma_0}$ is a steady state of the equation and the only one steady solution with mean equal to zero is $u = 0$.

The nontrivial long time dynamics occurs when the steady state u^* is not unique. A uniqueness condition is

$$|w|_\gamma^2 + \frac{1}{2}\int_0^L v_x w^2 dx \geq 0.$$

We have

$$\widehat{v_x w^2} = \widehat{v_x} * \widehat{w} * \widehat{w}.$$

Setting $\theta = v_x w^2$, we get

$$\int \theta dx = \frac{L}{2}\widehat{\theta}_0,$$

so

$$\widehat{\theta}_0 = \sum_{k\in\mathbb{Z}} \frac{-2i\pi k}{L}\widehat{v}_{-k}\left(\sum_{n\in\mathbb{Z}} \widehat{w}_{k-n}\widehat{w}_n\right).$$

Finally the decreasing condition reads as

$$\sum_{k\in\mathbb{Z}} |\hat{w}_k|^2 + \sum_{k\in\mathbb{Z}} ik\pi\widehat{v}_k\left(\sum_{n\in\mathbb{Z}} \widehat{w}_{-k-n}\widehat{w}_n\right) \geq 0.$$

When bounding from above the second term with the Cauchy-Schwarz inequality, we obtain

$$\sum_{k\in\mathbb{Z}} |\hat{w}_k|^2 - \sum_{k\in\mathbb{Z}} |k\pi\widehat{v}_k|\left(\sum_{n\in\mathbb{Z}} \widehat{w}_n^2\right) \geq 0.$$

Noting that

$$|v_x| = |\sum_{k\in\mathbb{Z}} \frac{2ik\pi}{L}\hat{v}_k e^{\frac{2ik\pi x}{L}}| \leq \sum_{k\in\mathbb{Z}} \frac{2k\pi}{L}|\hat{v}_k|,$$

we see that the decreasing condition can be satisfied only when γ_k are large enough.

3 Numerical schemes

3.1 Spatial discretization

Since the boundary conditions are periodic, it is natural to first consider a spatial Fourier-like approximation, in addition in that case the computation of the nonlocal damping terms will be easy. However, we shall develop also a compact finite difference approximation scheme, to have a comparison, but also to obtain a ground for the simulation when the boundary conditions can be non-periodic.

3.1.1 Fourier-like discretization

We set $\Omega = [0, L]$. Let $N \in \mathbb{N}^*$ we consider the expansion of L-periodic function u as

$$u_N(x) = \sum_{k=-N/2+1}^{N/2} \hat{u}_k e^{i\frac{2k\pi x}{L}},$$

with $\hat{u}_k = \dfrac{2}{L}\displaystyle\int_0^L u(x)e^{-i\frac{2k\pi x}{L}}dx$.

In such a way, we can define

$$(u_N)_x = \sum_{k=-N/2+1}^{N/2} \left(\frac{2k\pi}{L}\right) \hat{u}_k e^{i\frac{2k\pi x}{L}},\ (u_N)_{xxx} = \sum_{k=-N/2+1}^{N/2} \left(\frac{i2k\pi}{L}\right)^3 \hat{u}_k e^{i\frac{2k\pi x}{L}}.$$

The non local term $|D|^\alpha u_N(x)$ is defined *via* its Fourier serie as

$$|D|^\alpha u_N(x) = \sum_{k=-N/2+1}^{N/2} \left|\frac{2k\pi}{L}\right|^\alpha \hat{u}_k e^{i\frac{2k\pi x}{L}}.$$

The nonlinear term is evaluated in the physical space, then transformed in the spectral one. More precisely, setting $v = u^2$,

$$\hat{v}_k = \frac{2}{L}\int_0^L u^2(x)e^{-i\frac{2k\pi x}{L}}dx.$$

Of course, in a computational point of view, it is preferable to consider interpolation values of the truncated trigonometric expansion in such a way to use the FFT routines. To this end, we fix N points of $[0, L]$, $x_m = m\frac{L}{N}$, $m = 0, \cdots, N-1$ and we compute approximations of $U_N(x_m)$ using the relations

$$U_m = U_N(x_m) = \sum_{k=-N/2+1}^{N/2} \hat{u}_k e^{i\frac{2k\pi x_m}{L}} = \sum_{k=-N/2+1}^{N/2} \hat{u}_k e^{i\frac{2k\pi m}{N}}$$

and

$$\hat{u}_k = \frac{2}{N}\sum_{m=0}^{N-1} u_m e^{-i\frac{2k\pi m}{N}},$$

these two sums being efficiently computed with FFT. Hence we have also, using the same notations,

$$|D|^\alpha u_N(x_m) = NL_m = \sum_{k=-N/2+1}^{N/2} \left|\frac{2k\pi}{L}\right|^\alpha \hat{u}_k e^{i\frac{2k\pi m}{N}}$$

and

$$\widehat{\partial_x(u^2)}_k = i\left(\frac{2k\pi}{L}\right)\frac{2}{N}\sum_{m=0}^{N-1} u_m^2 e^{-i\frac{2k\pi m}{N}}.$$

3.1.2 Finite differences discretization

As before, we give ourselves N regularly spaced discretization points $x_m = m\frac{L}{N},\ m = 0, \cdots, N$ and we implement the periodicity with the relations

$$u(x_{m+kN}) = u(x_m).$$

In order to preserve the symmetry and the antisymmetry of the operators, we consider the following family of schemes for the three first derivatives

$$u_x(x_m) \simeq \sum_{\ell=1}^{p} \alpha_\ell \frac{u_{m+\ell} - u_{m-\ell}}{2\ell h}, \tag{17}$$

$$u_{xx}(x_m) \simeq \sum_{\ell=1}^{p} \beta_\ell \frac{u_{m+\ell} - 2u_m + u_{m-\ell}}{(\ell h)^2}, \tag{18}$$

$$u_{xxx}(x_m) \simeq \sum_{\ell=1}^{p} \theta_\ell \frac{-2(u_{m+\ell} + u_{m-\ell}) + (u_{m+\ell+1} + u_{m-\ell-1})}{(2\ell h)^3}. \tag{19}$$

$$\tag{20}$$

Coefficients α_k, β_k and θ_k are chosen in such a way, for a given p, the scheme is of maximal order of accuracy. If $p = 1$ then $\alpha_1 = \beta_1 = \theta_1 = 1$ and the schemes are second order accurate, see appendix. Notice that another possibility, not considered here consists in using compact schemes as presented e.g. in [18].

3.2 Time marching schemes

We present hereafter 4 implicit/semi-implicit time marching schemes for the damped KdV equation:

- Backward Euler's
- Crank Nicolson
- Sanz-Serna
- Strang Splitting

We write them considering only the semi discretization in time and give for 3 of them L^2 stability results which remain valid when finite dimension approximation in space is considered: this is simply due to orthogonality property of the interpolation trigonometric polynomials.
Finally, we need to solve numerically at each time step a fixed point problem. It can be done by using the classical Picard iterate. In some situations, e.g. for Sanz-Serna, the Picard fixed point method needs a small time step Δt to converge: this is artificial since the scheme is unconditionally L^2-stable. Such drawback can be overcome by using other fixed point solver which has a better stability, as proposed in [1], see also subsection 3.2.5 below.

3.2.1 Backward Euler

As first numerical scheme, we propose

$$\frac{u^{(n+1)} - u^{(n)}}{\Delta t} + L_\gamma u^{(n+1)} + \mathcal{L}^3 u^{(n+1)} + \frac{1}{2}\mathcal{L}(u^{(n+1)})^2 = f. \tag{21}$$

Here $\mathcal{L}$ is the skew symmetric linear operator of the first spatial derivative or of its discretization. We prove the following result:

Proposition 11. *Assume that $u^{(0)} = u_0 \in L^2$ and $f \in H_{\frac{1}{\gamma}}$. Then the sequence $u^{(n)}$ generated by the Forward Euler scheme is well defined, belongs in L^2 and*

$$|u^{(n+1)}|_2^2 + |u^{(n+1)} - u^{(n)}|_2^2 + \Delta t \sum_{k\in\mathbb{Z}} \gamma_k |\hat{u}_k^{(n+1)}|^2 \leq |u^{(n)}|_2^2 + \Delta t \sum_{k\in\mathbb{Z}} \frac{1}{\gamma_k} |\hat{f}_k|^2.$$

In addition if $f = 0$, then $\lim_{n\to+\infty} |u^{(n)}|_{L^2} = 0$.

Proof. Using the identity

$$< u^{(n+1)} - u^{(n)}, u^{(n+1)} >= -\frac{1}{2}\left(|u^{(n)}|_2^2 - |u^{(n+1)} - u^{(n)}|_2^2 - |u^{(n+1)}|_2^2\right),$$

we obtain after usual computations

$$|u^{(n+1)}|_2^2 + |u^{(n+1)} - u^{(n)}|_2^2 + 2\Delta t < L_\gamma u^{(n+1)}, u^{(n+1)} >= |u^{(n)}|_2^2 + 2\Delta t < u^{(n+1)}, f >, \tag{22}$$

where

$$< L_\gamma u^{(n+1)}, u^{(n+1)} >= \sum_{k\in\mathbb{Z}} \gamma_k |\hat{u}_k^{(n+1)}|^2 \geq 0.$$

At this point, we use the Young's inequality

$$< u^{(n+1)}, f >\leq \frac{\epsilon}{2}\sum_{k\in\mathbb{Z}} \gamma_k |\hat{u}_k^{(n+1)}|^2 + \frac{1}{2\epsilon}\sum_{k\in\mathbb{Z}} \frac{1}{\gamma_k}|\hat{f}_k|^2,$$

for $\epsilon > 0$ that will be fixed later on. Hence

$$|u^{(n+1)}|_2^2 + |u^{(n+1)} - u^{(n)}|_2^2 + 2\Delta t(1 - \frac{\epsilon}{2})\sum_{k\in\mathbb{Z}} \gamma_k |\hat{u}_k^{(n+1)}|^2 \leq |u^{(n)}|_2^2 + 2\Delta t\frac{1}{2\epsilon}\sum_{k\in\mathbb{Z}} \frac{1}{\gamma_k}|\hat{f}_k|^2.$$

Hence the result with $\epsilon = 1$.

If $f = 0$, the identity (22) becomes

$$|u^{(n+1)}|_2^2 + |u^{(n+1)} - u^{(n)}|_2^2 + 2\Delta t|u^{(n+1)}|_\gamma^2 = |u^{(n)}|_2^2 \tag{23}$$

Hence, the sequence $|u^{(n)}|_2$ is decreasing, limited from below (by 0), then convergent to C. It follows that

$$\lim_{n\to+\infty} \sum_{k\in\mathbb{Z}} \gamma_k |\hat{u}_k^{(n)}|^2 = 0.$$

Therefore, since $\gamma_k > 0$, we have $\lim_{n\to+\infty} \hat{u}_k^n = 0$ and then $C = 0$. □

We give also a discrete version of proposition **??**:

Proposition 12. *Let $u^{(n)}$ the sequence generated by the backward Euler scheme. We set $G^{(n)} = \frac{|u^{(n)}|_\gamma}{|u^{(n)}|_{L^2}}$. We have*

$$|u^{(n)}|_{L^2}^2 \leq \left(\prod_{j=1}^{n} \frac{1}{1 + 2\Delta t(G^{(j)})^2}\right)|u_0|_{L^2}^2.$$

In addition, if $(G^{(j)})_{j\in\mathbb{Z}} \notin \ell^2$, then $\lim_{n\to+\infty} |u^{(n)}|_{L^2} = 0$.

Proof. Taking the scalar product in L^2 with $u^{(n+1)}$ we obtain

$$\frac{1}{2\Delta t}\left(|u^{(n+1)}|_{L^2}^2 - |u^{(n)}|_{L^2}^2 + |u^{(n+1)} - u^{(n)}|_{L^2}^2\right) + (G^{(n+1)})^2|u^{(n+1)}|_{L^2}^2 = 0.$$

Therefore

$$(1 + 2\Delta t(G^{(n+1)})^2)|u^{(n+1)}|_{L^2}^2 + |u^{(n+1)} - u^{(n)}|_{L^2}^2 \leq |u^{(n)}|_{L^2}^2.$$

Now, for Δt small enough we have

$$\log\left(\prod_{j=1}^{n} \frac{1}{1 + 2\Delta t(G^{(j)})^2}\right) = -\sum_{j=1}^{n} \log(1 + 2\Delta t(G^{(j)})^2) \simeq -2\Delta t\sum_{j=1}^{n}(G^{(j)})^2.$$

Hence, if $G^{(j)} \notin \ell^2$ then $\lim_{n\to+\infty} |u^{(n)}|_{L^2} = 0$. □

3.2.2 Crank-Nicolson Scheme

The classical Crank-Nicolson scheme writes as

$$\frac{u^{(n+1)}-u^{(n)}}{\Delta t}+L_\gamma\frac{u^{(n+1)}+u^{(n)}}{2}+\mathcal{L}^3\frac{u^{(n+1)}+u^{(n)}}{2}+\frac{1}{4}\mathcal{L}\left((u^{(n+1)})^2+(u^{(n)})^2\right)=f, \tag{24}$$

with the notations as above. This scheme is second order accurate in time. Here we do not have

$$\left\langle \mathcal{L}\left((u^{(n+1)})^2+(u^{(n)})^2\right),\frac{u^{(n+1)}+u^{(n)}}{2}\right\rangle=0,$$

so we can not derive uniform L^2 bounds for $u^{(n)}$ from the scheme. However is practice, this scheme gives satisfactory numerical results, see section 4.

3.2.3 Sanz-Serna Scheme

The Sanz-Serna scheme is second order accurate in time and corresponds to a mid point quadrature formula in the evaluation of the vector field, see [26]. It writes here as

$$\frac{u^{(n+1)}-u^{(n)}}{\Delta t}+L_\gamma\frac{u^{(n+1)}+u^{(n)}}{2}+\mathcal{L}^3\frac{u^{(n+1)}+u^{(n)}}{2}+\frac{1}{2}\mathcal{L}\left(\frac{u^{(n+1)}+u^{(n)}}{2}\right)^2=f, \tag{25}$$

with always the same the notations.

Proposition 13. *Assume that $u_0\in L^2$ and $f\in L^2\bigcap H_\gamma$. Then the scheme (25) is stable in L^2 for all $\Delta t>0$.*

Proof. We take the L^2 scalar product of each term of (25) with $\dfrac{u^{(n+1)}+u^{(n)}}{2}$ and obtain

$$\frac{|u^{(n+1)}|^2_{L^2}-|u^{(n)}|^2_{L^2}}{2\Delta t}+\frac{1}{4}|u^{(n+1)}+u^{(n)}|^2_\gamma=\left\langle f,\frac{u^{(n+1)}+u^{(n)}}{2}\right\rangle$$

So, using duality and Young's inequality, we have

$$\frac{|u^{(n+1)}|^2_{L^2}-|u^{(n)}|^2_{L^2}}{2\Delta t}+\frac{1}{4}|u^{(n+1)}+u^{(n)}|^2_\gamma\leq\frac{1}{2}|f|^2_{\frac{1}{\gamma}}+\frac{1}{2}\left|\frac{u^{(n+1)}+u^{(n)}}{2}\right|^2_\gamma.$$

Finally, after the usual simplifications

$$|u^{(n+1)}|^2_{L^2}+\frac{\Delta t}{4}|u^{(n+1)}+u^{(n)}|^2_\gamma\leq|u^{(n)}|^2_{L^2}+\Delta t|f|^2_{\frac{1}{\gamma}}.$$

Hence the L^2 stability on every time interval $[O,T]$. □

The scheme (25) is indeed second order accurate and L^2 stable but we can not establish contraction properties as for Backward Euler's which is only first order accurate in time. Indeed, with $f=0$ we only obtain the relation

$$|u^{(n+1)}|^2_{L^2}+\frac{\Delta t}{4}|u^{(n+1)}+u^{(n)}|^2_\gamma=|u^{(n)}|^2_{L^2}$$

which implies that $|u^{(n)}|_{L^2}$ is decreasing (then convergent) but we cannot conclude that the limit is 0. In order to establish both accuracy and contraction properties we consider in the sequel a scheme based on the Strang Splitting.

3.2.4 A Strang splitting time scheme

The main idea of a time splitting scheme is to treat separately the time integration in the one hand of pure dispersive part of the equation and the damped, and on the other hand of the damped part. Of course this last one is less expensive in computations, so a natural approach is to apply the classical Strang splitting as follows:

$$u^{(n+1/3)} = e^{-\frac{\Delta t}{2}L_\gamma} u^{(n)}, \tag{26}$$

$$\frac{u^{(n+2/3)} - u^{(n+1/3)}}{\Delta t} + \frac{1}{2}\mathcal{L}^3\left(u^{(n+2/3)} + u^{(n+1/3)}\right) + \frac{1}{8}\mathcal{L}((u^{(n+2/3)} + u^{(n+1/3)})^2) = f, \tag{27}$$

$$u^{(n+1)} = e^{-\frac{\Delta t}{2}L_\gamma} u^{(n+2/3)}. \tag{28}$$

Here, the operator $\mathcal{S}_\gamma = e^{-\frac{\Delta t}{2}L_\gamma}$ is for every $u \in L^2(\mathbb{T})$ as

$$\mathcal{S}_\gamma u = \sum_{k\in\mathbb{Z}} e^{-\frac{\Delta t}{2}L_{\gamma_k}} \hat{u}_k e^{\frac{2i\pi kx}{L}}.$$

When using an exact time integration, the Strang splitting is second order time accurate. Steps (26) and (28) correspond to exact integration while (27) is a Sanz Serna's which is second order accurate. The resulting so, as we will check numerically. At this point we derive stability bounds

Proposition 14. *Assume that $\gamma_k > 0, \forall k$ and $u^{(0)} \in L^2(\mathbb{T})$. Then the sequence $u^{(n)}$ generated by the scheme (26)-(27)-(28) is well defined and the scheme is unconditionnally stable in L^2. If $f = 0$ then $\lim_{n\to+\infty} |u^{(n)}|_{L^2} = 0$. We have in addition the following estimates*

- *if $\exists c > 0,\ \gamma_k \geq c > 0, \forall k$, then*

$$|u^{(n)}|_{L^2} \leq \delta^{2n}|u^{(0)}|_{L^2} + \Delta t\delta\frac{1}{1-\delta^2}|f|_{L^2}$$

  with $\delta = e^{-\frac{\Delta t c}{2}}$

- *if $u^{(0)} \in L^2(\mathbb{T}) \cap H_{\frac{1}{\gamma}}$ and $f = 0$ then*

$$|u^{(n)}| \leq \frac{e^{-1}}{N\Delta t}|u^{(0)}|_{\frac{1}{\gamma}}.$$

Proof. We first assume that $\gamma_k \geq \gamma = cst, \forall k \in \mathbb{Z}$. We have then $|\mathcal{S}_\gamma u|_{L^2} \leq e^{-\frac{\Delta t\gamma}{2}}|u|_{L^2} = \delta|u|_{L^2}$. We obtain directly the relations

$$|u^{(n+1/3)}|_{L^2} \leq \delta|u^{(n)}|_{L^2} \text{ and } |u^{(n+1)}|_{L^2} \leq \delta|u^{(n+2/3)}|_{L^2}.$$

Taking the scalar product in $L^2(\mathbb{T})$ of each term of (27) with $u^{(n+2/3)} + u^{(n+1/3)}$, we get

$$|u^{(n+2/3)}|^2_{L^2} - |u^{(n+1/3)}|^2_{L^2} \leq \Delta t < f, u^{(n+2/3)} + u^{(n+1/3)} > \leq \Delta t|f|\left(|u^{(n+2/3)}|_{L^2} + |u^{(n+1/3)}|_{L^2}\right),$$

therefore

$$|u^{(n+2/3)}|_{L^2} - |u^{(n+1/3)}|_{L^2} \leq \Delta t|f|_{L^2}.$$

Finally

$$|u^{(n+1)}|_{L^2} \leq \delta|u^{(n+2/3)}|_{L^2} \leq \delta\left(\delta|u^{(n)}|_{L^2} + \Delta t|f|_{L^2}\right).$$

In summary

$$|u^{(n+1)}|_{L^2} \leq \delta^2|u^{(n)}|_{L^2} + \Delta t\delta|f|_{L^2},$$

and by induction we find

$$|u^{(n)}|_{L^2} \leq \delta^{2n}|u^{(0)}|_{L^2} + \Delta t\delta\frac{1}{1-\delta^2}|f|_{L^2},$$

hence the uniform L^2 stability, the sequence $u^{(n)}$ is well defined in L^2. Also, we infer from the previous relation that if $f = 0$ then $\lim_{n\to+\infty} |u^{(n)}|_{L^2} = 0$.

Let us now study the general case $\gamma_k > 0$, with possibly $\lim_{k\to+\infty} \gamma_k = 0$. We first need to show that

$$\lim_{k\to+\infty} |\mathcal{S}_\gamma^N v|_{L^2} = 0$$

for any $v \in L^2(\mathbb{T})$. We have the following result

Lemma 15. *Let $v \in L^2(\mathbb{T})$. Then*

$$\lim_{N\to+\infty} |S_\gamma^N v|_{L^2} = 0.$$

In addition, if $v \in L^2(\mathbb{T}) \cap H_{\frac{1}{\gamma}}$ we have the estimate

$$|S_\gamma^N v|_{L^2} \leq 2\frac{e^{-1}}{N\Delta t}|v|_{\frac{1}{\gamma}}.$$

Proof. Since $v \in L^2(\mathbb{T})$, for a given $\varepsilon > 0$, there exists $N_1 \in \mathbb{N}$ such that

$$\forall N \geq N_1, \sum_{|k|>N_1} |\hat{v}_k|^2 < \frac{\varepsilon}{\sqrt{2}M}.$$

where we have set $M = |v|_{L^2}$. Now, we write $\mathcal{S}^N v$ as

$$|\mathcal{S}^N v|_{L^2}^2 = \sum_{|k|\leq N_1} e^{-N\Delta t\gamma_k}|\hat{v}_k|^2 + \sum_{|k|>N_1} e^{-N\Delta t\gamma_k}|\hat{v}_k|^2$$

The second part is bounded by $\frac{\varepsilon^2}{2}$. Now, since N_1 is fixed, we define $\underline{\gamma}$ as $\underline{\gamma} = \inf_{|k|\leq N_1} \gamma_k > 0$. We can write

$$\sum_{|k|\leq N_1} e^{-N\Delta t\gamma_k}|\hat{v}_k|^2 \leq e^{-N\Delta t\underline{\gamma}}M^2.$$

Finally for the same $\varepsilon > 0$ there exists N_2 such that for every $N \geq N_2$, $e^{-N\Delta t\underline{\gamma}} < \frac{\varepsilon^2}{2M^2}$. Summing these inequalities, we obtain the result. Notice that we do not have any estimate of the rate of convergence; the rate depends on both v and γ.

Assume now that $v \in L^2(\mathbb{T}) \cap H_{\frac{1}{\gamma}}$. Proceeding exactly as in Proposition 4, we find

$$|\mathcal{S}_\gamma^N v|_{L^2} \leq \frac{e^{-1}}{N\Delta t}|v|_{\frac{1}{\gamma}}.$$

This achieves the proof of the lemma. □

Let us now turn back to the time marching scheme. We have the relations

$$u^{(n+1/3)} = \mathcal{S}_\gamma u^{(n)}, \tag{29}$$

$$|u^{(n+2/3)}| \leq |u^{(n+1/3)}| + \Delta t|f|, \tag{30}$$

$$u^{(n+1)} = \mathcal{S}_\gamma u^{(n+2/3)}. \tag{31}$$

Hence,

$$|u^{(n+1)}| \leq \Delta t|f| + |Su^{(n)}|.$$

The L^2-stability follows by induction since $|\mathcal{S}_\gamma u^{(n)}|_{L^2} \leq |u^{(n)}|_{L^2}$. Now, if $f = 0$, we have directly

$$|u^{(n)}|_{L^2} \leq |\mathcal{S}^n u^{(0)}|_{L^2}$$

and we conclude with the previous lemma. □

This splitting scheme combines thus both second order accuracy in time (as Crank-Nicolson's or Sanz-Serna's) and good L^2 stability properties (as Backward Euler's). We illustrate these properties in the numerical simulations.

Remark 16. *The Strang-type splitting scheme*

$$\frac{u^{(n+1/3)} - u^{(n)}}{\Delta t/2} + L_\gamma u^{(n+1/3)} = 0, \tag{32}$$

$$\frac{u^{(n+2/3)} - u^{(n+1/3)}}{\Delta t} + \mathcal{L}^3 u^{(n+2/3)} + \frac{1}{2}\mathcal{L}(u^{(n+2/3)})^2 = f, \tag{33}$$

$$\frac{u^{(n+1)} - u^{(n+2/3)}}{\Delta t/2} + L_\gamma u^{(n+1)} = 0, \tag{34}$$

allows to recover comparable L^2 stability properties. However, it is only first order accurate (see numerical tests), the first and all the three steps being only first order accurate in time.

3.2.5 Implementation

The schemes presented above are implicit or semi implicit and a fixed point problem must be solved at each iteration that can be written as

$$u^{(n+1)} = \Phi(\Delta t, u^{(n)}, u^{(n+1)}), \tag{35}$$

where the definition of Φ depends on the chosen time marching scheme. The simplest method to solve (35) is Picard's iterate:

```
For n=0 ···
Set          v^(0) = u^(n), m = 0
             while ‖φ(Δt, u^(n), v^(m)) − v^(m)‖ > ε
             v^(m+1) = Φ(Δt, u^(n), v^(m))
             m = m + 1
             End while
Set          u^(n+1) = v^(m)
End for
```

Here $\epsilon > 0$ is a small parameter fixed, e.g. $\epsilon = 1.e-12$.
Following [1], we underline that, even when the time marching scheme is stable, and sometimes unconditionally stable, a numerical blow up can be observed because the Picard iterates do not converge if Δt is not small enough. In such a case an artificial restriction on the time step destroys the interest of the numerical method. This occurs here, e.g., when using Sanz-Serna scheme. A way to overcome this drawback is to implement more stable fixed point schemes such as Lemarechal or Marder-Weitzner, see [1] and the references therein for more details.

4 Numerical results

The results presented here have been obtained using Matlab software. We have used the Crank-Nicolson scheme together with the standard Picard iterate to solve the fixed point at each step. The other time schemes (Euler's, Sanz-Serna, Splitting) give comparable results.

4.1 Long time behavior : measure of the numerical Sobolev regularity, special solutions

As said in the introduction, one of the aims of the present work is to observe an asymptotic regularization of the solutions. This have been done for the so-called weak damping ($\gamma_k = c$), but it remains to be done for $\gamma_k \to 0$. To this end we capture the discrete smoothing by analyzing the convergence of the truncated Fourier expansion of the solution. More precisely if, for a fixed time t, we expand $u(x,.)$ as

$$u(x,.) = \sum_{k=1}^{+\infty} \widehat{u}_k w_k(x), \tag{36}$$

where $w_{2k}(x) = \sin(2k\pi x)$, $k \geq 1$, $w_{2k+1}(x) = \cos(2k\pi x)$, $k \geq 0$.
The smoothness of the function $u(x)$ shows on the decay of the high frequency modes. As in [1], we follow [20] starting from the fact that a function u that is in L^2 belongs to H^s, $s > 0$ iff

$$\sum_{N=1}^{+\infty} N^{2s-1} ||u - u_N||_{L^2}^2 < +\infty, \tag{37}$$

where

$$u_N = \sum_{|k|>N} \widehat{u}(k) e_k(x). \tag{38}$$

Of course, in practice, this formula will be applied with a finite number of Fourier modes. If we use two levels of approximations, the fine one u_N which will play the role of u in (37) and the coarse one $u_{N/2}$ which will play the role of u_N in (37), we have to compute s such that

$$\sum_{k=1}^{N/2} k^{2s-1} \left(\sum_{\ell=k}^{N} |\hat{u}_k|^2 \right) < +\infty.$$

The numerical Sobolev exponent is computed by considering the queue of the spectral energy of the solution. More precisely, we look to a linear behavior of the high frequencies Fourier coefficients as

$$\sum_{\ell=k}^{N} |\hat{u}_\ell|^2 \simeq \frac{C}{k^{2s}}, \text{ for } k \gg 1,$$

or equivalently

$$v_k = \ln \sum_{\ell=k}^{N} |\hat{u}_\ell|^2 \simeq \ln(C) - 2s \ln k, \text{ for } k \gg 1.$$

It suffices then to compute s by a linear regression (least square fitting). In practice, we will select a few number (m) of $\hat{u}_k$. Hence s (and $\kappa = \ln(C)$) are computed as minimizers of

$$\sum_{k=N-m}^{N} (v_k - (\kappa - 2s \ln(k))^2.$$

We now apply this technique to the forced damped KdV equation for different sequences γ_k and more precisely

- Constant damping $\gamma_k = 1, \forall k$.
- Band limited damping: $\gamma_k = \chi_{k_1 \le k \le k_2}$.
- Comb-like damping: $\gamma_k = \begin{cases} 1 \text{ if } k \text{ is even} \\ 0 \text{ otherwise} \end{cases}$.

  In that case we have $\widehat{\partial_x u^2}_k = \hat{v}_k = \dfrac{2i\pi k}{L} \displaystyle\sum_{n \in \mathbb{Z}} \hat{u}_{k-n} \hat{u}_n$.

  Hence, if $\hat{u}_{2p+1} = 0$, for $p \in \mathbb{Z}$ then $\hat{v}_{2k+1} = 0$. Therefore, it is easy to show that if $\hat{u}_0$ and f have only even nonzero frequency, then the sequence generated by the different schemes enjoy of the same property. Consequently a comb damping supported by even frequency will damp all the solution while a comb-damping supported only by odd frequency will have no damping effect. Indeed let $u \in L^2$ such that $\hat{u}_{2k+1} = 0, \forall k \in \mathbb{Z}$. We set $v = \partial_x u^2$. We have

$$\hat{v}_k = \frac{2i\pi k}{L} \sum_{n \in \mathbb{Z}} \hat{u}_{k-n} \hat{u}_n = \frac{2i\pi k}{L} \left(\sum_{n \in \mathbb{Z}} \hat{u}_{k-2n} \hat{u}_{2n} + \sum_{n \in \mathbb{Z}} \hat{u}_{k-2n-1} \hat{u}_{2n+1} \right).$$

  If $k = 2p + 1$, we have

$$\hat{v}_{2p+1} = \frac{2i\pi k}{L} \left(\sum_{n \in \mathbb{Z}} \hat{u}_{2p+1-2n} \hat{u}_{2n} + \sum_{n \in \mathbb{Z}} \hat{u}_{2p+1-2n-1} \hat{u}_{2n+1} \right) = 0.$$

  More generally, we can prove the following result

  Lemma 17. *Let $u, v \in L^\infty(\mathbb{T})$. Assume that $\hat{u}_{2k+1} = \hat{v}_{2k+1} = 0$. Then*

$$\widehat{uv}_{2k+1} = 0, \ k \in \mathbb{Z}.$$

  It follows by induction that if $\hat{u}_{2k+1} = 0$, then $\hat{u}^p_{2k+1} = 0$.
- $\gamma_k > 0$ with $\lim\limits_{k \to +\infty} \gamma_k = 0$, such as $\gamma_k = \dfrac{1}{(1 + |k|)^\alpha}$, with $\alpha = 1/4, 1, 2, \cdots$

4.2 The numerical tests

We first illustrate the effect of the damping for different sequences γ_k on both the linear and the nonlinear equation.
At first, we illustrate the damping effect in the two energy norms $|.|_{L^2}$ and $|.|_\gamma$. We see in particular that, as expected, when $\gamma_k > 0$ the solution of the homogeneous equation converges toward 0 in $L^2 \bigcap H_\gamma$. However, when $\lim\limits_{k \to +\infty} \gamma_k = 0$ the rate of convergence depends on u_0 and on its Fourier decomposition.
When $\gamma_k = 0$ on a band frequency, the solution do not automatically converge to 0; it depends on both the Fourier decomposition of the initial data and of the right hand side.
In Figures 1 to 18 we observe a perfect agreement with the results established above: when $\gamma_k > 0, \forall k$ the solution converges to 0 in L^2 and H_γ norms, however, when $\lim\limits_{k \to +\infty} \gamma_k = 0$ the rate (slope in log scale) depends both on the initial data u_0 and on γ_k; in the case of a bandpass, i.e., when $\gamma_k = 0$ for $N_1 \le |k| \le N_2$, we observe according to the cases convergence to 0 if enough frequencies are damped but this is not the case when the damping is not sufficient.

In a second time, we consider the forced and damped equation. We give a special focus to the computation of special solutions as steady states and periodic solutions.
We report in figures 1 and 2 the different damping sequence γ that we will consider. Then in figures 3 to 15, we compare all the numerical schemes (Backward Euler's, Crank-Nicolson's, Sanz-Serna's and the two

Strang-splitting time schemes). All the scheme display comparable results and, as expected, we observe that Euler's and the second Strang-splitting are first order accurate while the others are second order accurate in time. After that all the computation have been realized with the Crank-Nicolson scheme. In figures 16 to 24, we illustrate the damping effects for the homogeneous equation. The results agree with propositions 6 and 8. Then, we consider a non zero source term in such a way we can obtain a non trivial dynamics and observe regularization effects. At first, figure 25 to 51, we compute the time evolution of different norm of the solution; in particular, we look to the time evolution of the (exponential) factors of Proposition 9 and observe that they behave like in the case of the presence of an absorbing set in L^2 (when $\gamma_k > 0$). After that, in figures 52 to 63, we compute non trivial steady states when varying γ_k, f and u_0. In Figures 64 to 70, implementing the technique presented in section 4.1, we point out numerically regularization effects even when $\lim_{k\to+\infty} \gamma_k = 0$: the numerical Sobolev regularity increases with the time. Finally, in figures 71 to 83, we point out numerically, *via* phase plots, the existence of time-periodic solutions, as in [4], but for sequences γ_k such that $\lim_{|k|\to+\infty} \gamma_k = 0$. This result traduces a non trivial dynamics for large times.

For simplicity we will use the following notation $u_0(x) = S1 = 3 \cdot c \cdot sech(\frac{\sqrt{c}}{2}(x - p \cdot L))^2$, where $c = 1,\ c = 0.16$, $p = 0.4,\ p = 0.5$, is the soliton; $u_0(x) = S2$ corresponds to the crennell $u_0(x) = (0.4 * L < x) * (x < 0.6 * L)$; $u_0(x) = S3$ is the sine data $u_0(x) = sin(2\pi x/L)$; finally $u_0(x) = S4 = 50\chi_{x>\pi} sin(4x)$ is the initial datum to compute time-periodic solutions.

Unless specified, for all the numerical simulations, we work with $L = 100$, $N = 2^9$ and $\Delta t = 0.005$.

4.2.1 Profiles of γ_k and $\widehat{u_{0k}}$

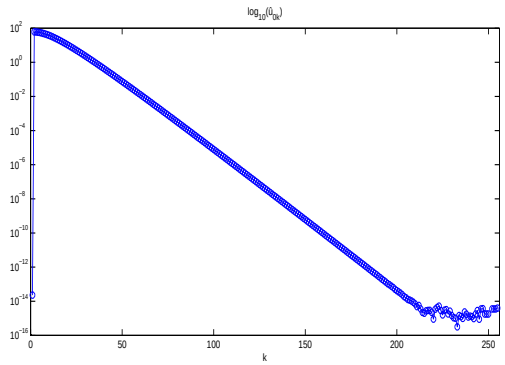

$u_0(x) = S1$

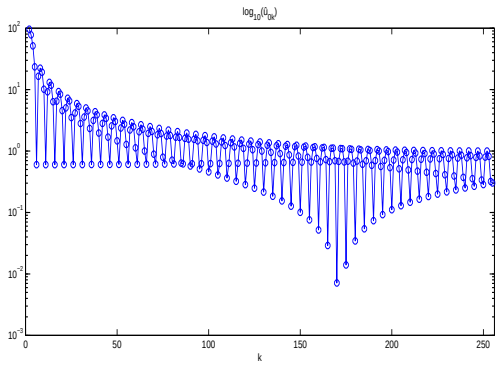

$u_0(x) = S2$

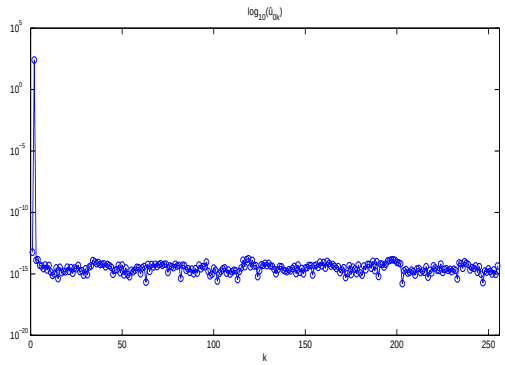

$u_0(x) = S3$

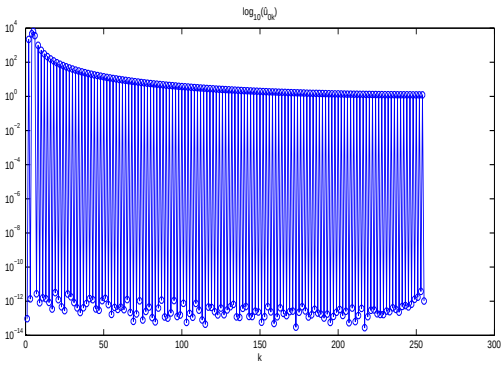

$u_0(x) = S4$

Table 1: Energy spectrum of various initial data.

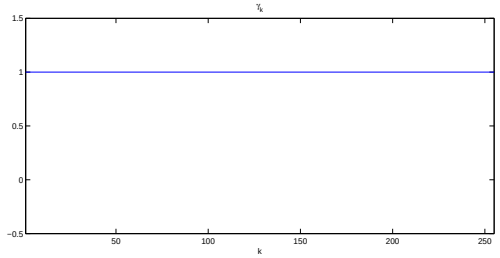	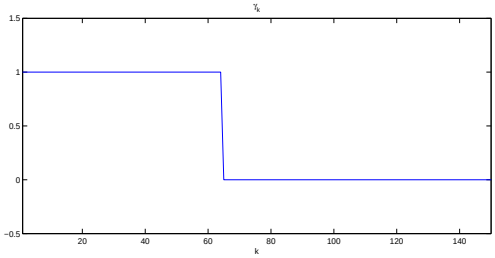
$\gamma_k = 1, \forall k$	$\gamma_k = 1$ if $\|k\| \leq k_0 = N/8$ else 0,
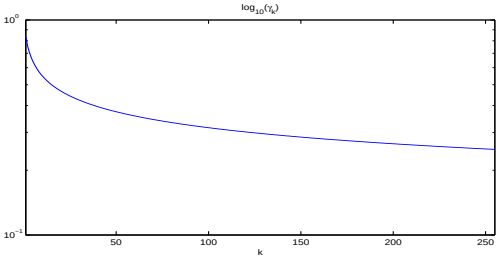	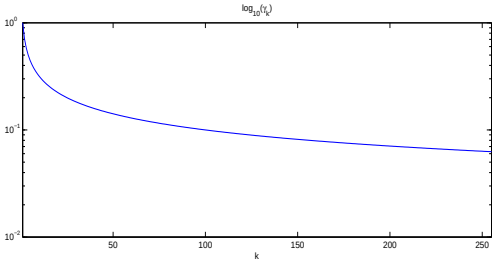
$\gamma_k = \frac{1}{(1+\|k\|)^{1/4}}$	$\gamma_k = \frac{1}{(1+\\|k\\|)^{1/2}}$
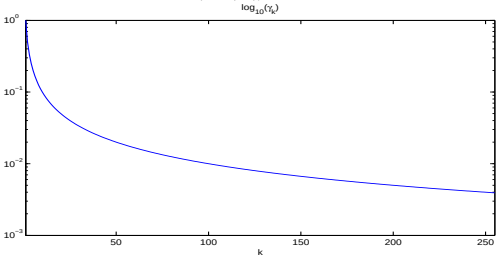	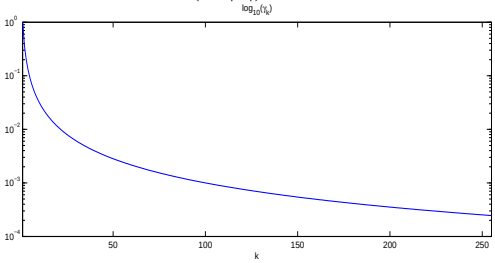
$\gamma_k = \frac{1}{(1+\|k\|)^{1}}$	$\gamma_k = \frac{1}{(1+\\|k\\|)^{3/2}}$
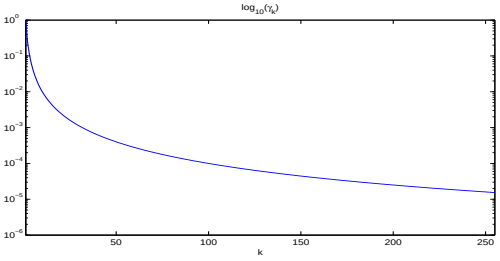	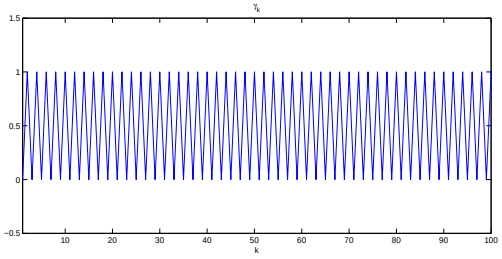
$\gamma_k = \frac{1}{(1+\|k\|)^{2}}$	$\gamma_k = 1$ if k is even , 0 if k is odd

Table 2: Various frequency damping profiles.

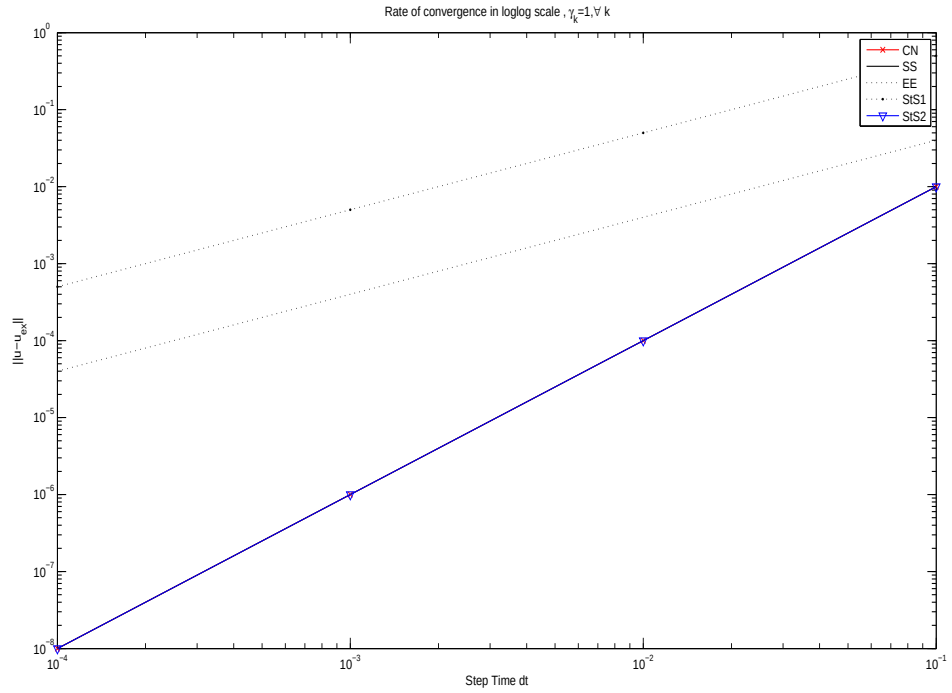

Figure 1: Comparison of the rate of the accuracy of the schemes for $\gamma = 1$

4.3 Homogeneous damped and forced KdV

4.3.1 Damping for different γ_k

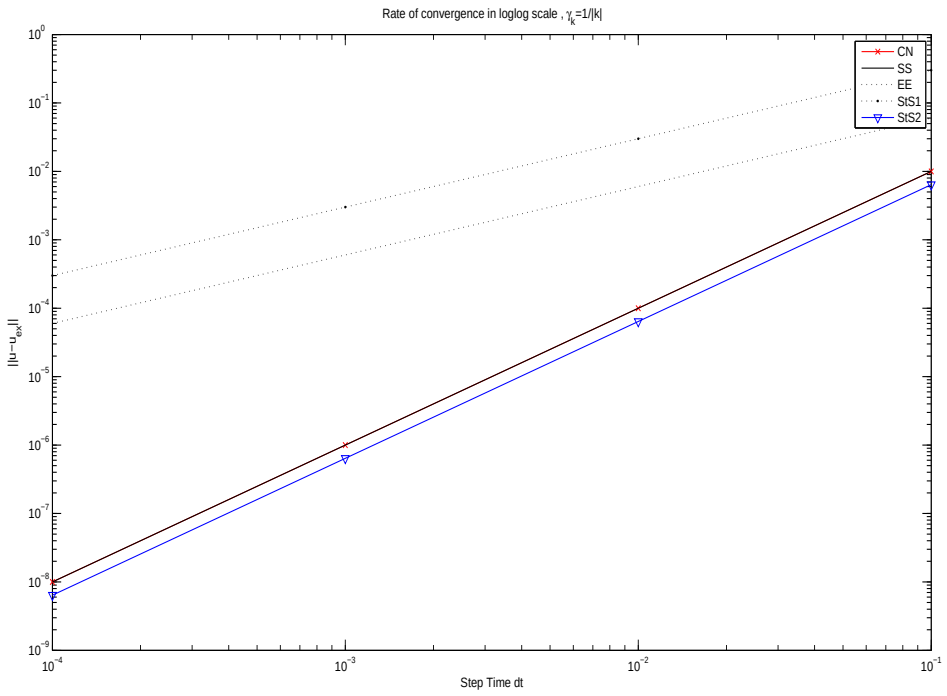

Figure 2: Comparison of the rate of the accuracy of the schemes for $\gamma_k = \dfrac{1}{1+|k|}$

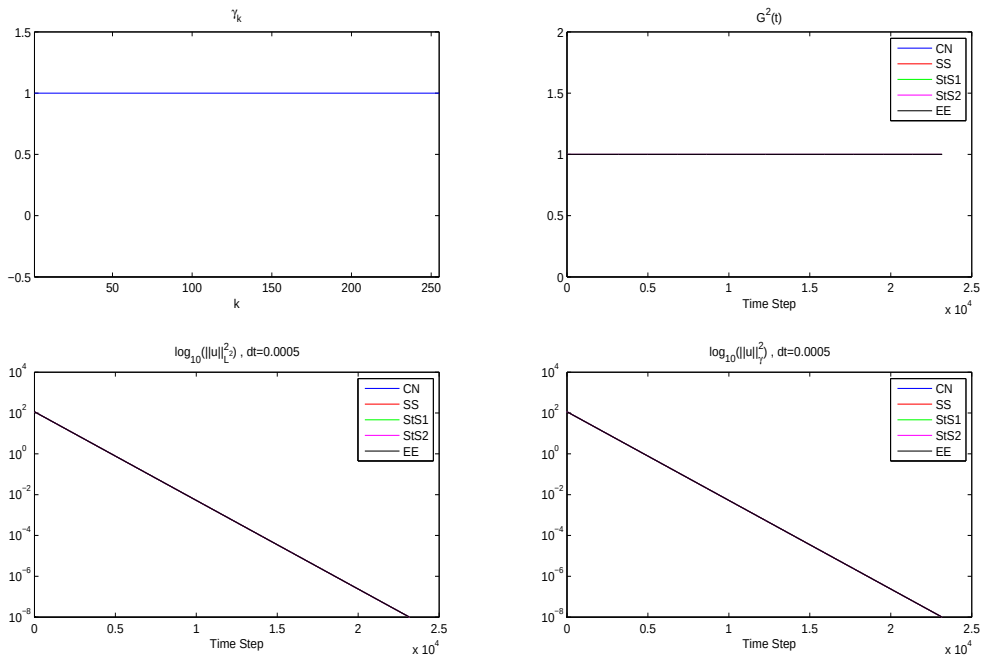

Figure 3: $u_0(x) = S1$, $\gamma_k = 1, \forall k$, $f(x) = 0$

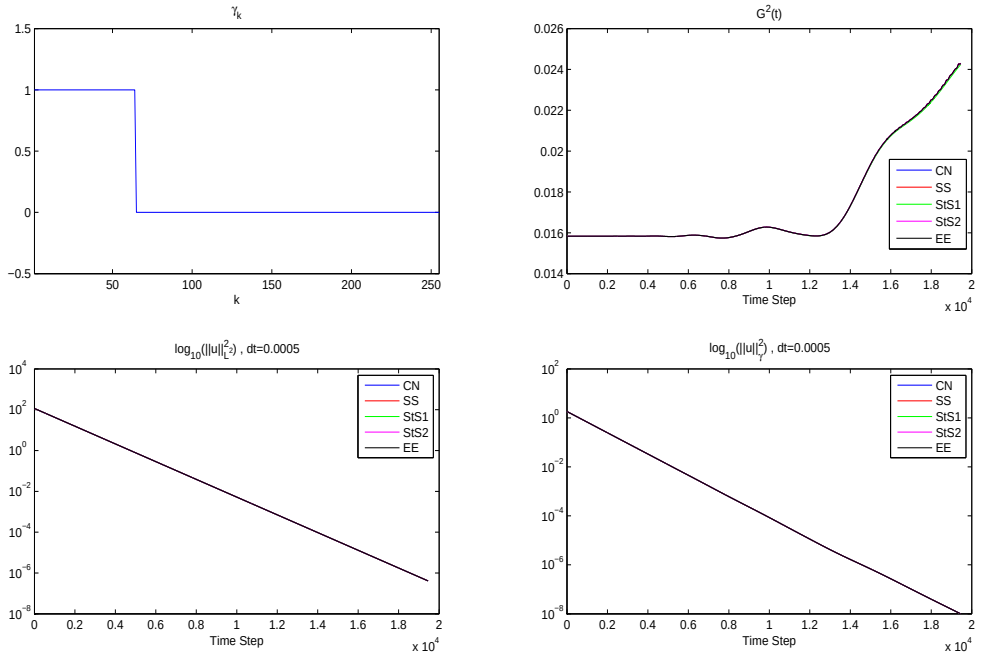

Figure 4: $u_0(x) = S1$,$\gamma_k = 1$ if $|k| \leq k_0 = N/8$ else 0, $f(x) = 0$

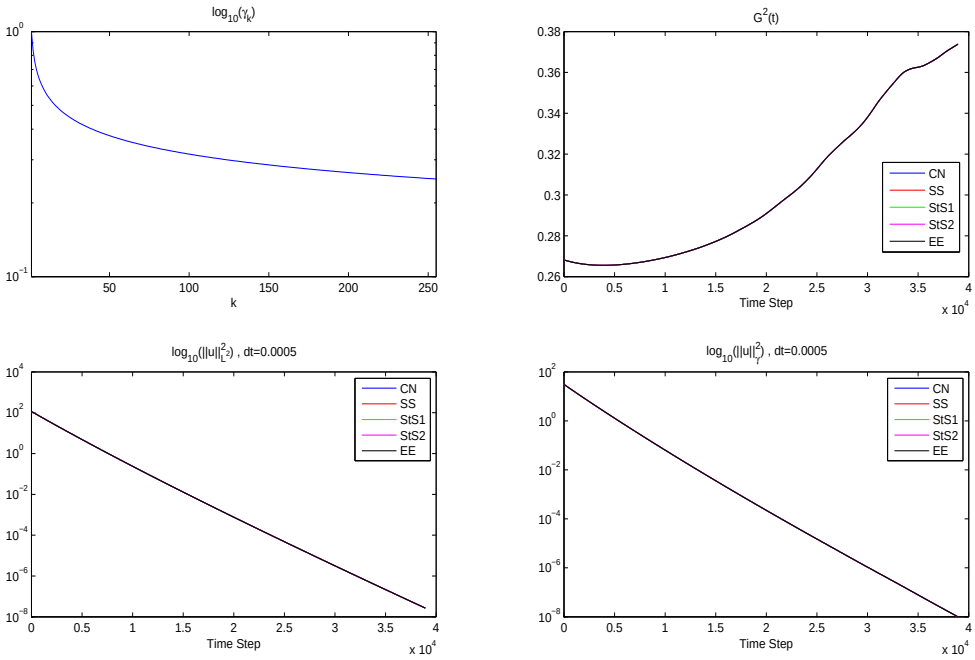

Figure 5: $u_0(x) = S1$,$\gamma_k = \frac{1}{(1+|k|)^{1/4}}$, $f(x) = 0$

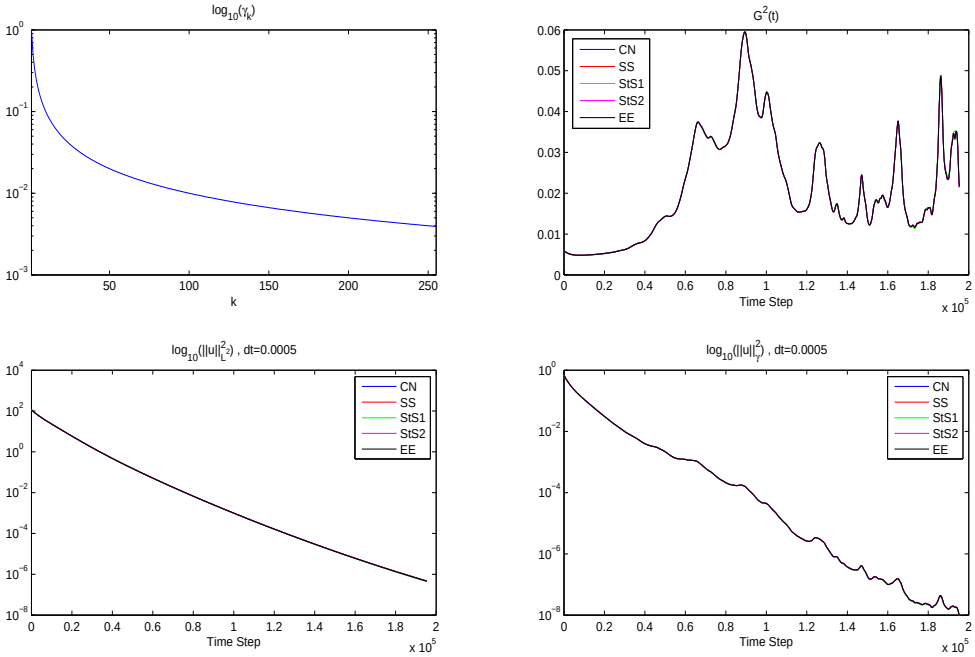

Figure 6: $u_0(x) = S1$,$\gamma_k = \frac{1}{(1+|k|)}$, $f(x) = 0$

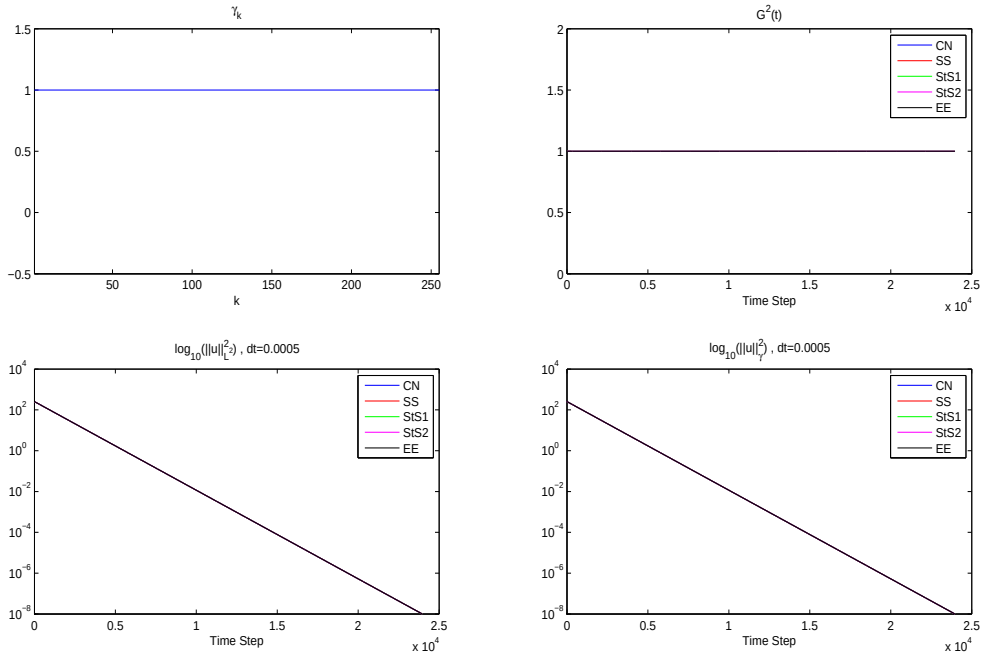

Figure 7: $u_0(x) = S3$,$\gamma_k = 1, \forall k,\ f(x) = 0$

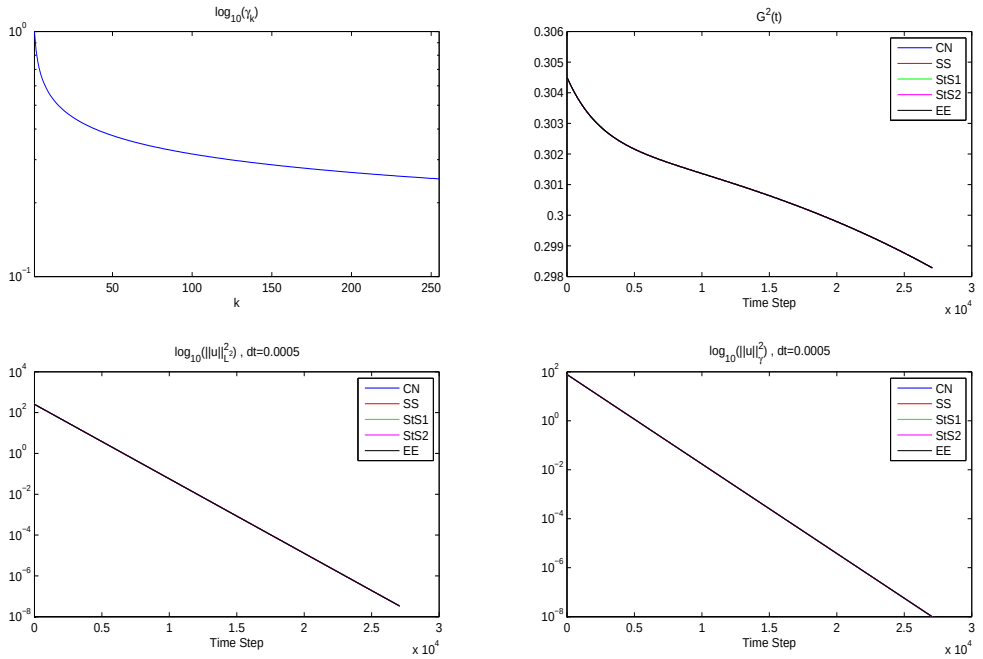

Figure 8: $u_0(x) = S3$,$\gamma_k = \frac{1}{(1+|k|)^{1/4}},\ f(x) = 0$

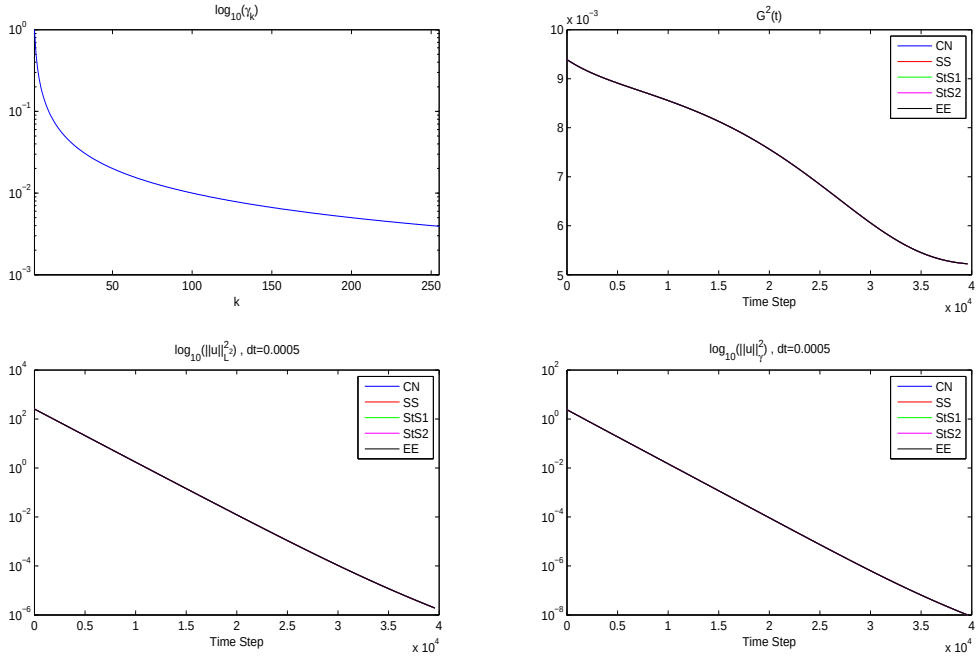

Figure 9: $u_0(x) = S3$,$\gamma_k = \frac{1}{(1+|k|)}$, $f(x) = 0$

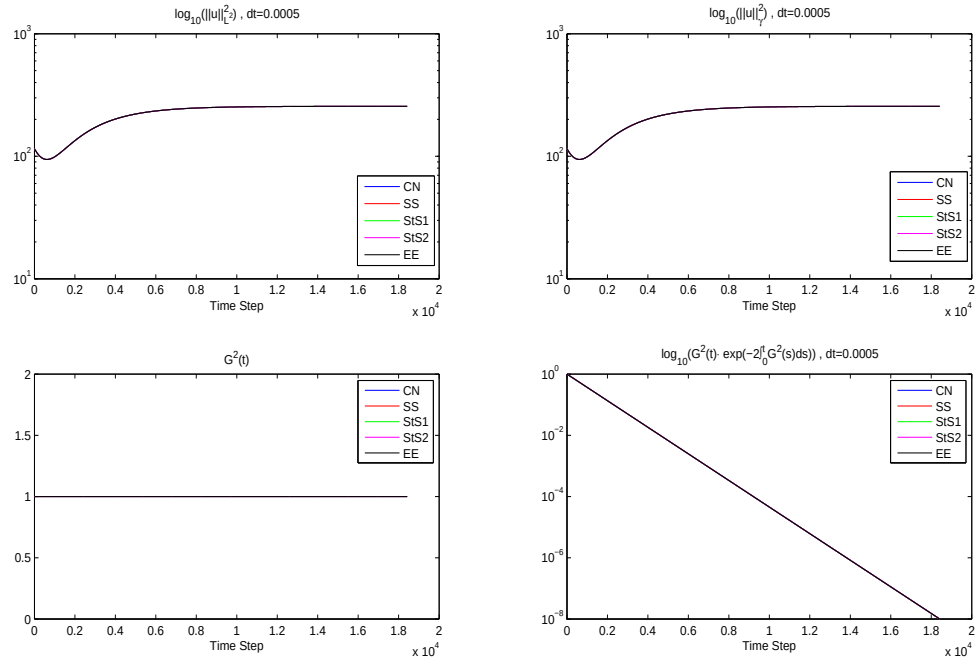

Figure 10: $u_0(x) = S1$, $\gamma_k = 1, \forall k$, $f(x) = \sin(2\pi x/L)$

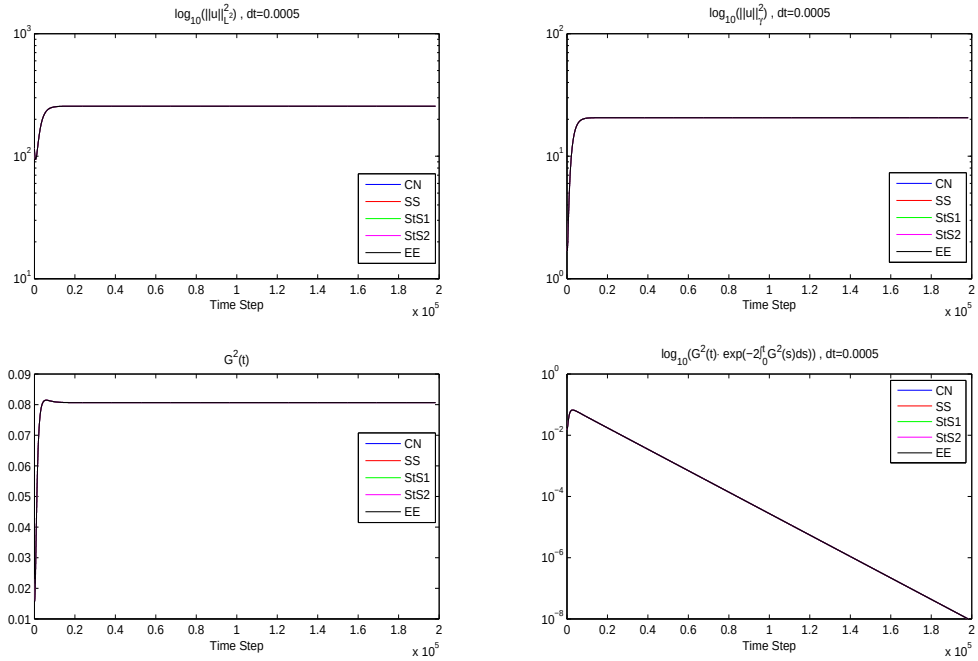

Figure 11: $u_0(x) = S1$,$\gamma_k = 1$ if $|k| \leq k_0 = N/8$ else 0, $f(x) = \sin(2\pi x/L)$

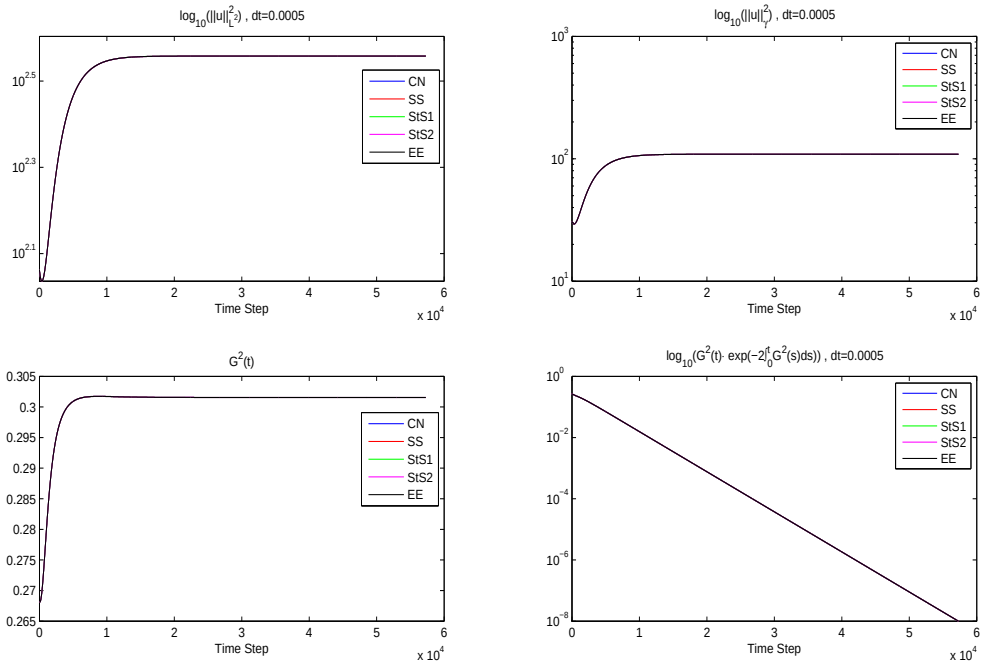

Figure 12: $u_0(x) = S1$,$\gamma_k = \frac{1}{(1+|k|)^{1/4}}$, $f(x) = \sin(2\pi x/L)$

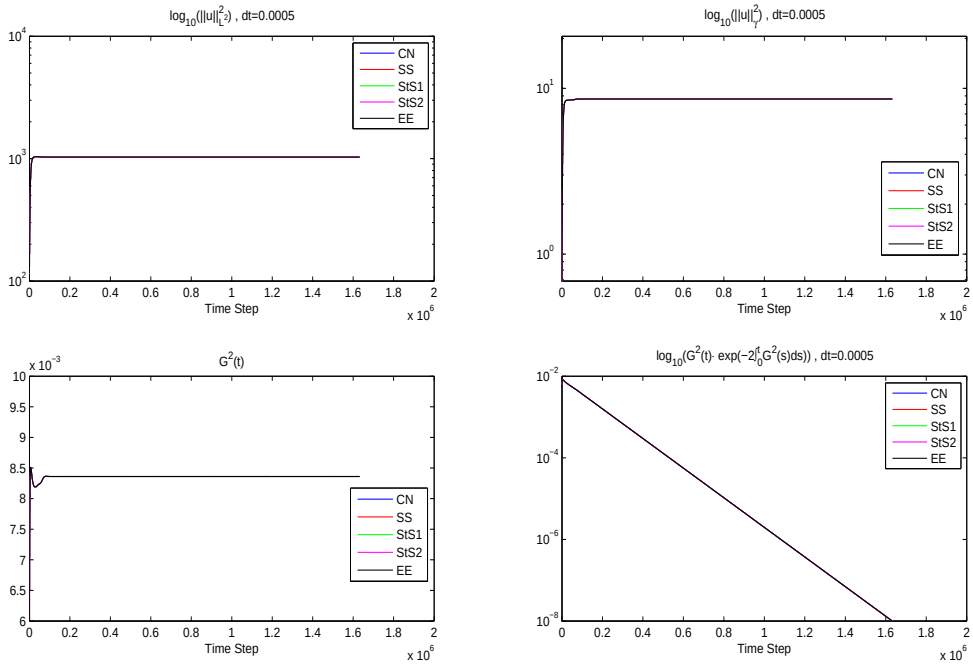

Figure 13: $u_0(x) = S1$,$\gamma_k = \frac{1}{(1+|k|)}$, $f(x) = \sin(2\pi x/L)$

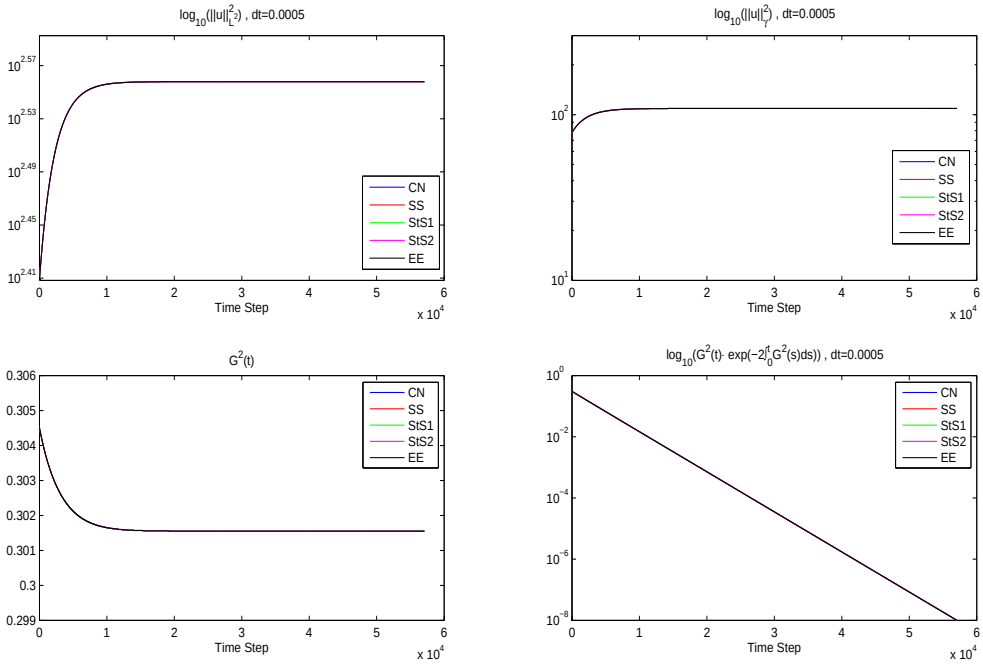

Figure 14: $u_0(x) = S3$,$\gamma_k = \frac{1}{(1+|k|)^{1/4}}$, $f(x) = 0$

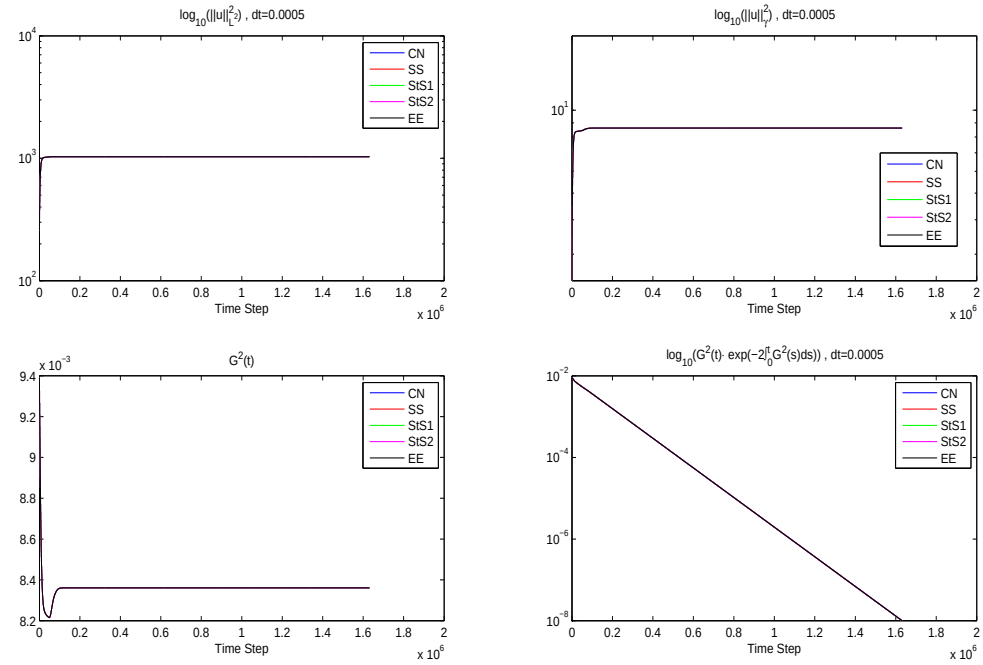

Figure 15: $u_0(x) = S3$,$\gamma_k = \frac{1}{(1+|k|)}$, $f(x) = 0$

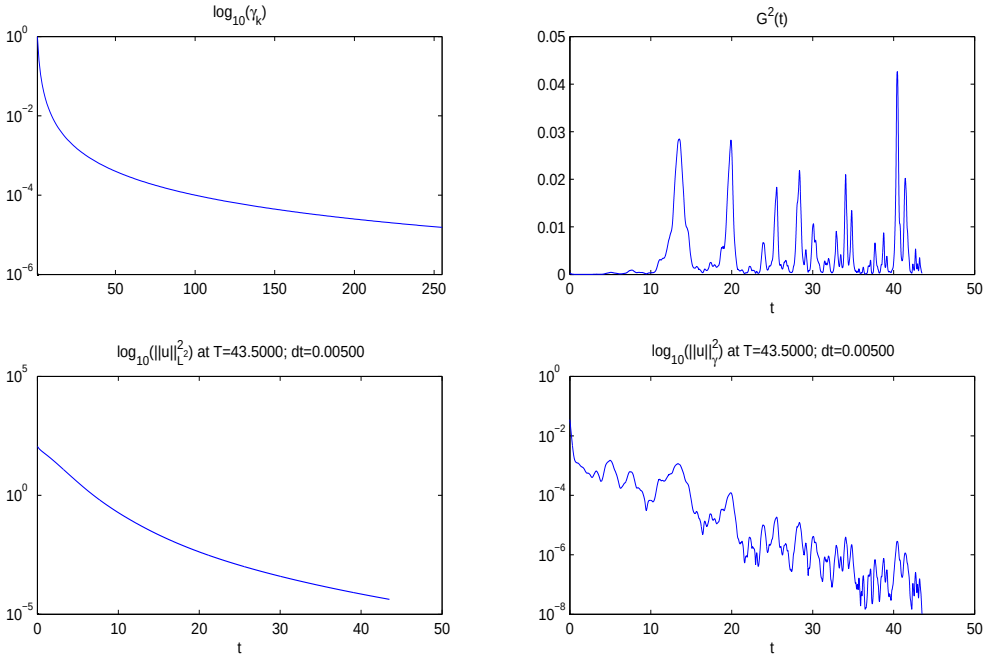

Figure 16: $u_0(x) = S1$,$\gamma_k = \frac{1}{(1+|k|)^2}$, $f(x) = 0$

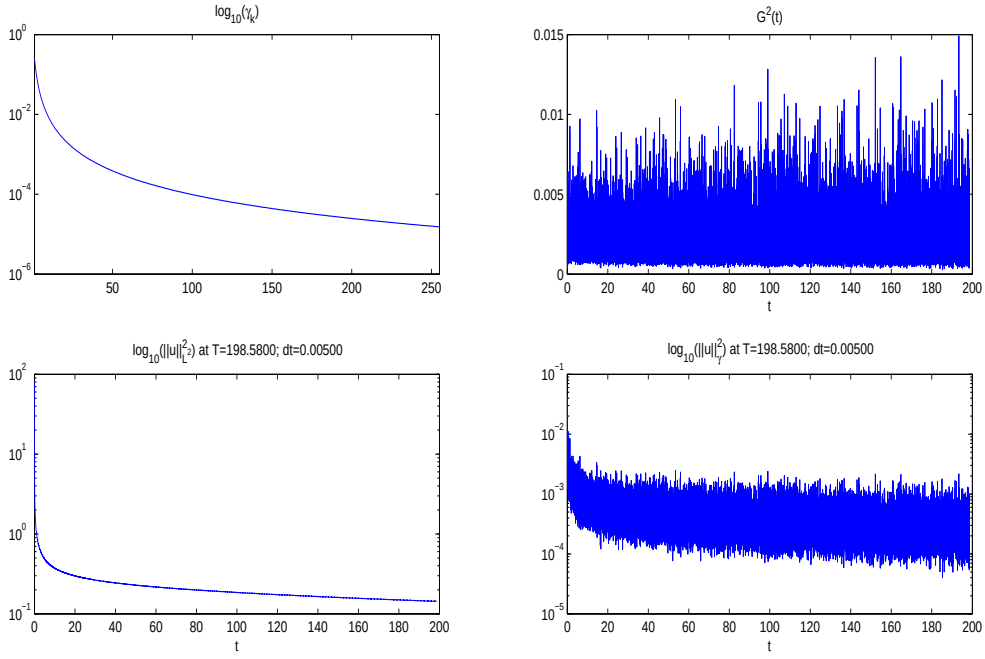

Figure 17: $u_0(x) = S2$, $\gamma_k = \frac{1}{(1+|k|)^2}$, $f(x) = 0$

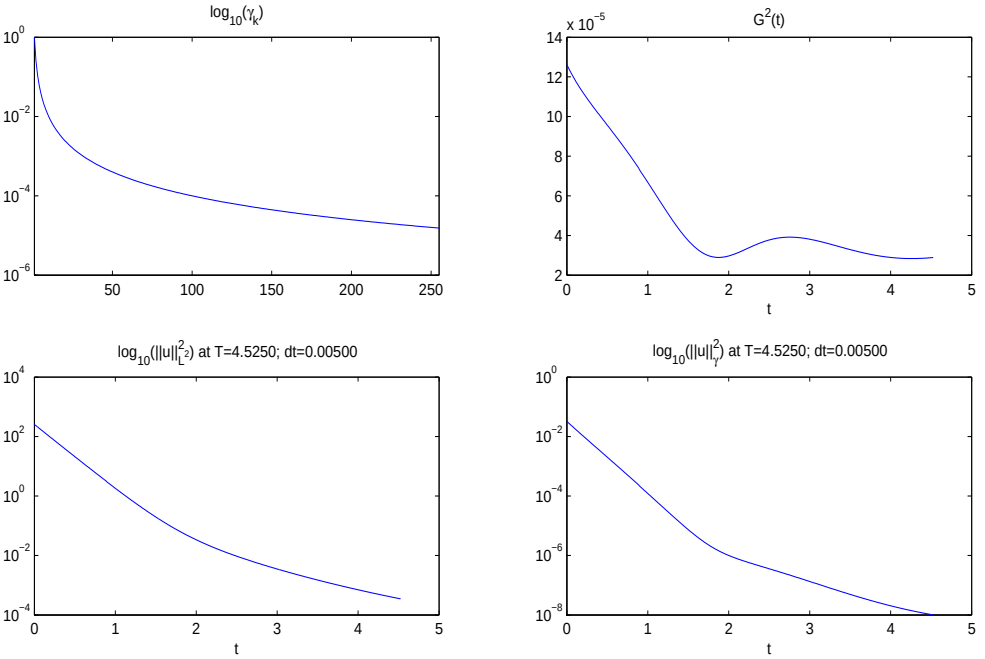

Figure 18: $u_0(x) = S3$, $\gamma_k = \frac{1}{(1+|k|)^2}$, $f(x) = 0$

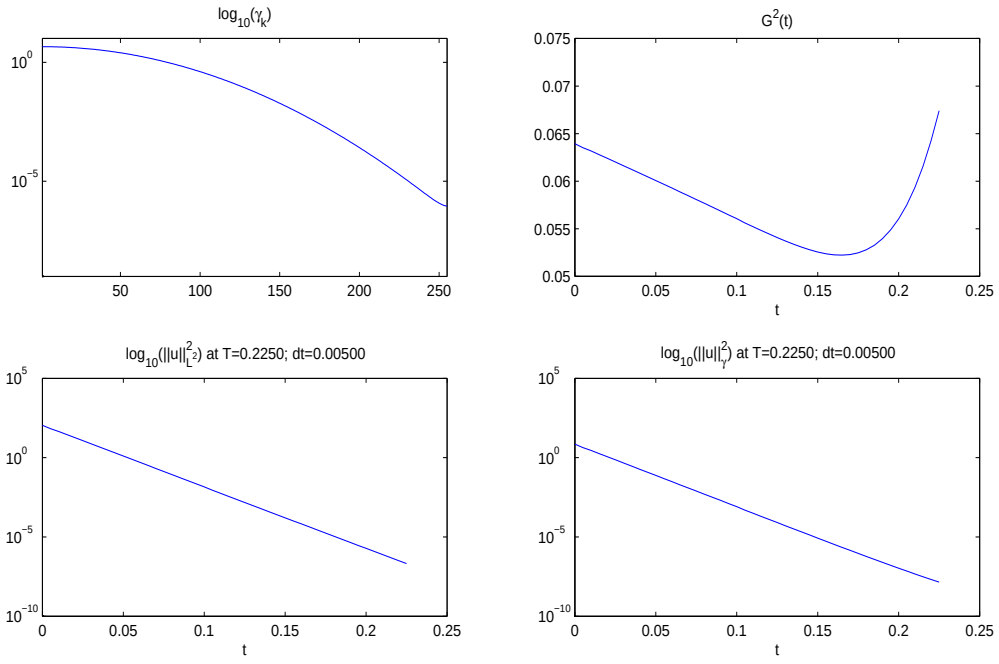

Figure 19: $u_0(x) = S1$,$\gamma_k = abs(fft(exp(-(k-L/2)^2/\sigma)), \sigma = 1/4;\ f(x) = 0$

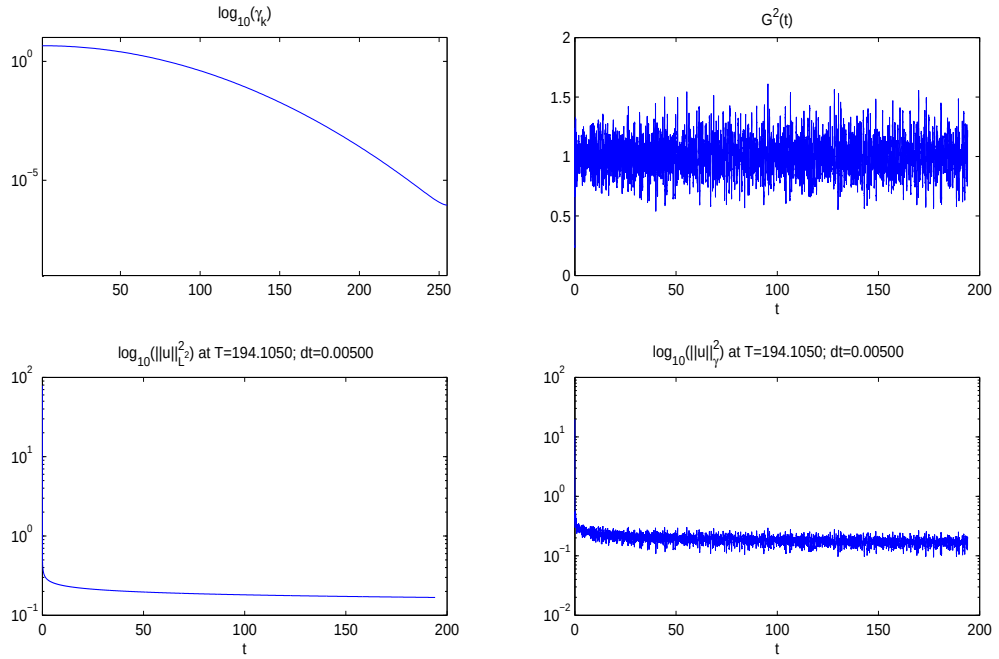

Figure 20: $u_0(x) = S2$,$\gamma_k = abs(fft(exp(-(k-L/2)^2/\sigma)), \sigma = 1/4;\ f(x) = 0$

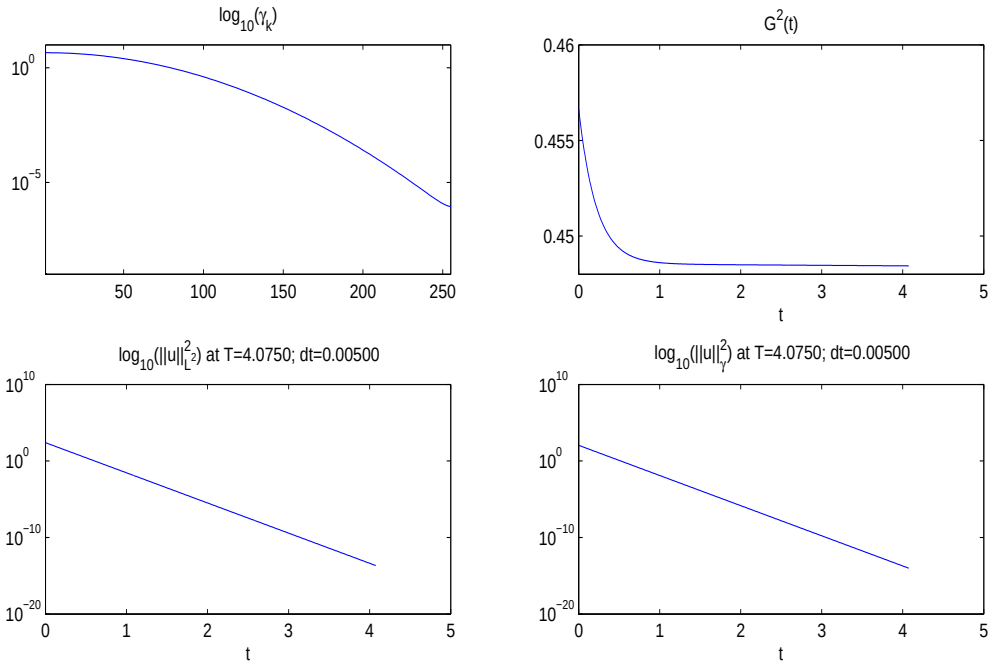

Figure 21: $u_0(x) = S3$, $\gamma_k = abs(fft(exp(-(k-L/2)^2/\sigma)), \sigma = 1/4;\ f(x) = 0$

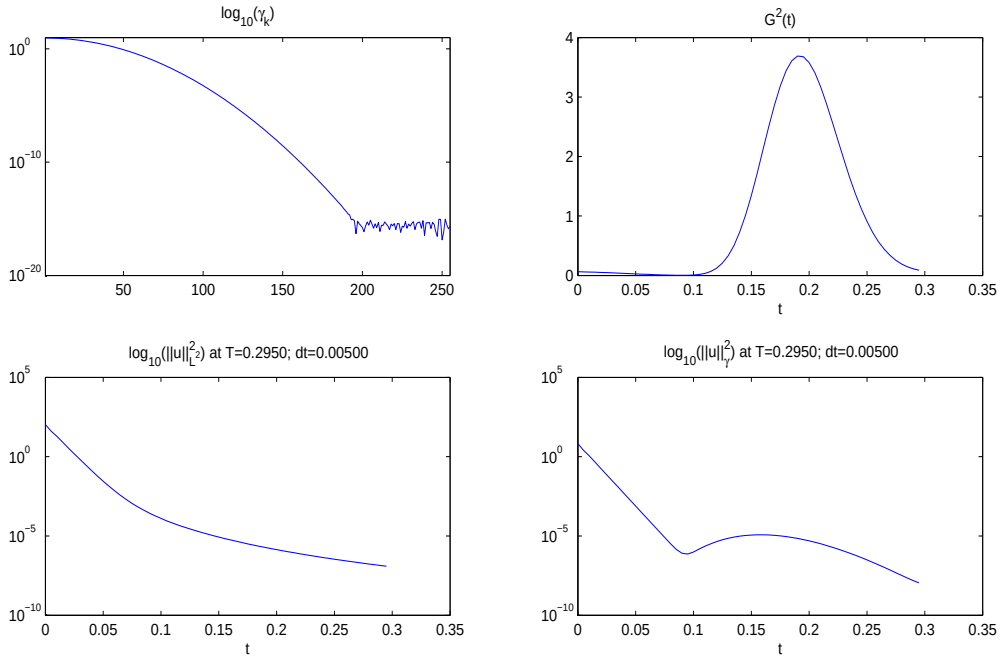

Figure 22: $u_0(x) = S1$,$\gamma_k = abs(fft(exp(-(k-L/2)^2/\sigma)), \sigma = 1;\ f(x) = 0$

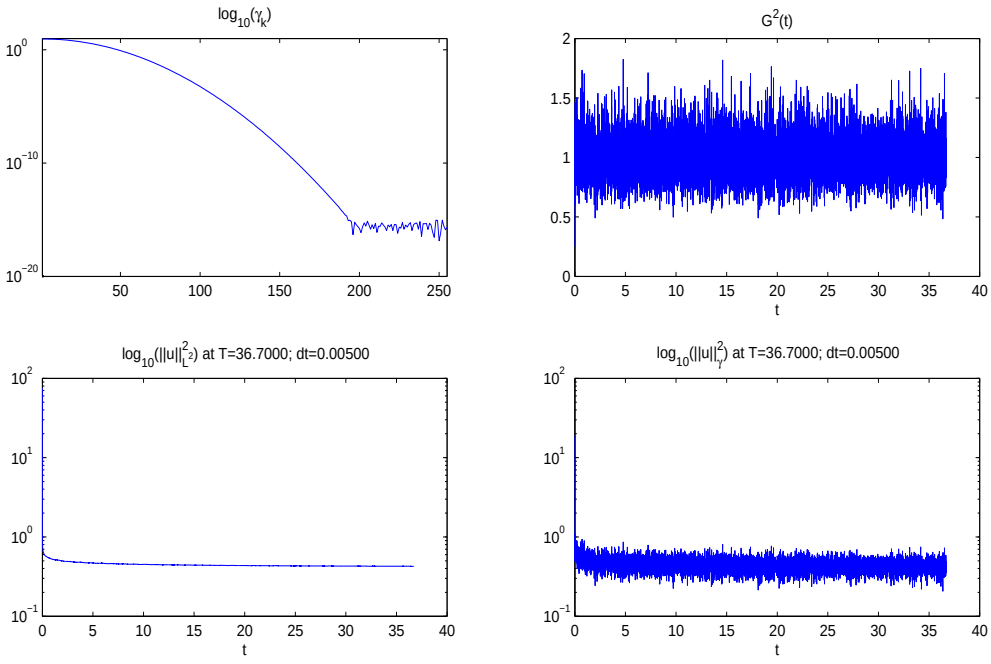

Figure 23: $u_0(x) = S2$,$\gamma_k = abs(fft(exp(-(k-L/2)^2/\sigma)), \sigma = 1;\ f(x) = 0$

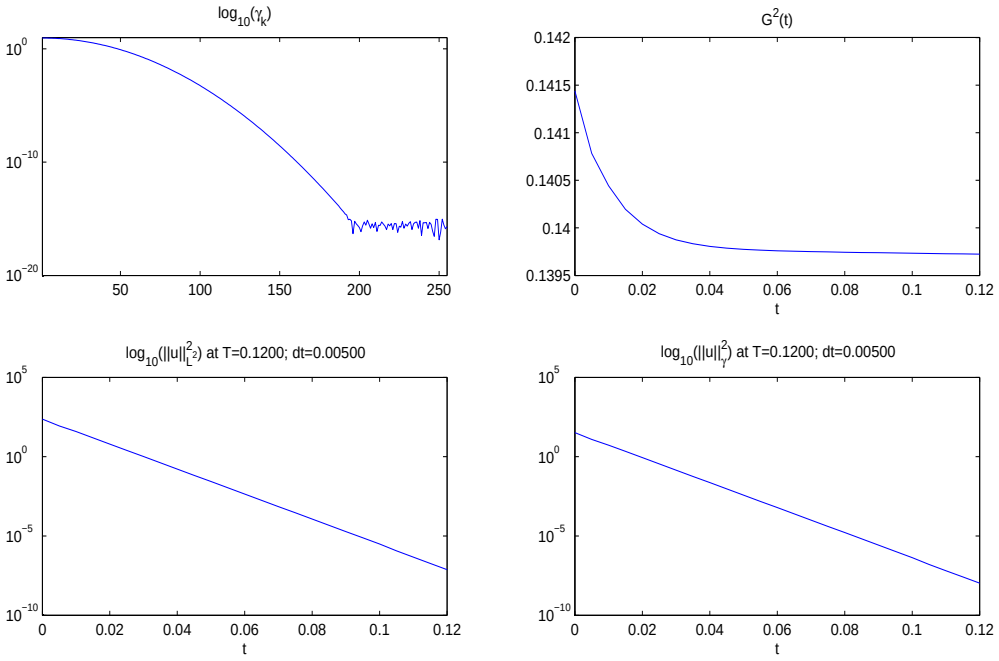

Figure 24: $u_0(x) = S3$, $\gamma_k = abs(fft(exp(-(k-L/2)^2/\sigma)), \sigma = 1;\ f(x) = 0$

4.3.2 Forced KdV

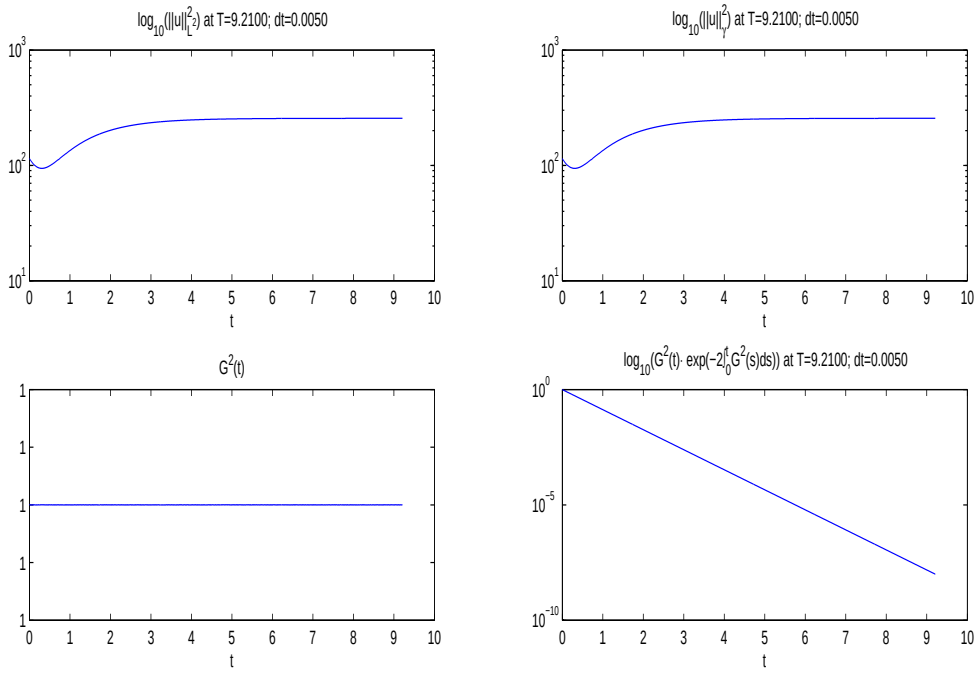

Figure 25: $u_0(x) = S1$,$\gamma_k = 1, \forall k,\ f(x) = \sin(2\pi x/L)$

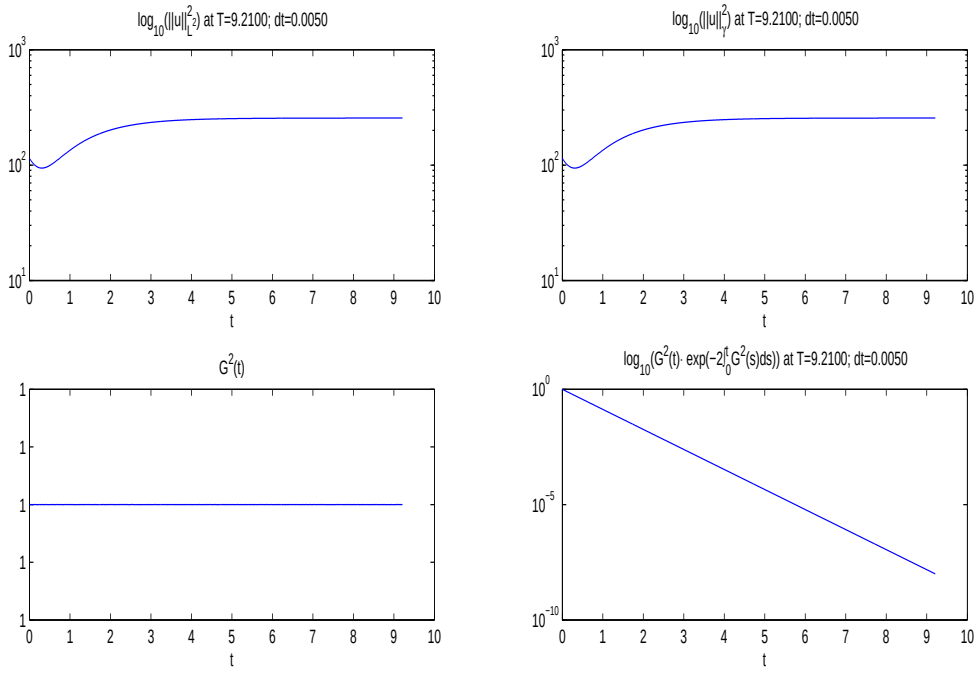

Figure 26: Sanz-Serna, $u_0(x) = S1$,$\gamma_k = 1, \forall k,\ f(x) = \sin(2\pi x/L)$

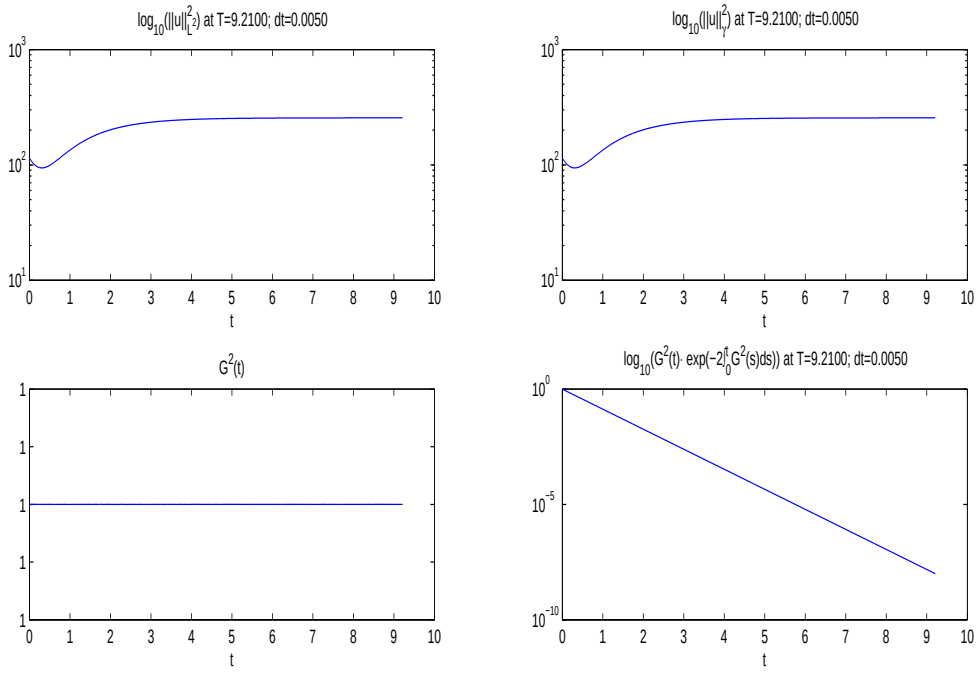

Figure 27: Euler-Explicite, $u_0(x) = S1$,$\gamma_k = 1, \forall k,\ f(x) = \sin(2\pi x/L)$

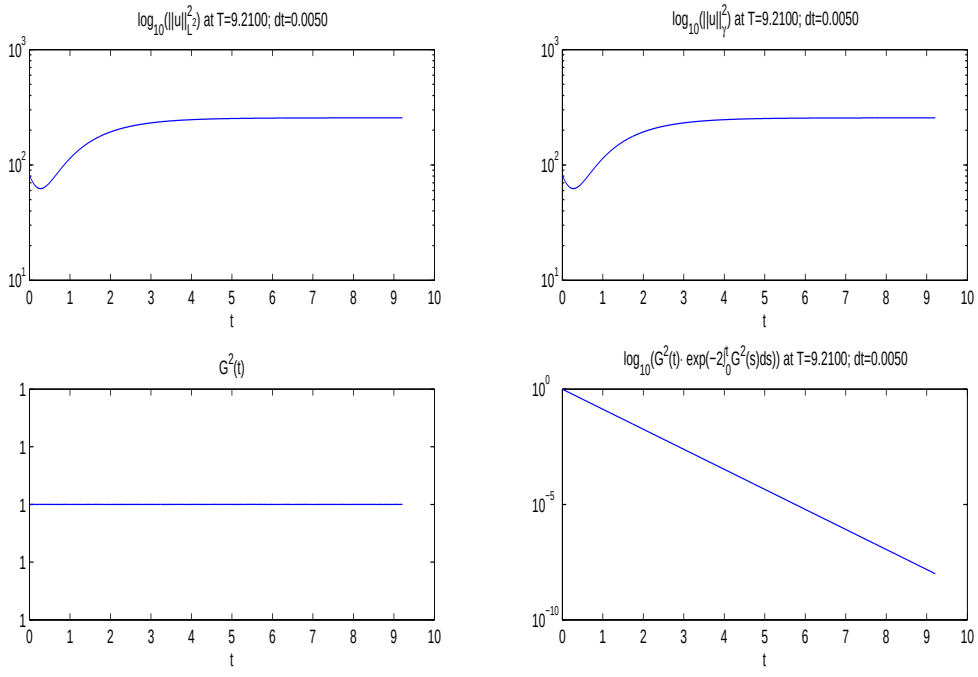

Figure 28: $u_0(x) = S2$, $\gamma_k = 1, \forall k,\ f(x) = \sin(2\pi x/L)$

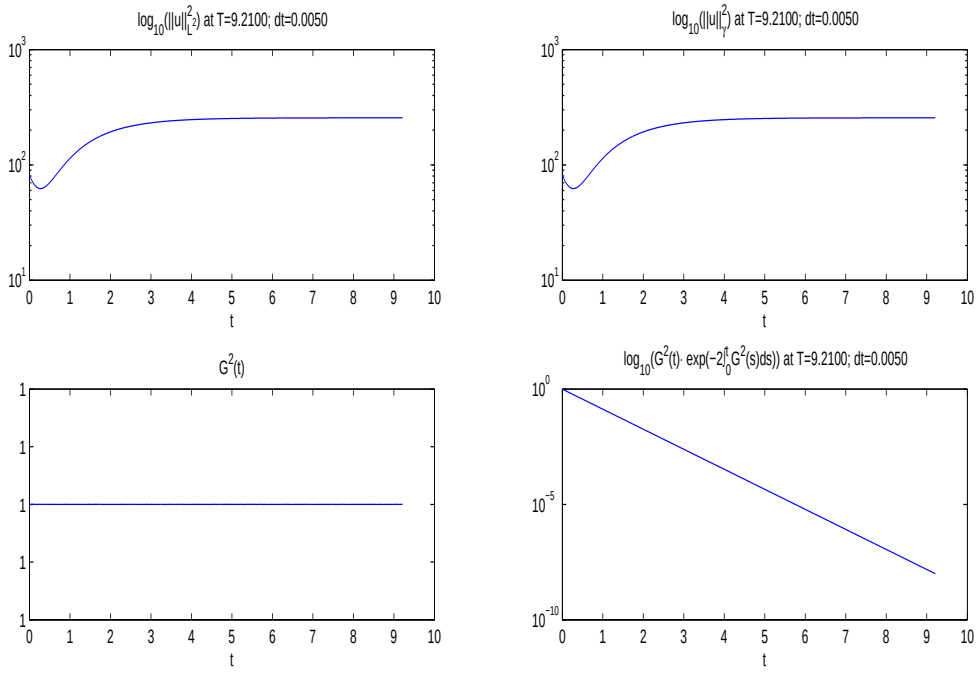

Figure 29: $u_0(x) = S2$, $\gamma_k = 1, \forall k$, $f(x) = \sin(2\pi x/L)$

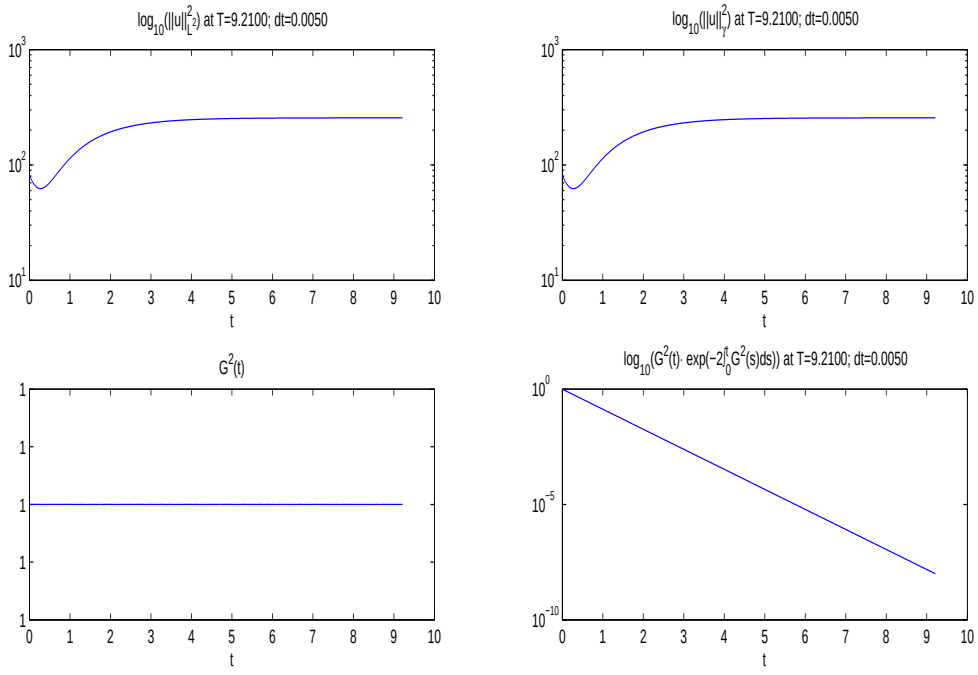

Figure 30: Sanz-Serna, $u_0(x) = S2$, $\gamma_k = 1, \forall k$, $f(x) = \sin(2\pi x/L)$

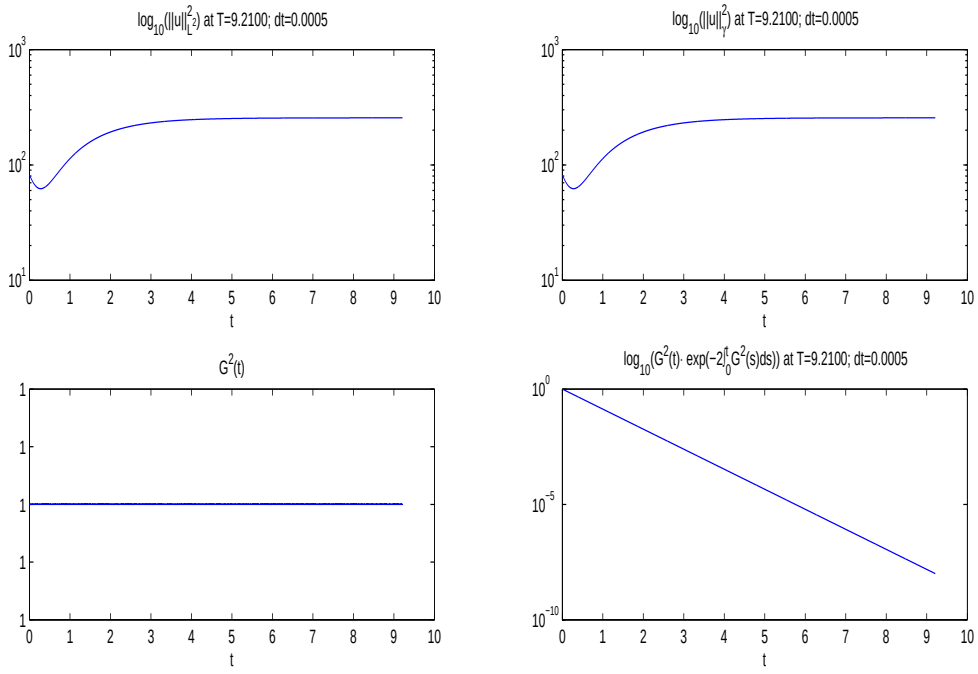

Figure 31: Euler-Explicite, $u_0(x) = S2$, $\gamma_k = 1, \forall k,\ f(x) = \sin(2\pi x/L)$

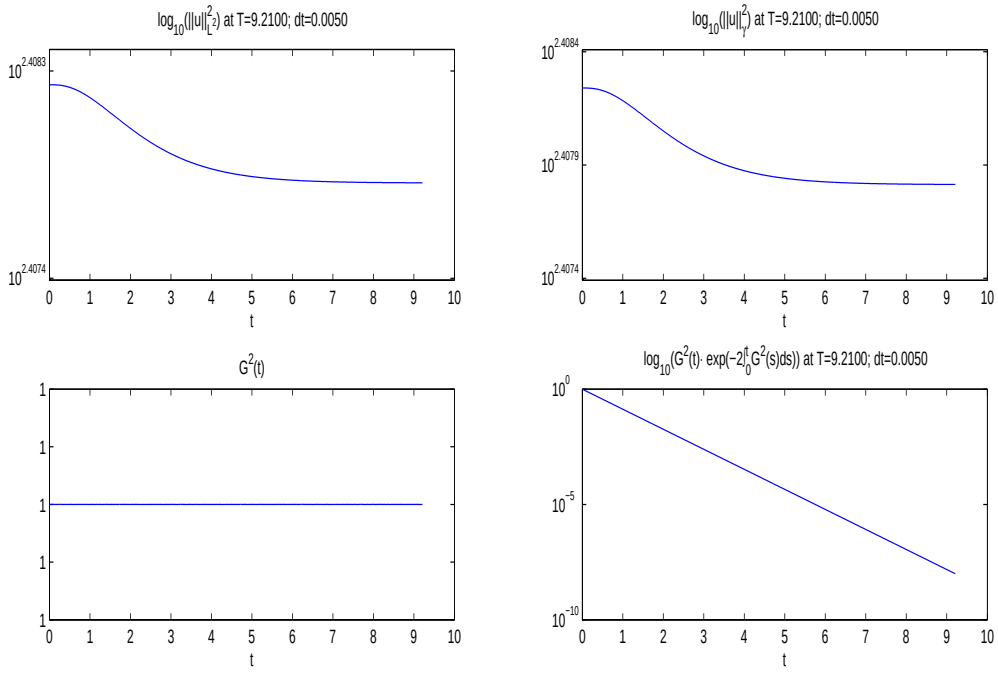

Figure 32: $u_0(x) = S3$, $\gamma_k = 1, \forall k,\ f(x) = \sin(2\pi x/L)$

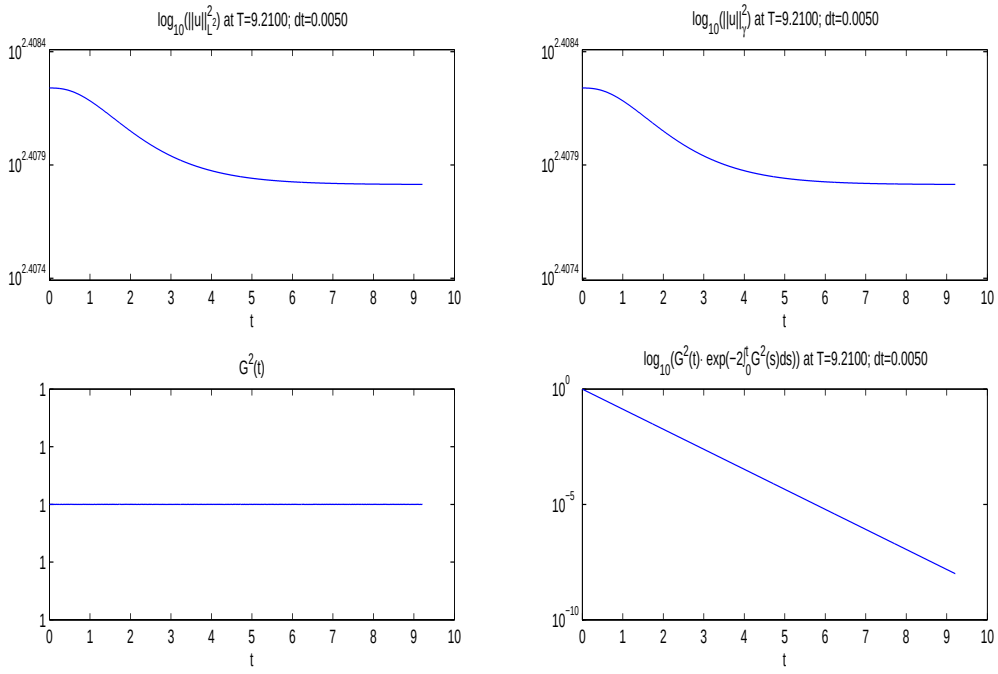

Figure 33: Sanz-Serna, $u_0(x) = S3$, $\gamma_k = 1, \forall k$, $f(x) = \sin(2\pi x/L)$

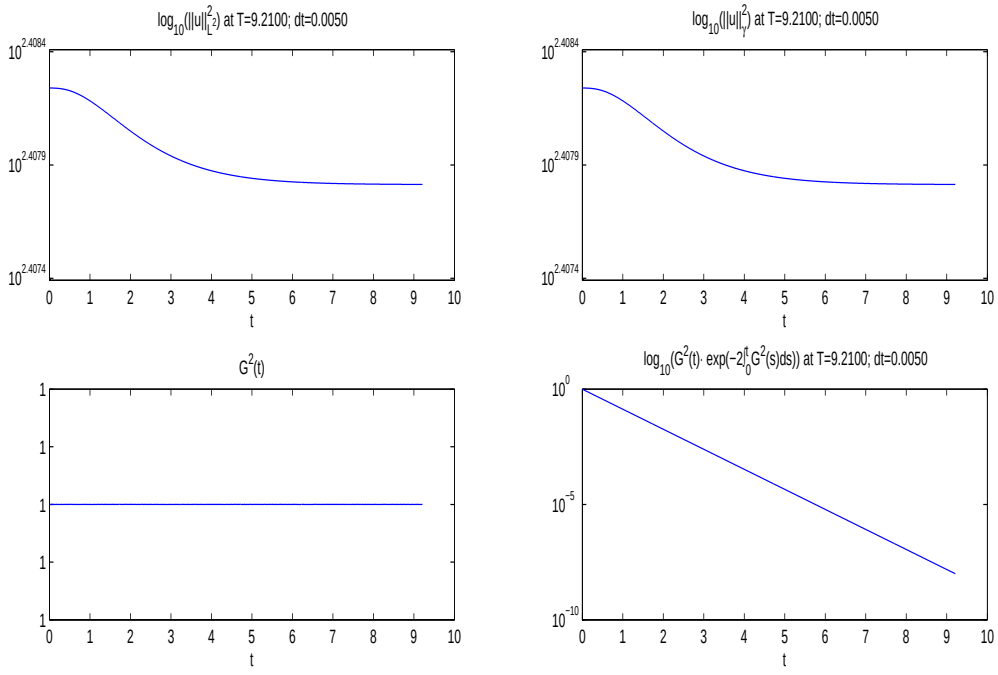

Figure 34: Euler-Explicite, $u_0(x) = S3$, $\gamma_k = 1, \forall k$, $f(x) = \sin(2\pi x/L)$

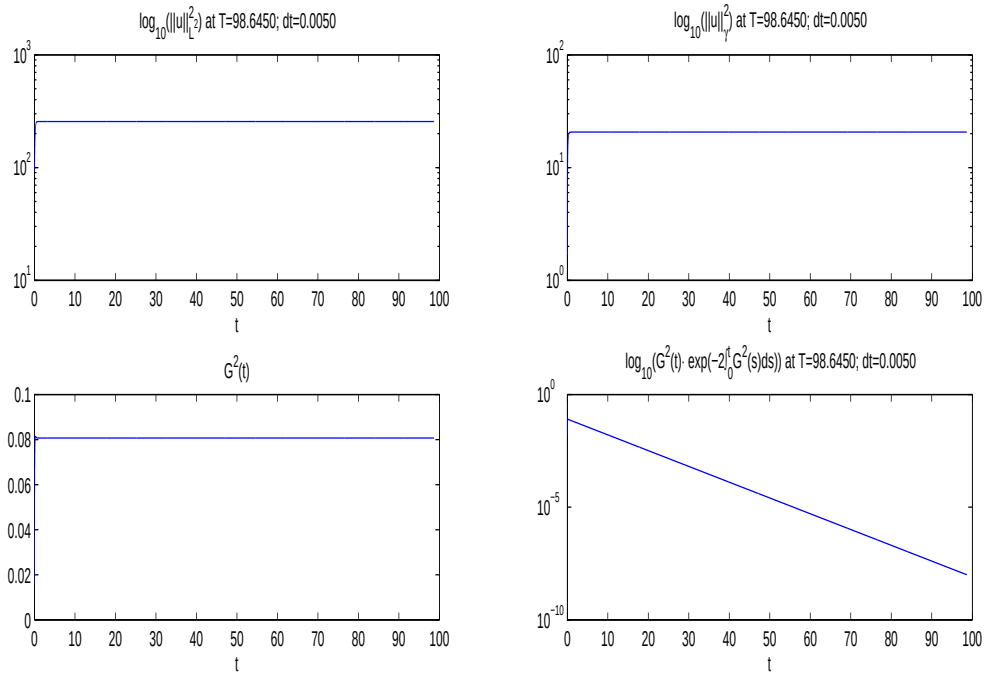

Figure 35: $u_0(x) = S1$,$\gamma_k = 1$ if $|k| \leq k_0 = N/8$ else 0, $f(x) = \sin(2\pi x/L)$

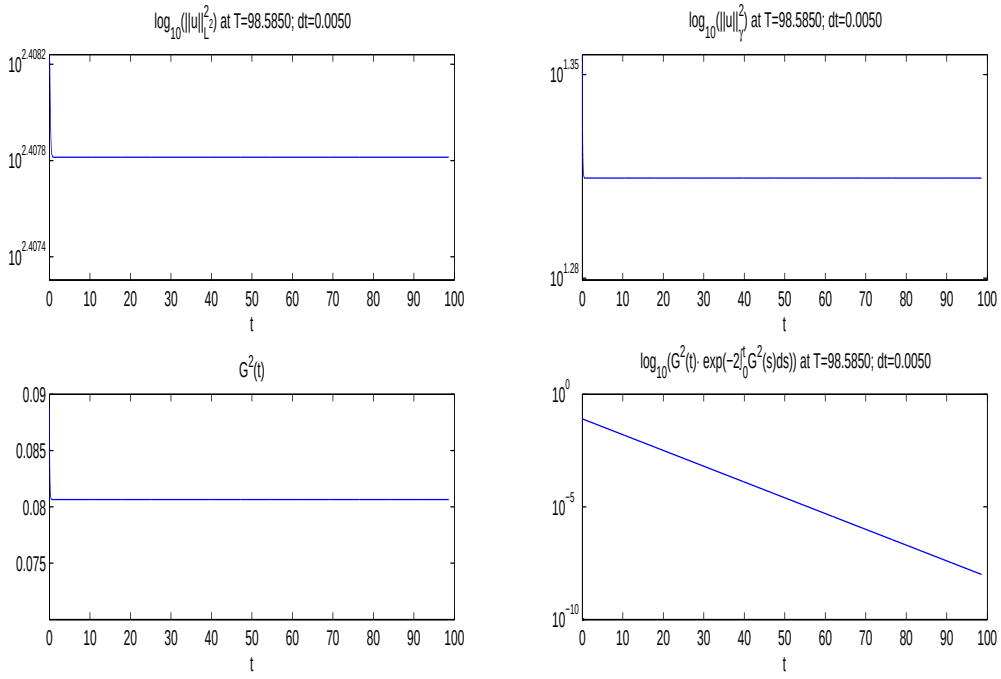

Figure 36: $u_0(x) = S3$, $\gamma_k = 1$ if $|k| \leq k_0 = N/8$ else 0, $f(x) = \sin(2\pi x/L)$

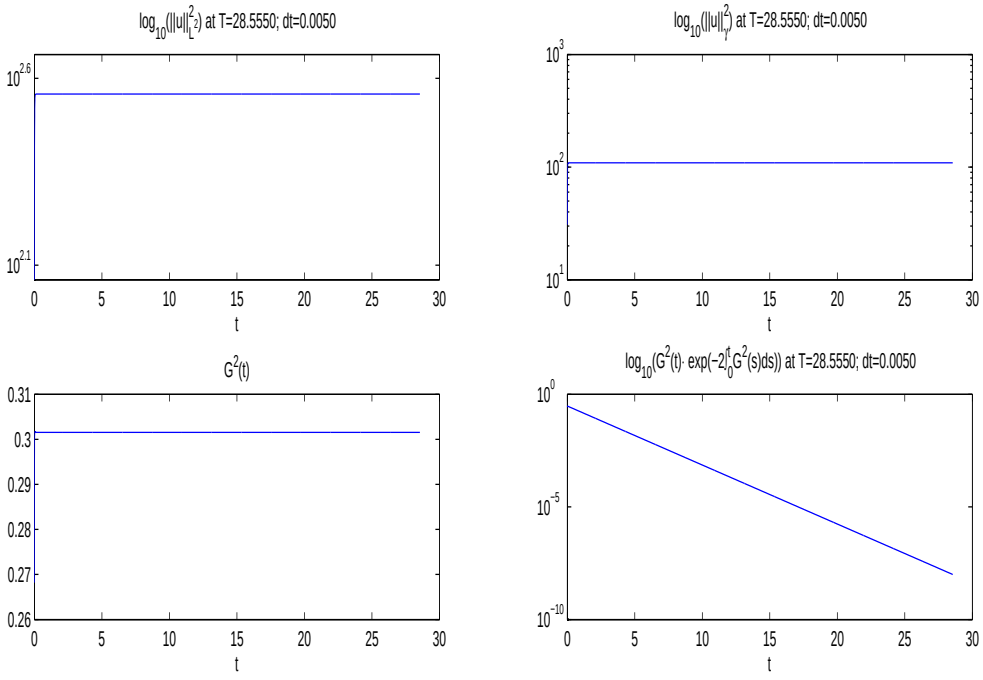

Figure 37: $u_0(x) = S1$,$\gamma_k = \frac{1}{(1+|k|)^{1/4}}$, $f(x) = \sin(2\pi x/L)$

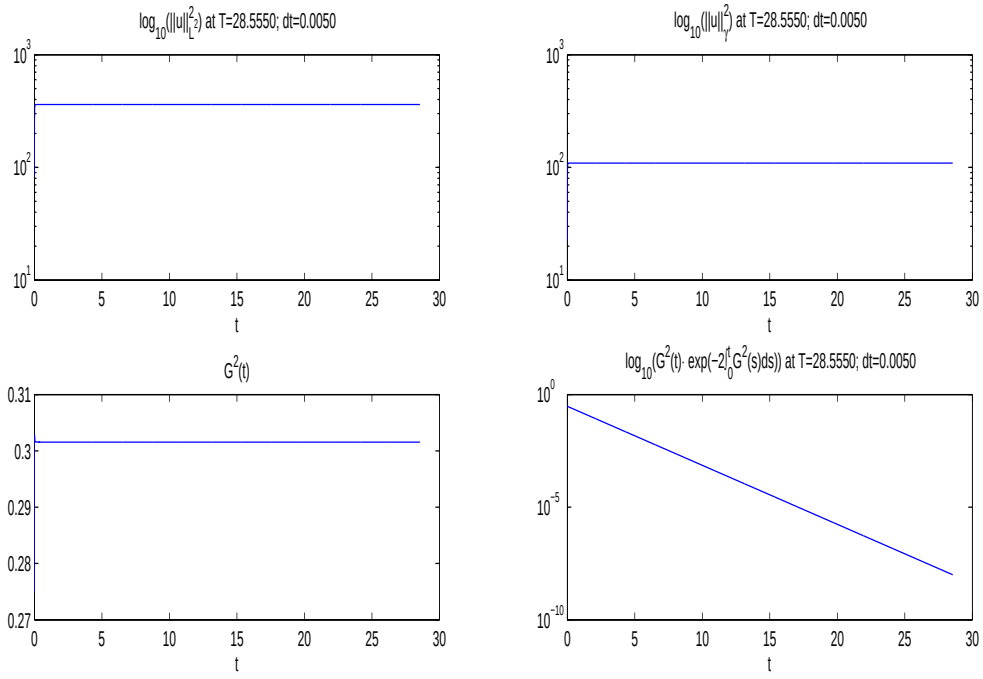

Figure 38: $u_0(x) = S2$, $\gamma_k = \frac{1}{(1+|k|)^{1/4}}$, $f(x) = \sin(2\pi x/L)$

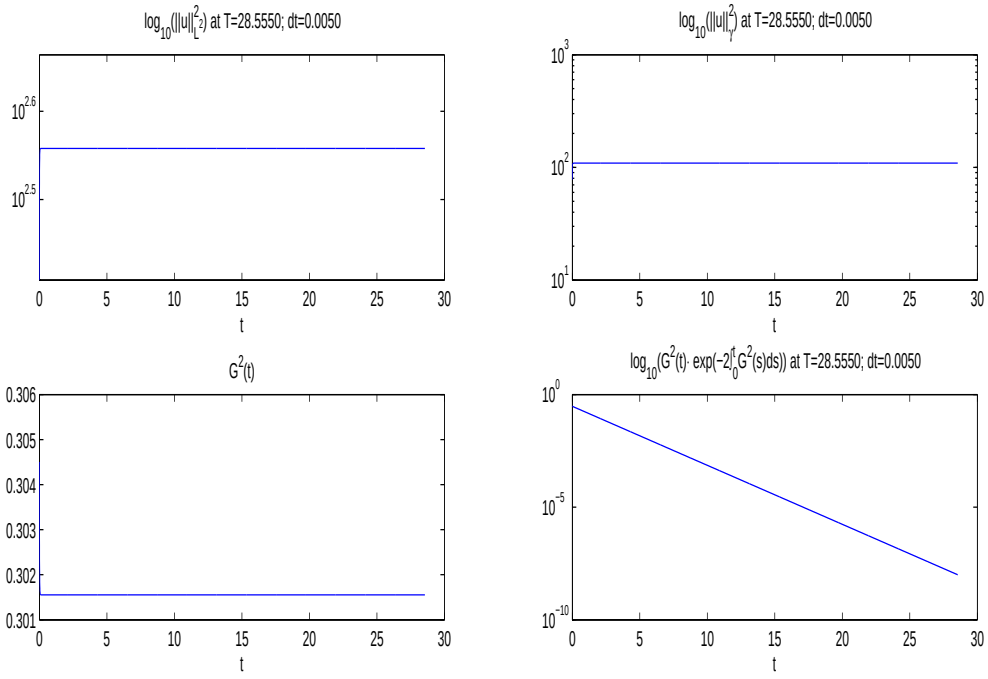

Figure 39: $u_0(x) = S3$, $\gamma_k = \frac{1}{(1+|k|)^{1/4}}$, $f(x) = \sin(2\pi x/L)$

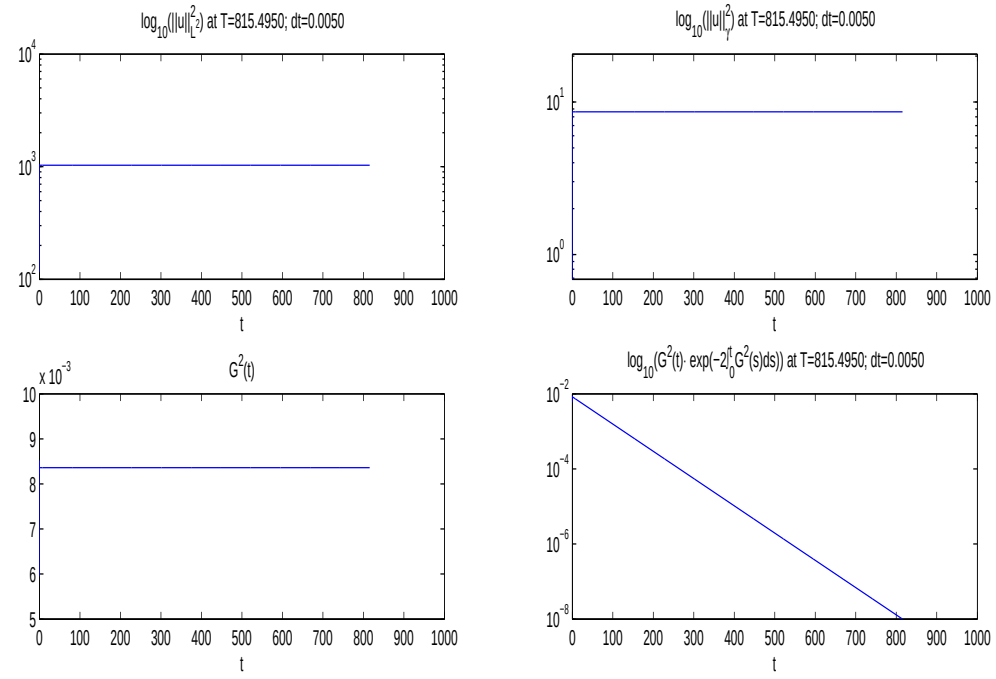

Figure 40: $u_0(x) = S1$, $\gamma_k = \frac{1}{(1+|k|)}$, $f(x) = \sin(2\pi x/L)$

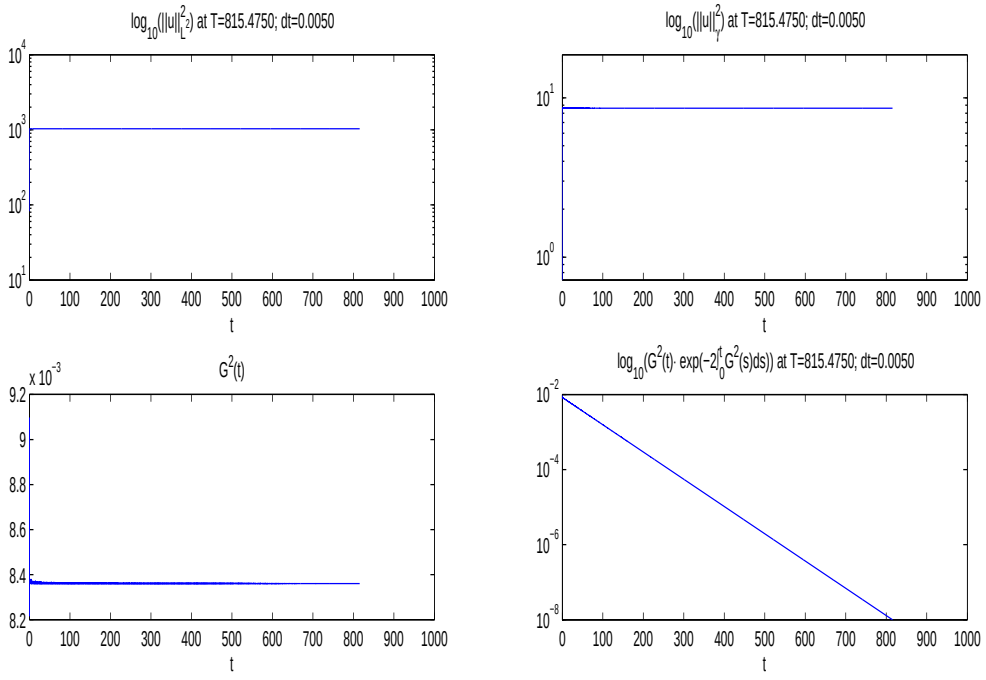

Figure 41: $u_0(x) = S2$, $\gamma_k = \frac{1}{(1+|k|)}$, $f(x) = \sin(2\pi x/L)$

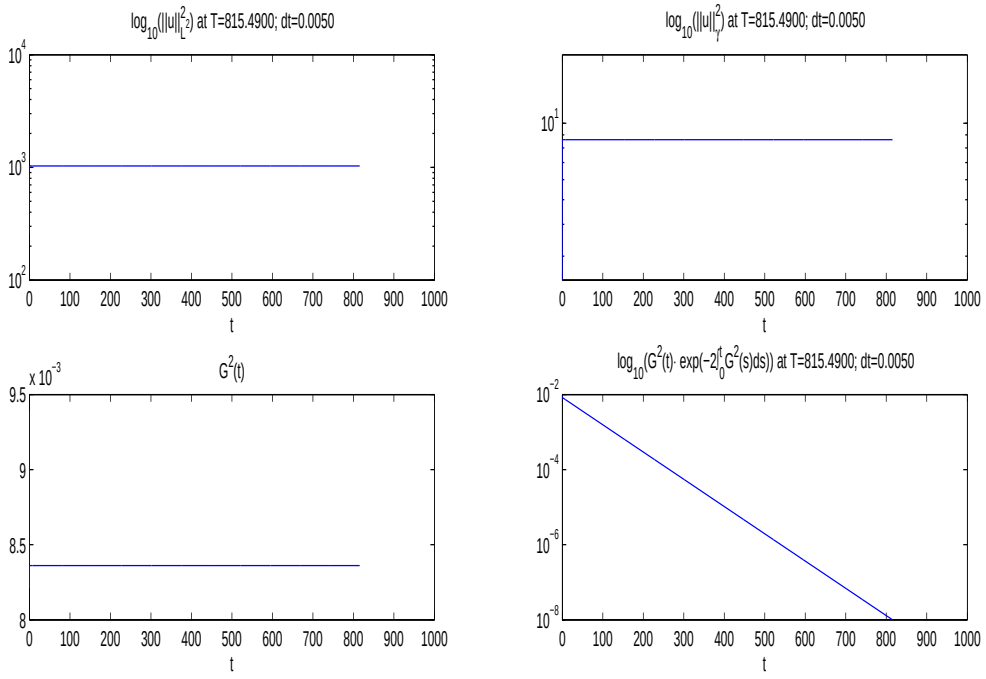

Figure 42: $u_0(x) = S3$, $\gamma_k = \frac{1}{(1+|k|)}$, $f(x) = \sin(2\pi x/L)$

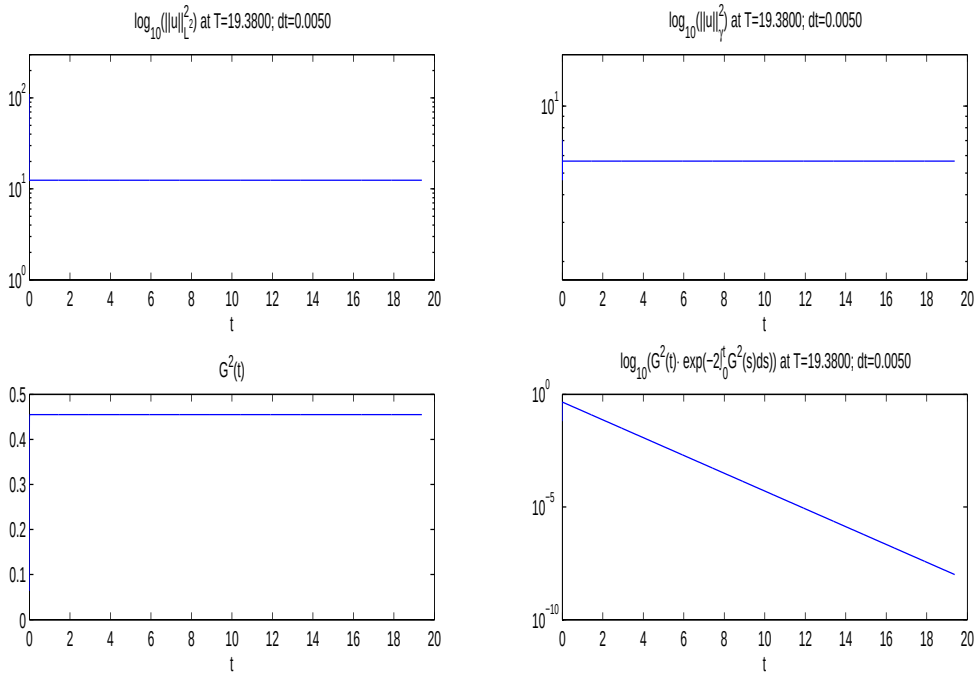

Figure 43: $u_0(x) = S1$,$\gamma_k = abs(fft(exp(-(k-L/2)^2/\sigma)), \sigma = 1/4;\ f(x) = \sin(2\pi x/L)$

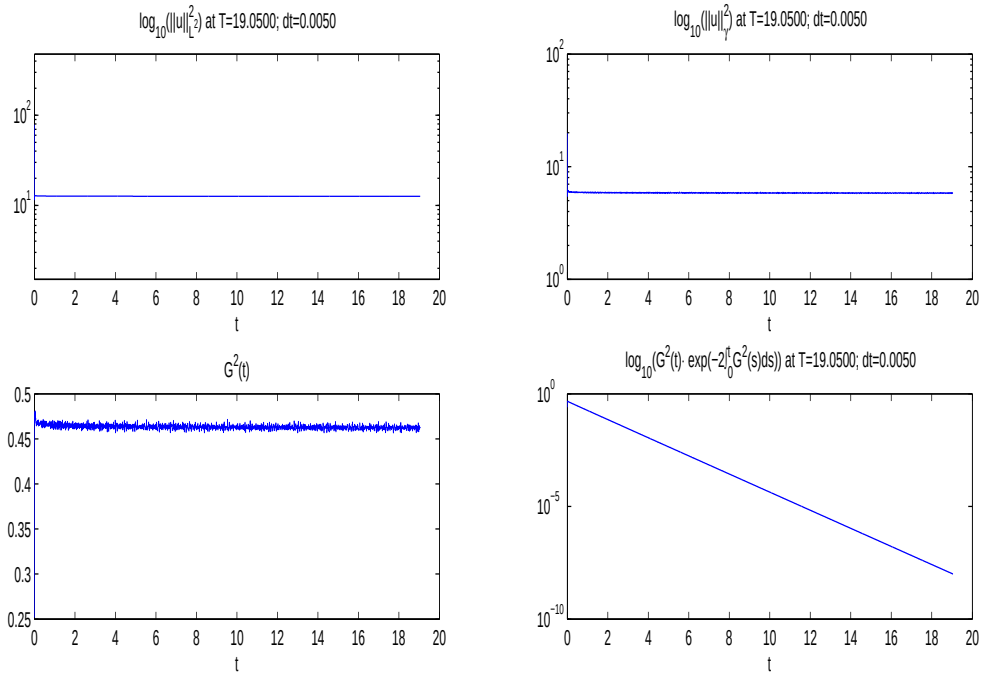

Figure 44: $u_0(x) = S2$,$\gamma_k = abs(fft(exp(-(k-L/2)^2/\sigma)), \sigma = 1/4;\ f(x) = \sin(2\pi x/L)$

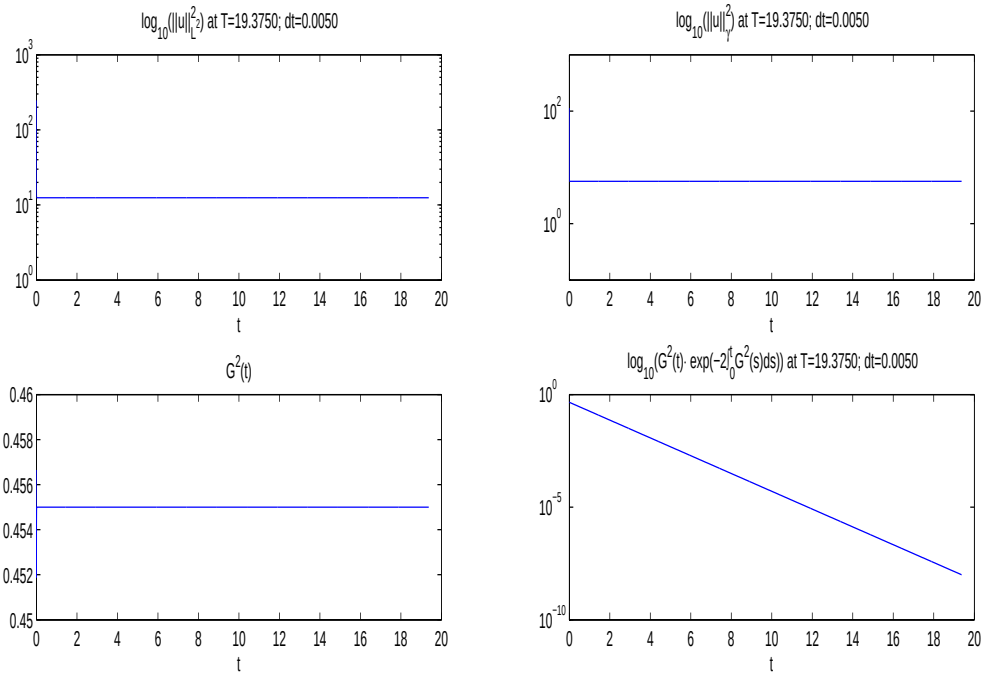

Figure 45: $u_0(x) = S3$, $\gamma_k = abs(fft(exp(-(k-L/2)^2/\sigma)), \sigma = 1/4;\ f(x) = \sin(2\pi x/L)$

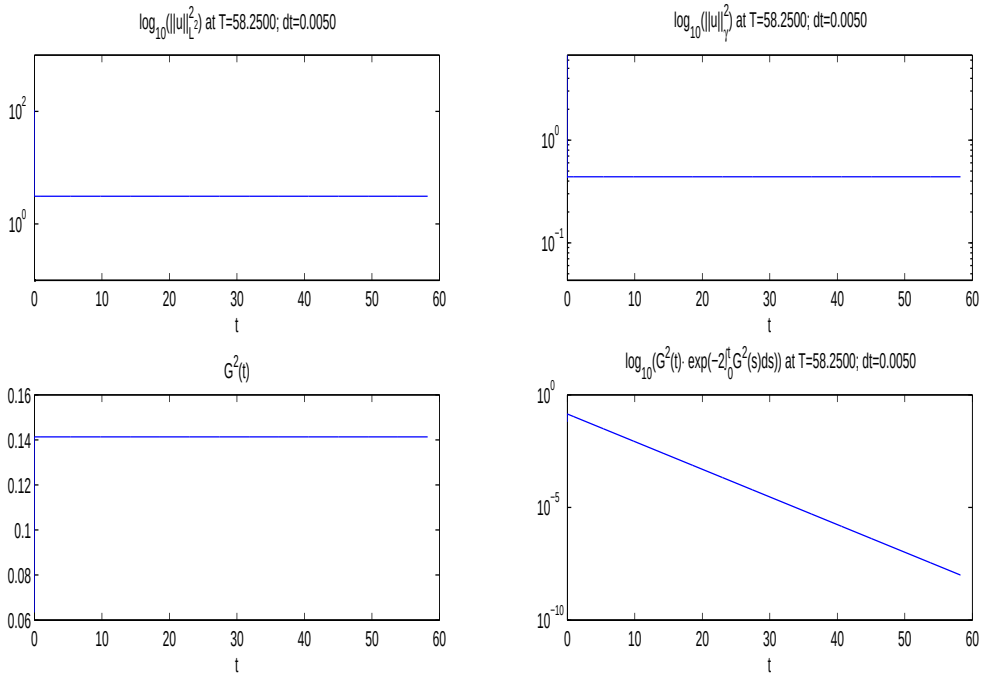

Figure 46: $u_0(x) = S1$,$\gamma_k = abs(fft(exp(-(k-L/2)^2/\sigma)), \sigma = 1/4;\ f(x) = \sin(2\pi x/L)$

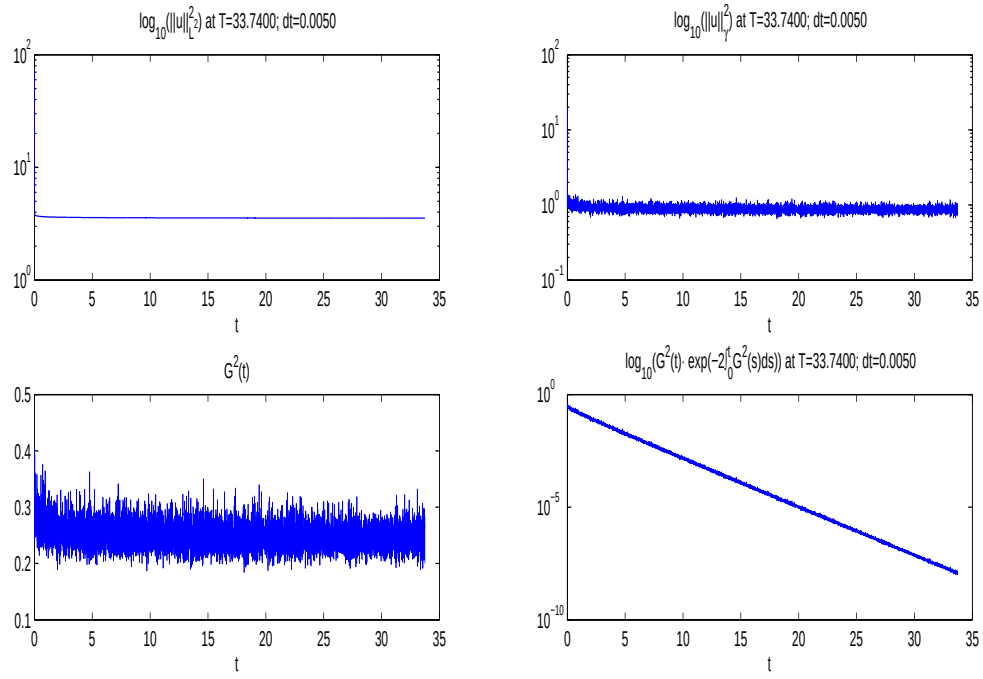

Figure 47: $u_0(x) = S2$,$\gamma_k = abs(fft(exp(-(k-L/2)^2/\sigma)), \sigma = 1;\ f(x) = \sin(2\pi x/L)$

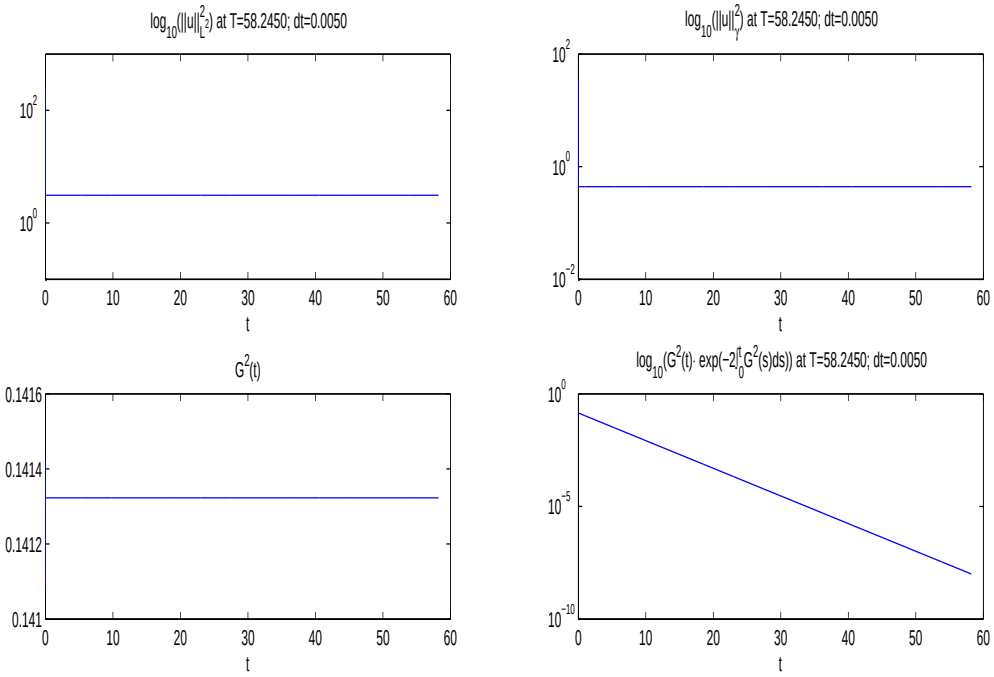

Figure 48: $u_0(x) = S3$, $\gamma_k = abs(fft(exp(-(k-L/2)^2/\sigma)), \sigma = 1;\ f(x) = \sin(2\pi x/L)$

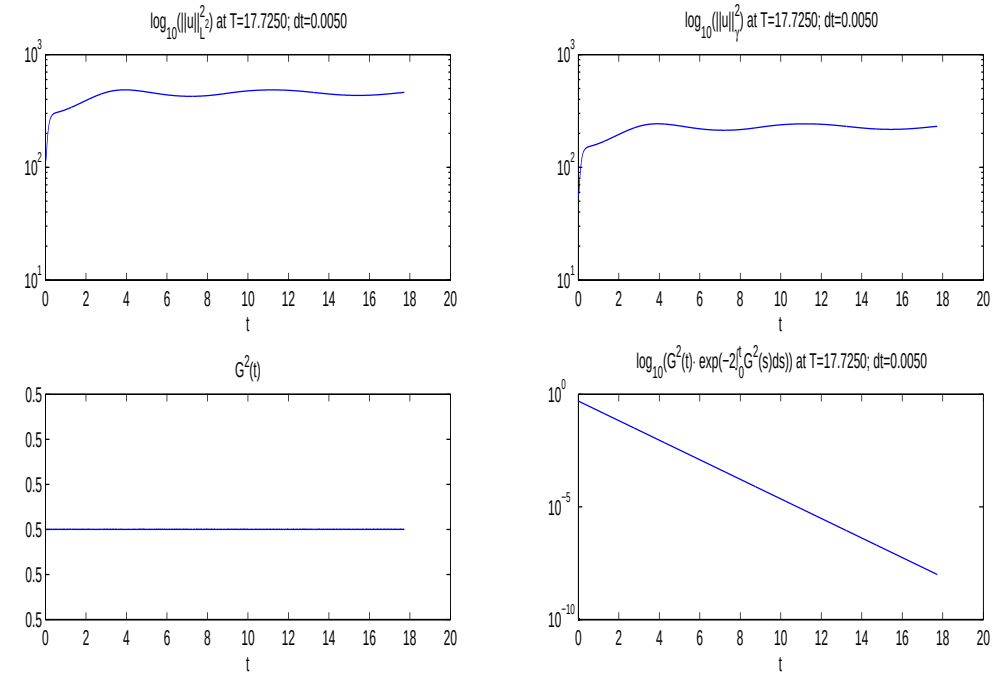

Figure 49: $u_0(x) = S1$,$\gamma_k = 1$ if k is even , 0 if k is odd; $f(x) = \sin(2\pi x/L)$

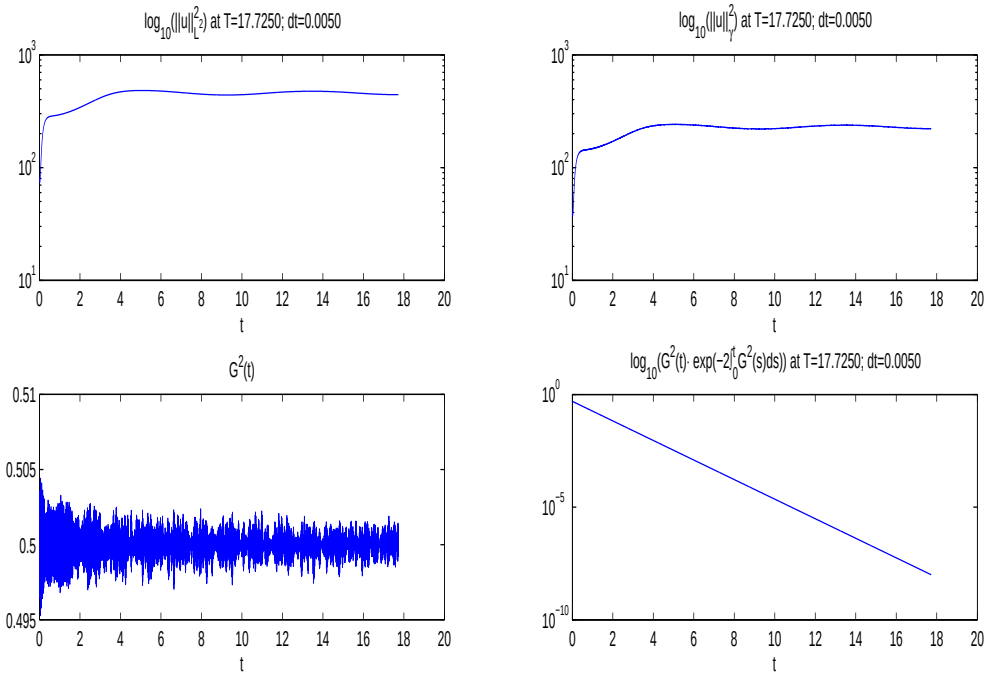

Figure 50: $u_0(x) = S2$,$\gamma_k = 1$ if k is even , 0 if k is odd; $f(x) = \sin(2\pi x/L)$

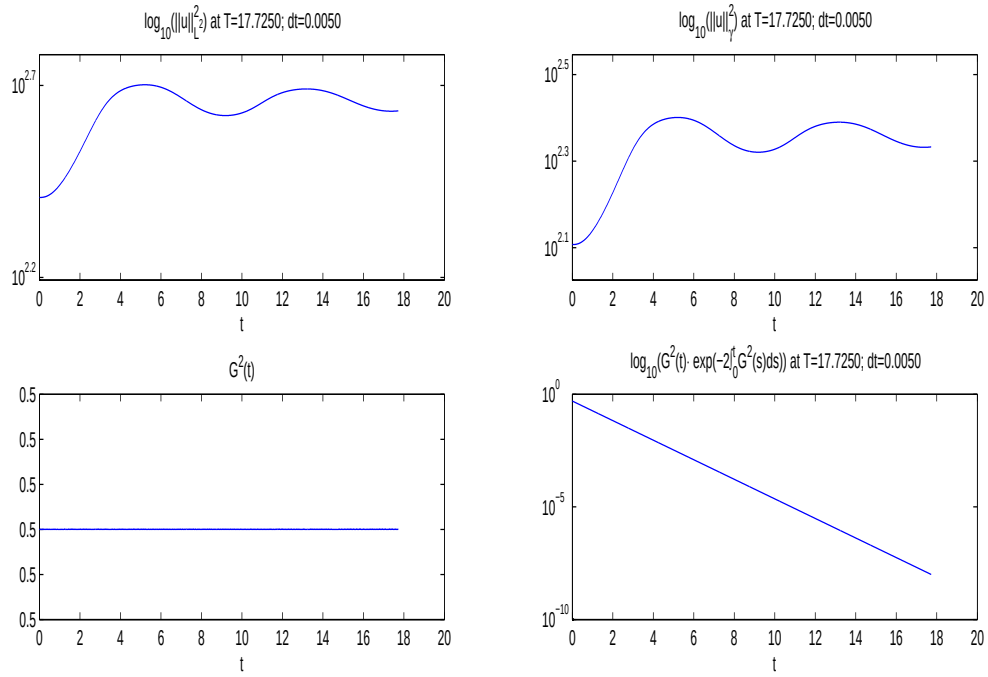

Figure 51: $u_0(x) = S3$, $\gamma_k = 1$ if k is even , 0 if k is odd; $f(x) = \sin(2\pi x/L)$

4.4 Steady state Solutions

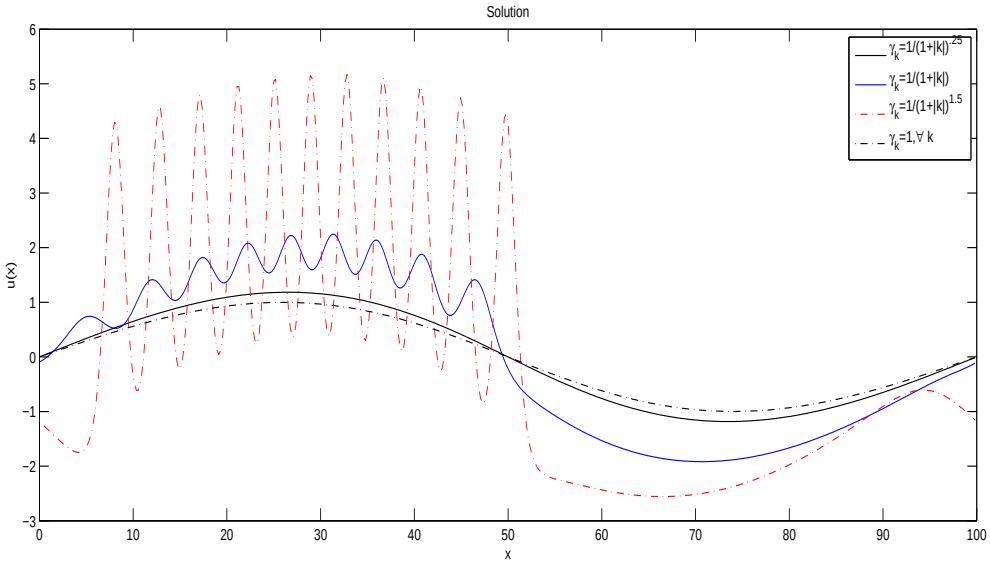

Figure 52: Computed steady states with different γ_k, $u_0(x) = S3$, $f(x) = \sin(2\pi x/L)$

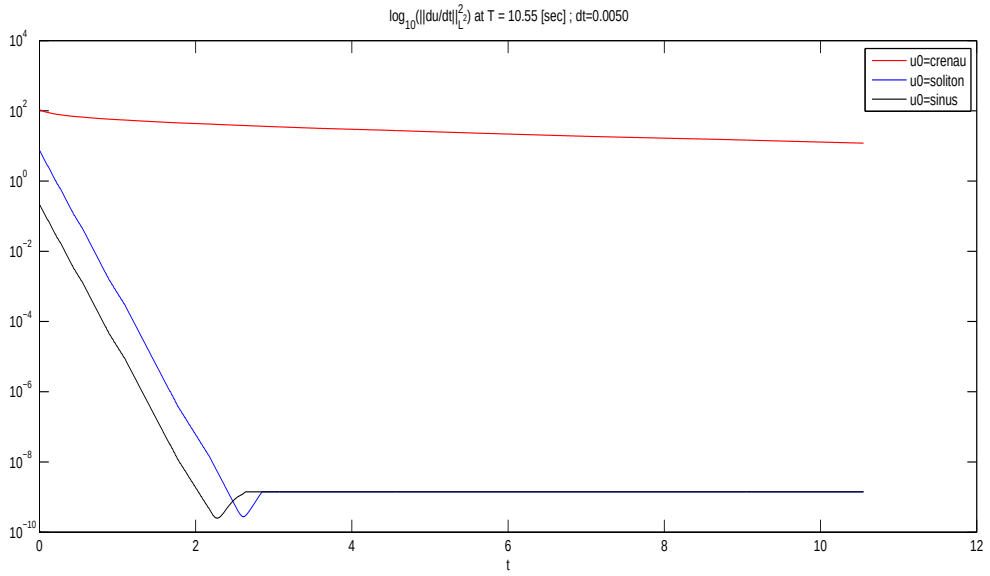

Figure 53: Computed steady states for $\gamma_k = 1, \forall k$, $f(x) = \sin(2\pi x/L)$, various $u_0(x)$: evolution of $\|\frac{du}{dt}\|^2_{L^2}$

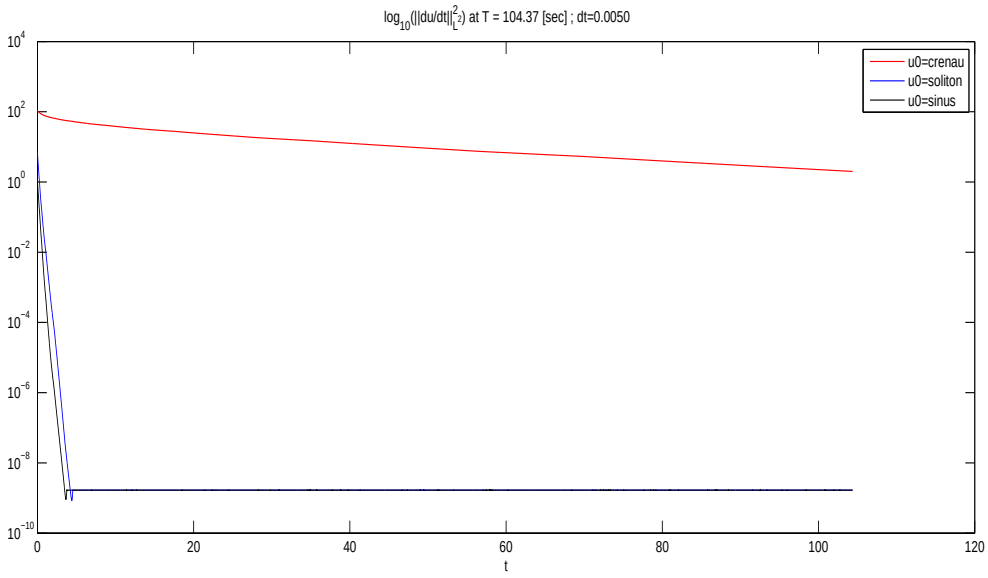

Figure 54: Computed steady states for $\gamma_k = \frac{1}{(1+|k|)^{.25}}$, $f(x) = \sin(2\pi x/L)$, various $u_0(x)$: evolution of $\|\frac{du}{dt}\|^2_{L^2}$

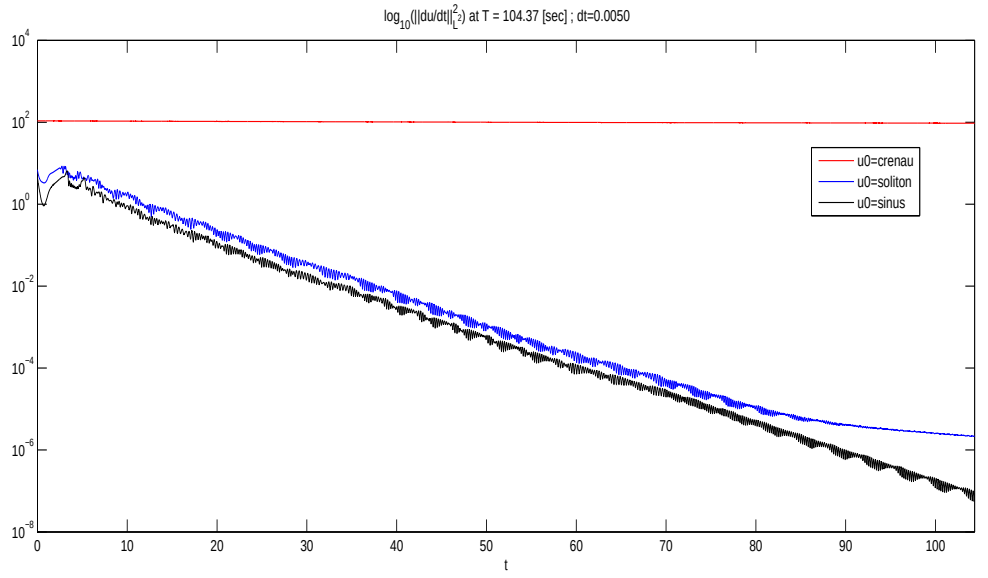

Figure 55: Computed steady states for $\gamma_k = \frac{1}{(1+|k|)^{1.5}}$, $f(x) = \sin(2\pi x/L)$, various $u_0(x)$: evolution of $\|\frac{du}{dt}\|^2_{L^2}$

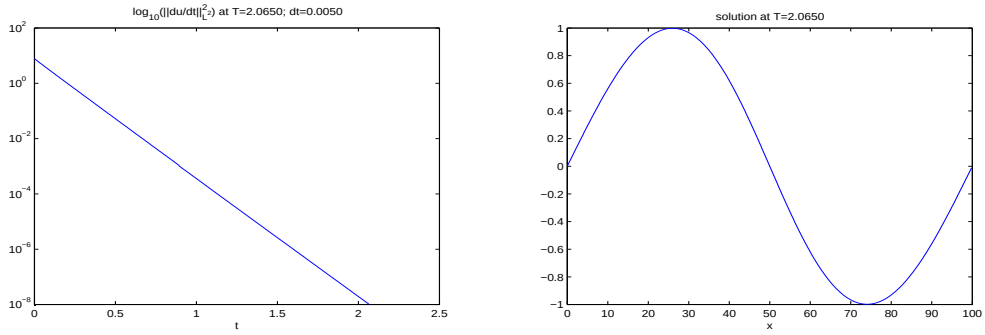

Figure 56: $u_0(x) = S1$,$\gamma_k = 1, \forall k,\ f(x) = \sin(2\pi x/L)$

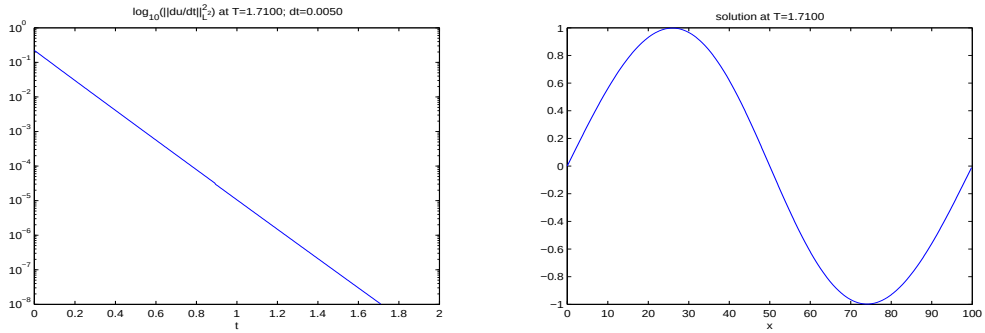

Figure 57: $u_0(x) = S3$, $\gamma_k = 1, \forall k,\ f(x) = \sin(2\pi x/L)$

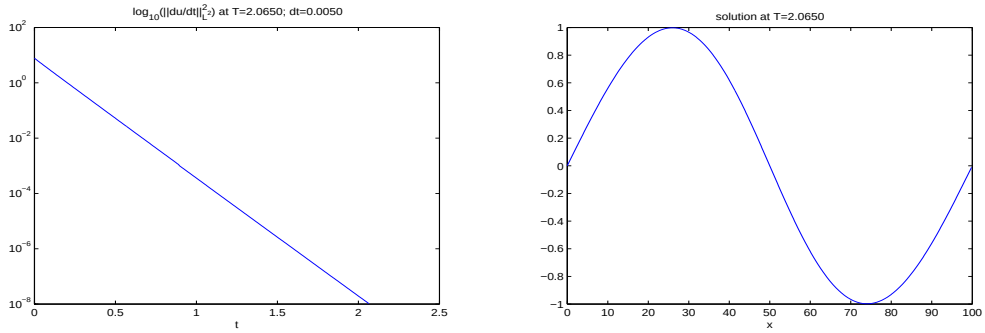

Figure 58: $u_0(x) = S1$,$\gamma_k = 1$ if $|k| \leq k_0 = N/8$ else 0, $f(x) = \sin(2\pi x/L)$

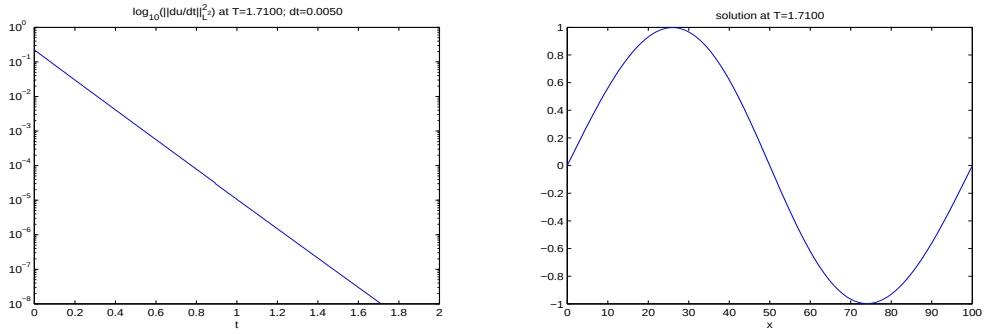

Figure 59: $u_0(x) = S3$, $\gamma_k = 1$ if $|k| \leq k_0 = N/8$ else 0, $f(x) = \sin(2\pi x/L)$

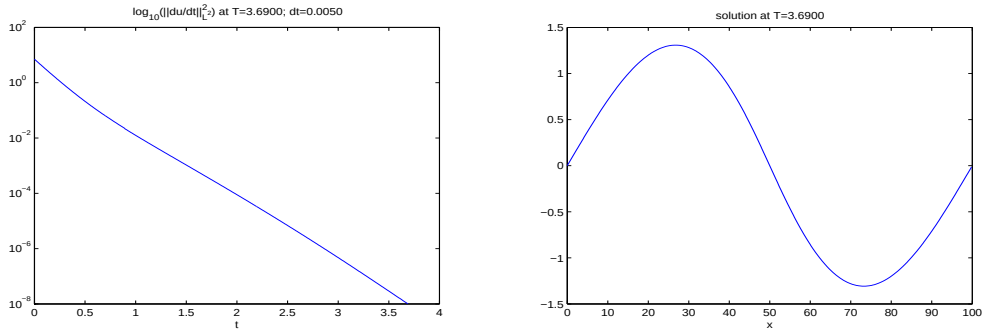

Figure 60: $u_0(x) = S1$, $\gamma_k = \frac{1}{(1+|k|)^{1/4}}$, $f(x) = \sin(2\pi x/L)$

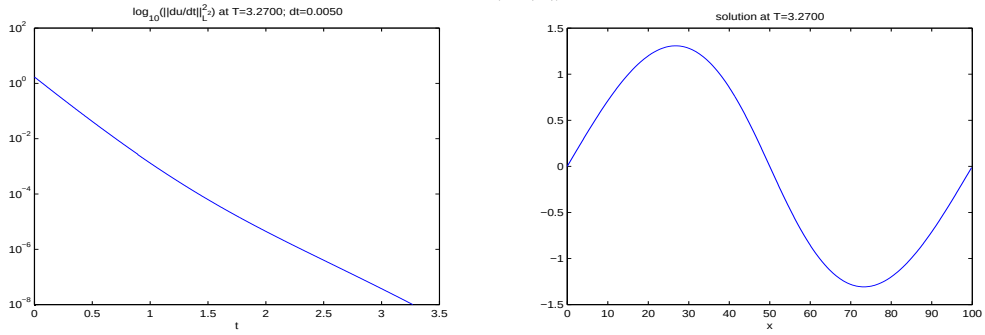

Figure 61: $u_0(x) = S3$, $\gamma_k = \frac{1}{(1+|k|)^{1/4}}$, $f(x) = \sin(2\pi x/L)$

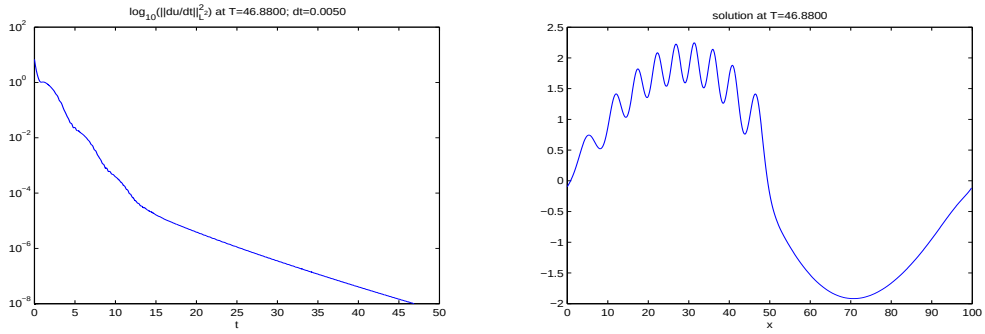

Figure 62: $u_0(x) = S1$, $\gamma_k = \frac{1}{(1+|k|)}$, $f(x) = \sin(2\pi x/L)$

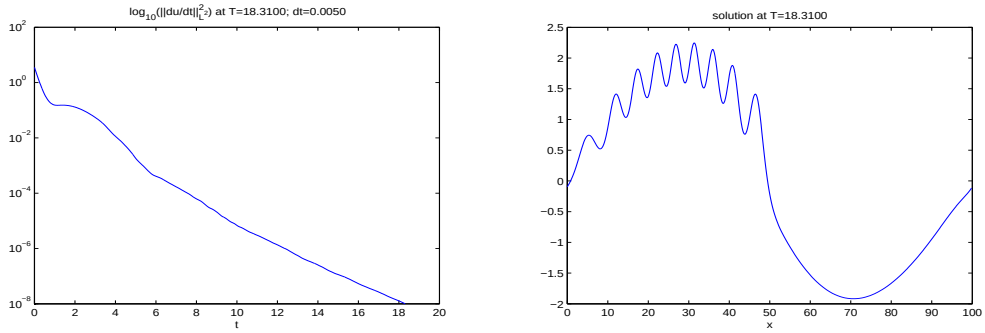

Figure 63: $u_0(x) = S3$, $\gamma_k = \frac{1}{(1+|k|)}$, $f(x) = \sin(2\pi x/L)$

4.5 Sobolev regularity

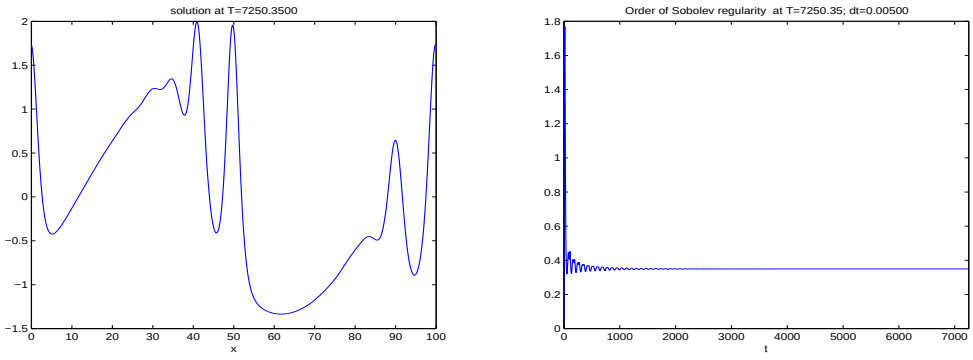

Figure 64: $\hat{u}_k(0) = 1/(1+|k|)$ if k is even, 0 if k is odd, $\gamma_k = 1$ if k is even , 0 if k is odd, $T = 35, f(x) = \sin(2\pi x/L)$

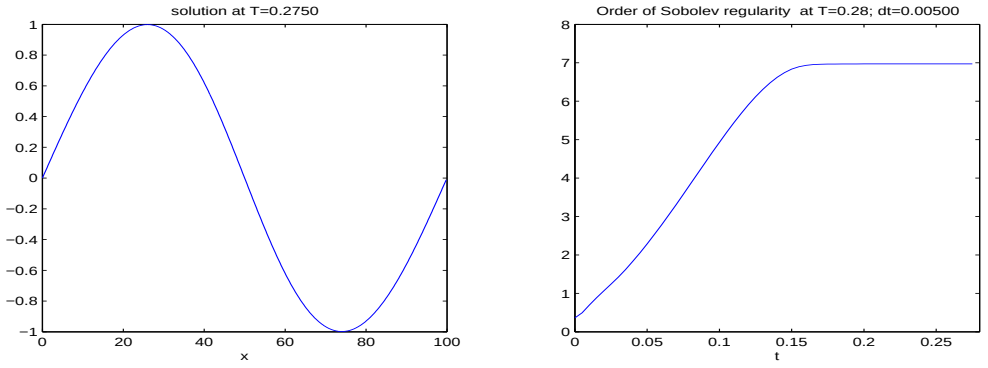

Figure 65: $u_0(x) = S1$,$\gamma_k = 1, \forall k$, $f(x) = \sin(2\pi x/L)$

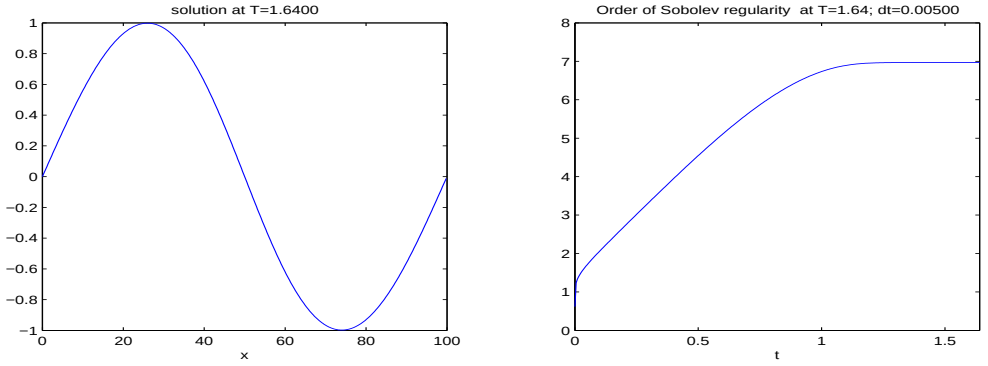

Figure 66: $u_0(x) = S2$,$\gamma_k = 1, \forall k$ $f(x) = \sin(2\pi x/L)$

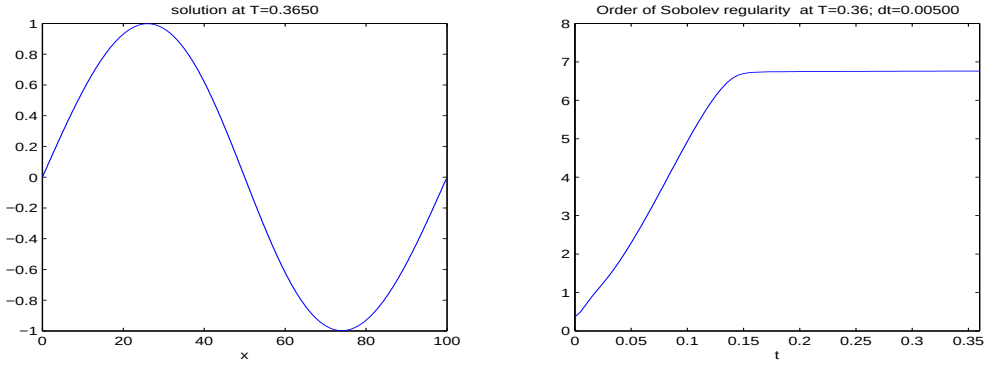

Figure 67: $u_0(x) = S1$,$\gamma_k = 1$ if $|k| \leq k_0 = N/8$ else 0, $f(x) = \sin(2\pi x/L)$

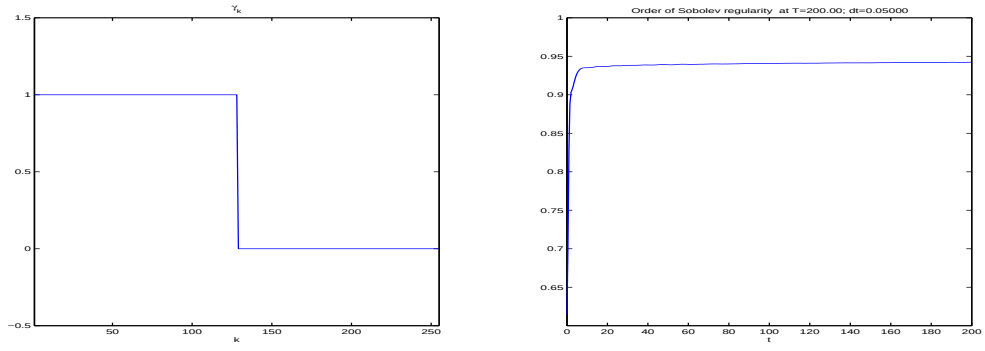

Figure 68: $u_0(x) = S2$,$\gamma_k = 1$ if $|k| \leq k_0 = N/4$ else 0, $f(x) = \sin(2\pi x/L)$

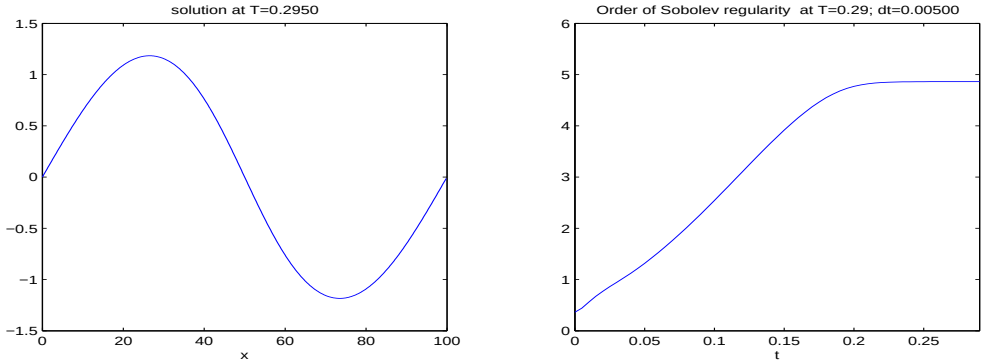

Figure 69: $u_0(x) = S1$,$\gamma_k = \frac{1}{(1+|k|)^{1/4}}$, $f(x) = \sin(2\pi x/L)$

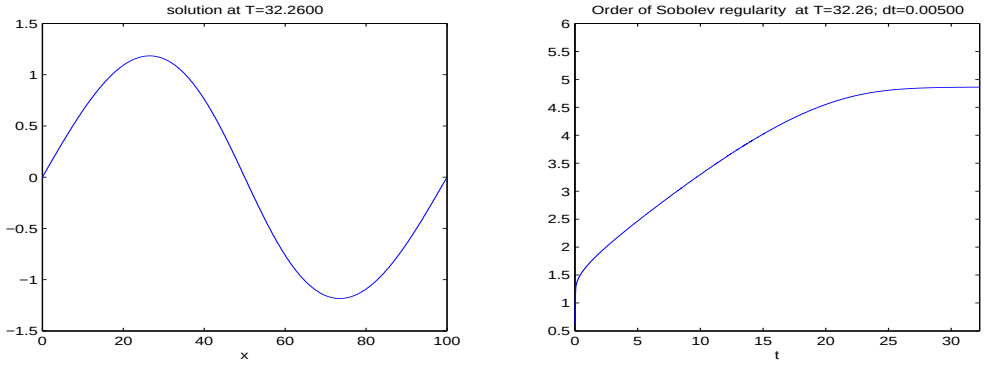

Figure 70: $u_0(x) = S2$,$\gamma_k = \frac{1}{(1+|k|)^{1/4}}$ else 0, $f(x) = \sin(2\pi x/L)$

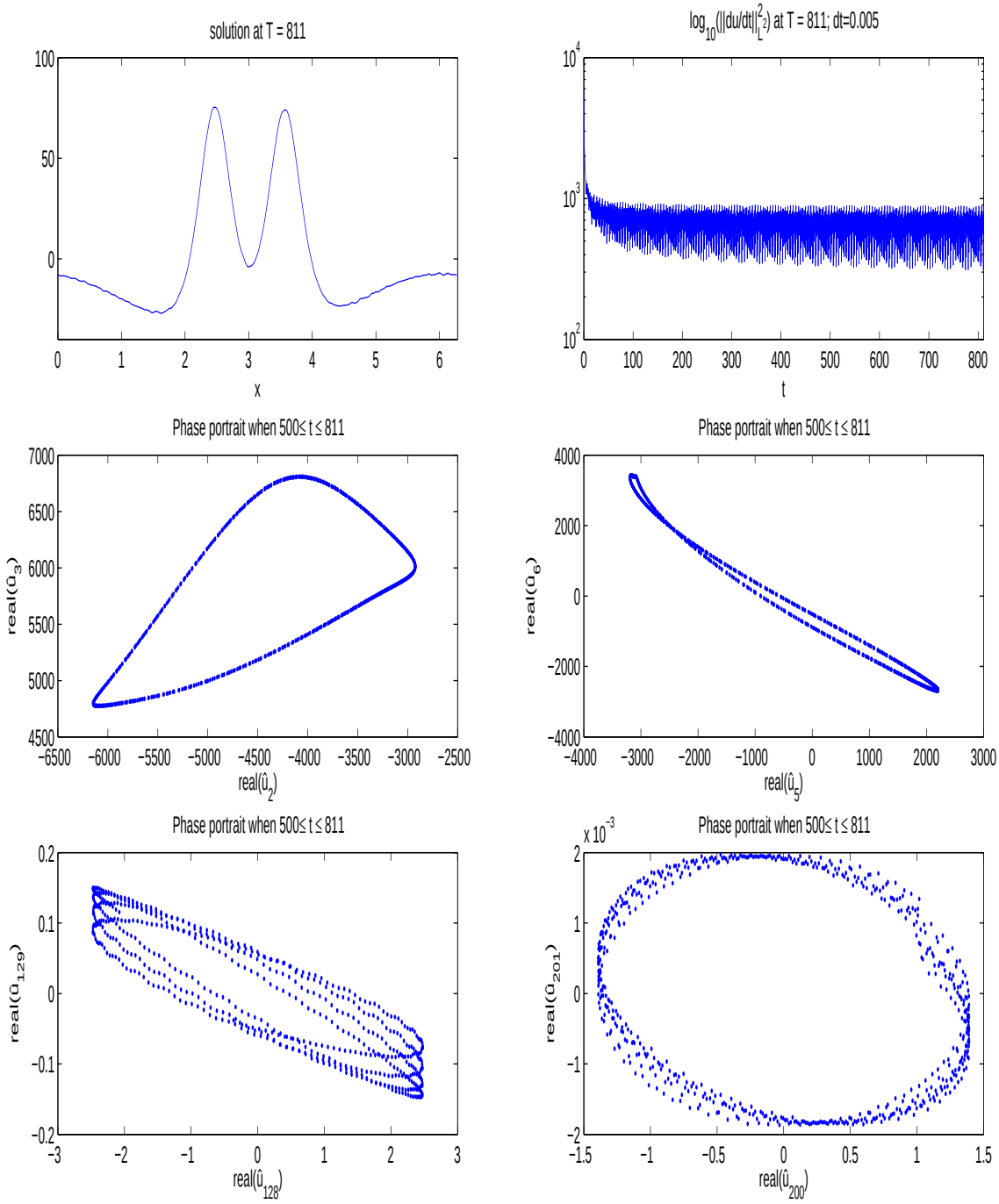

Figure 71: $u_0(x) = S4$,$\gamma_k = 2.7, \forall k,\ f(x) = \sin(2\pi x/L)$

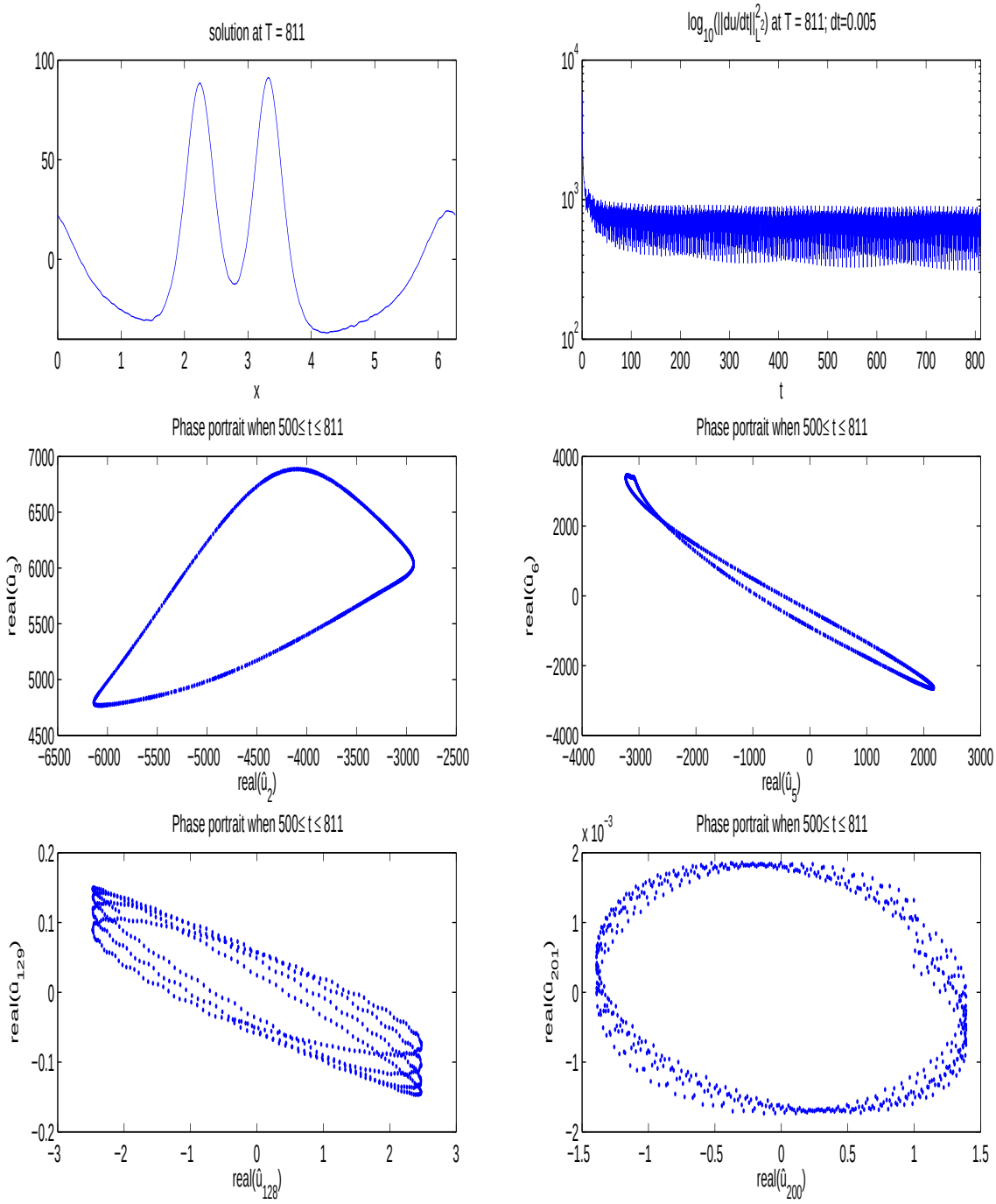

Figure 72: $u_0(x) = S4$,$\gamma_k = \dfrac{2.7}{(1+|k|)^{0.01}}$, $f(x) = \sin(2\pi x/L)$

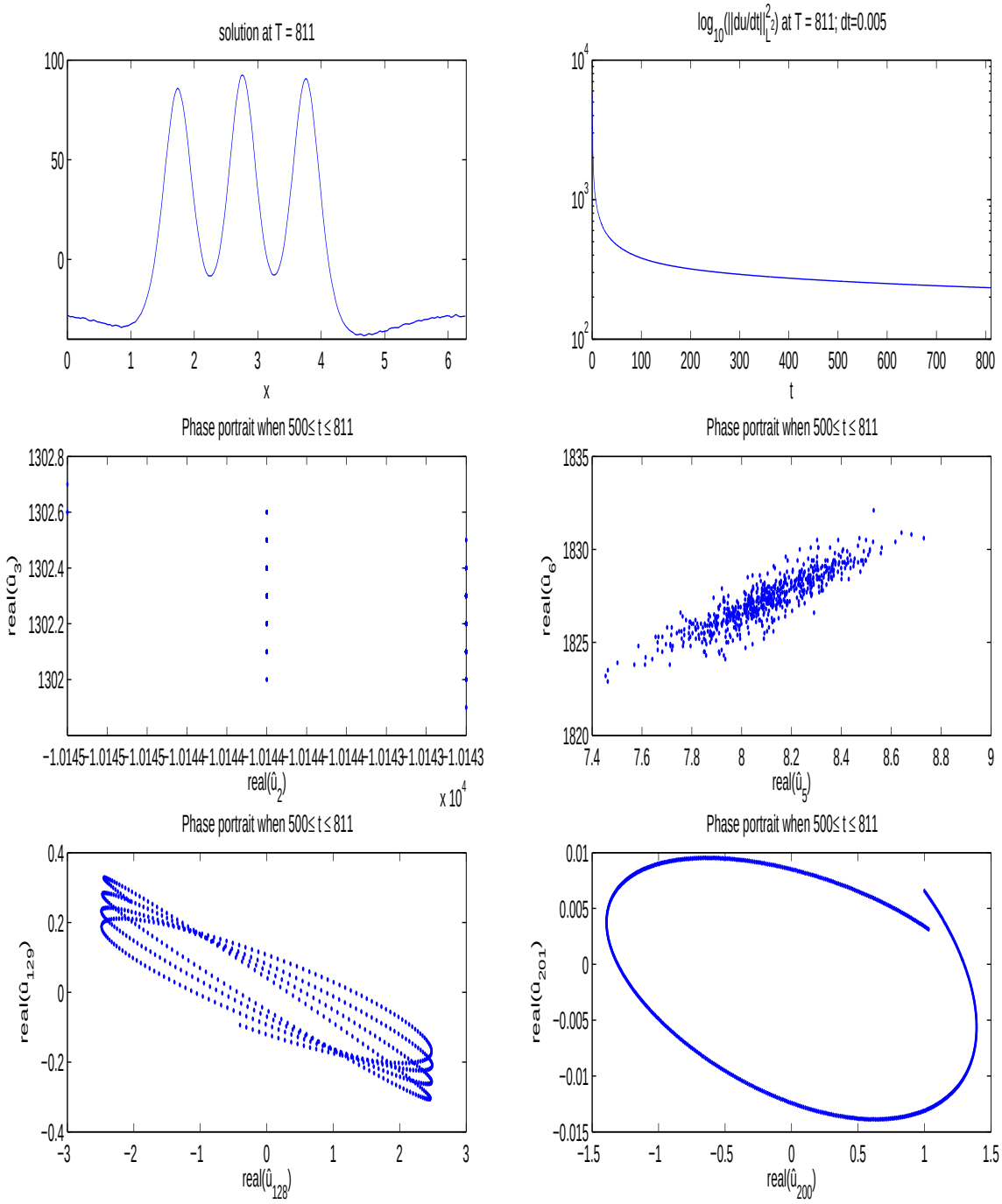

Figure 73: $u_0(x) = S4$,$\gamma_k = \dfrac{2.7}{(1+|k|)^{0.05}}$, $f(x) = \sin(2\pi x/L)$

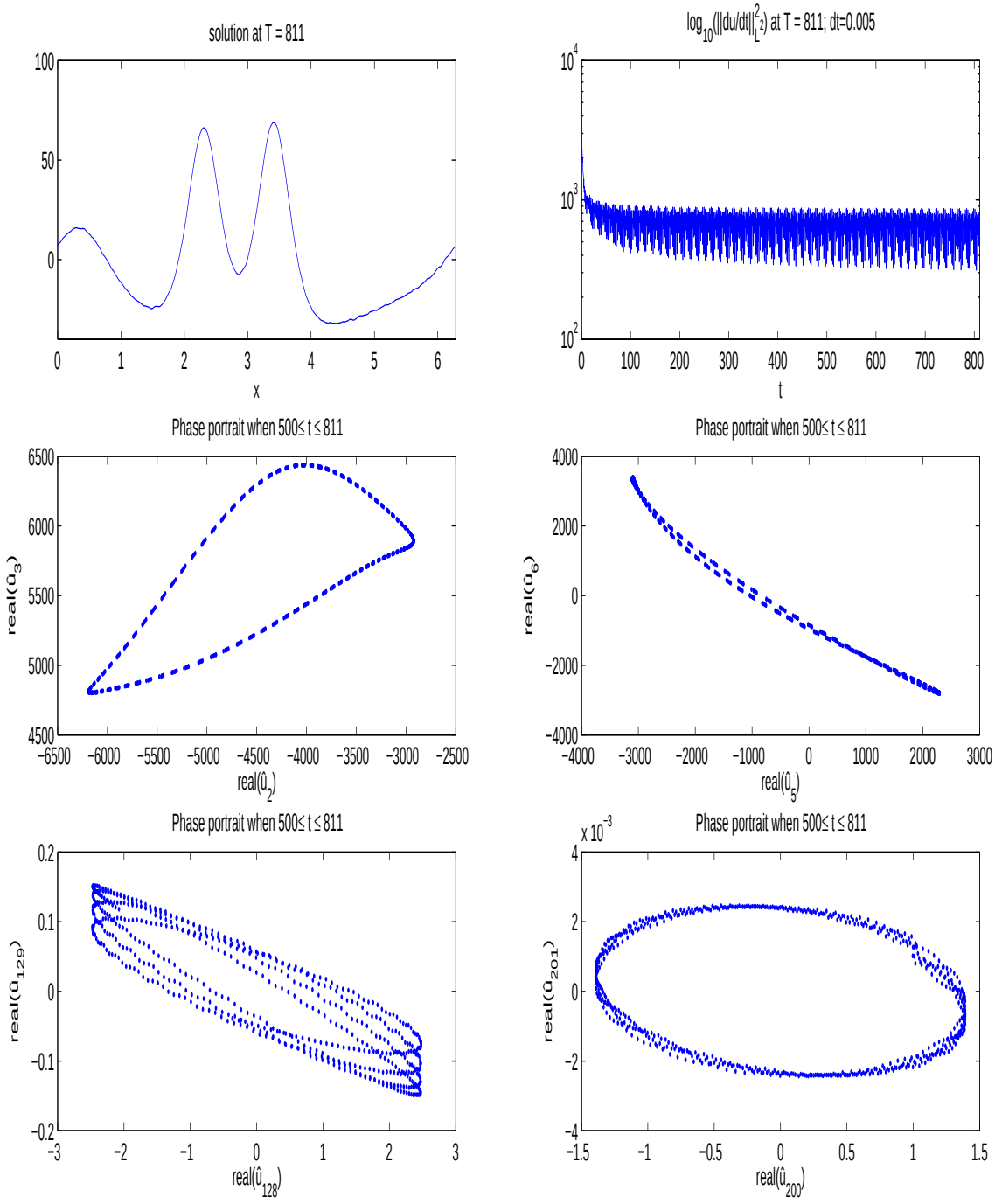

Figure 74: $u_0(x) = S4$,$\gamma_k = \dfrac{3}{(1+|k|)^{0.05}}$, $f(x) = \sin(2\pi x/L)$

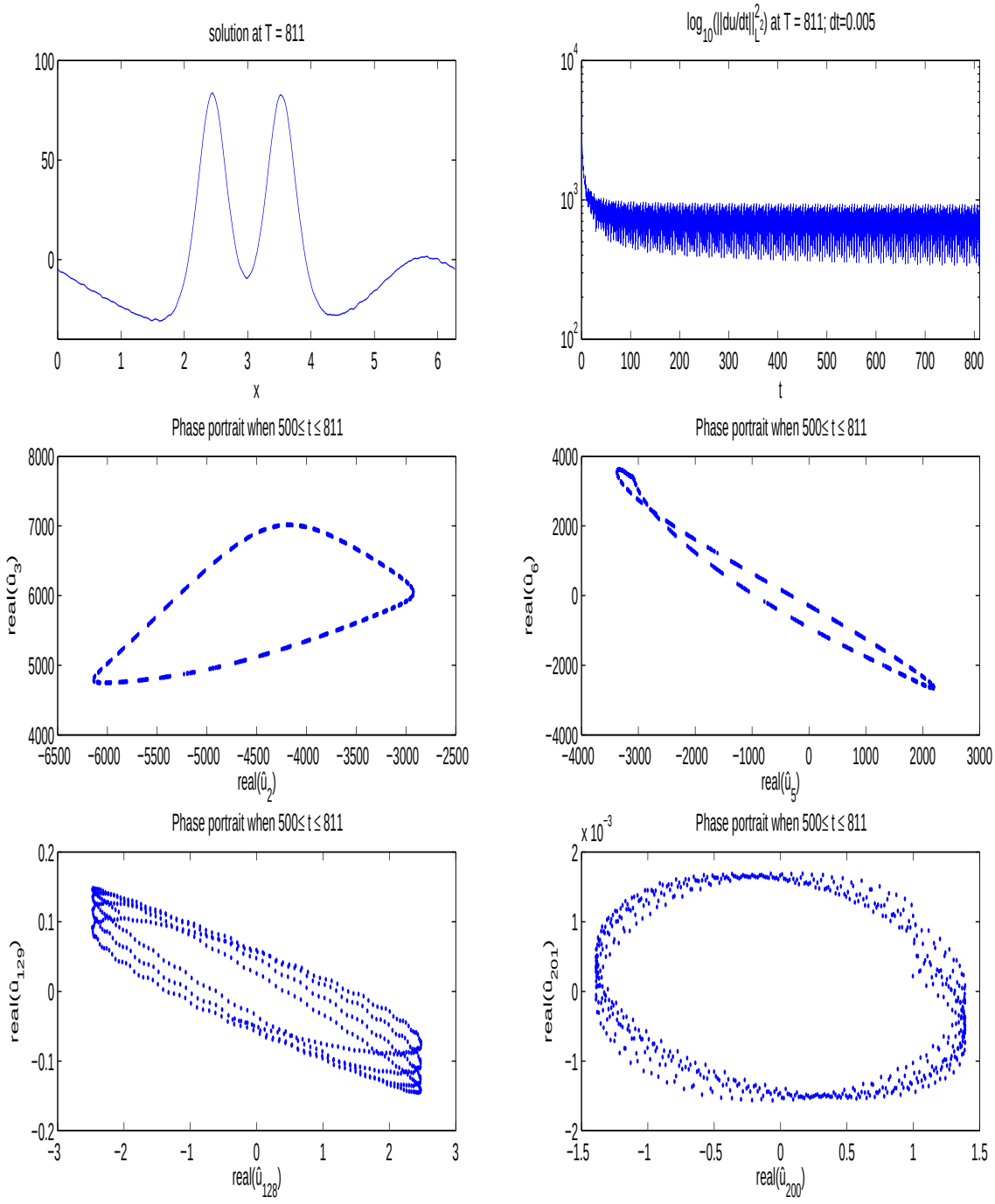

Figure 75: $u_0(x) = S4$,$\gamma_k = \dfrac{3.3}{(1+|k|)^{0.2}}$, $f(x) = \sin(2\pi x/L)$

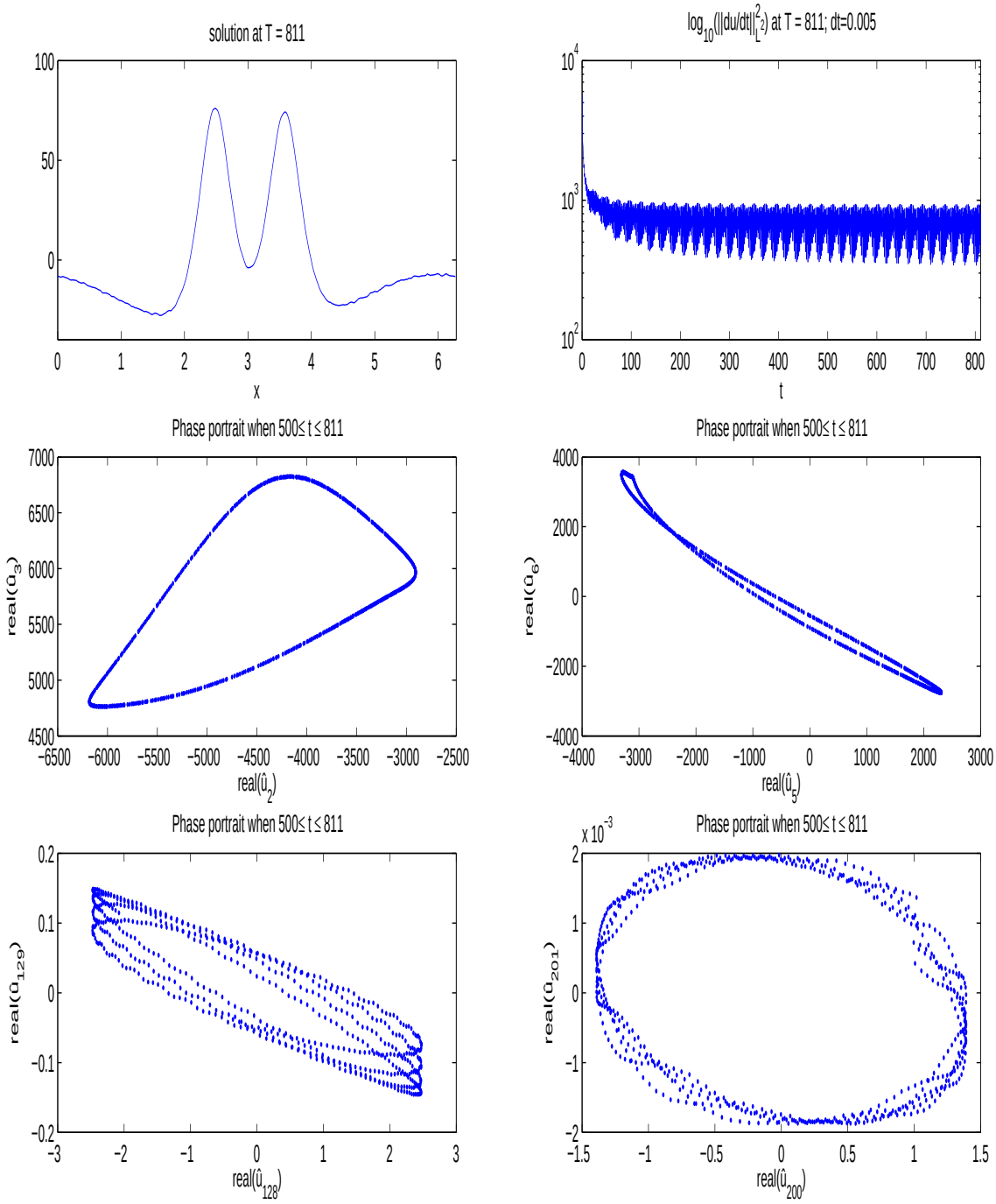

Figure 76: $u_0(x) = S4$,$\gamma_k = \dfrac{3.8}{(1+|k|)^{0.3}}$, $f(x) = \sin(2\pi x/L)$

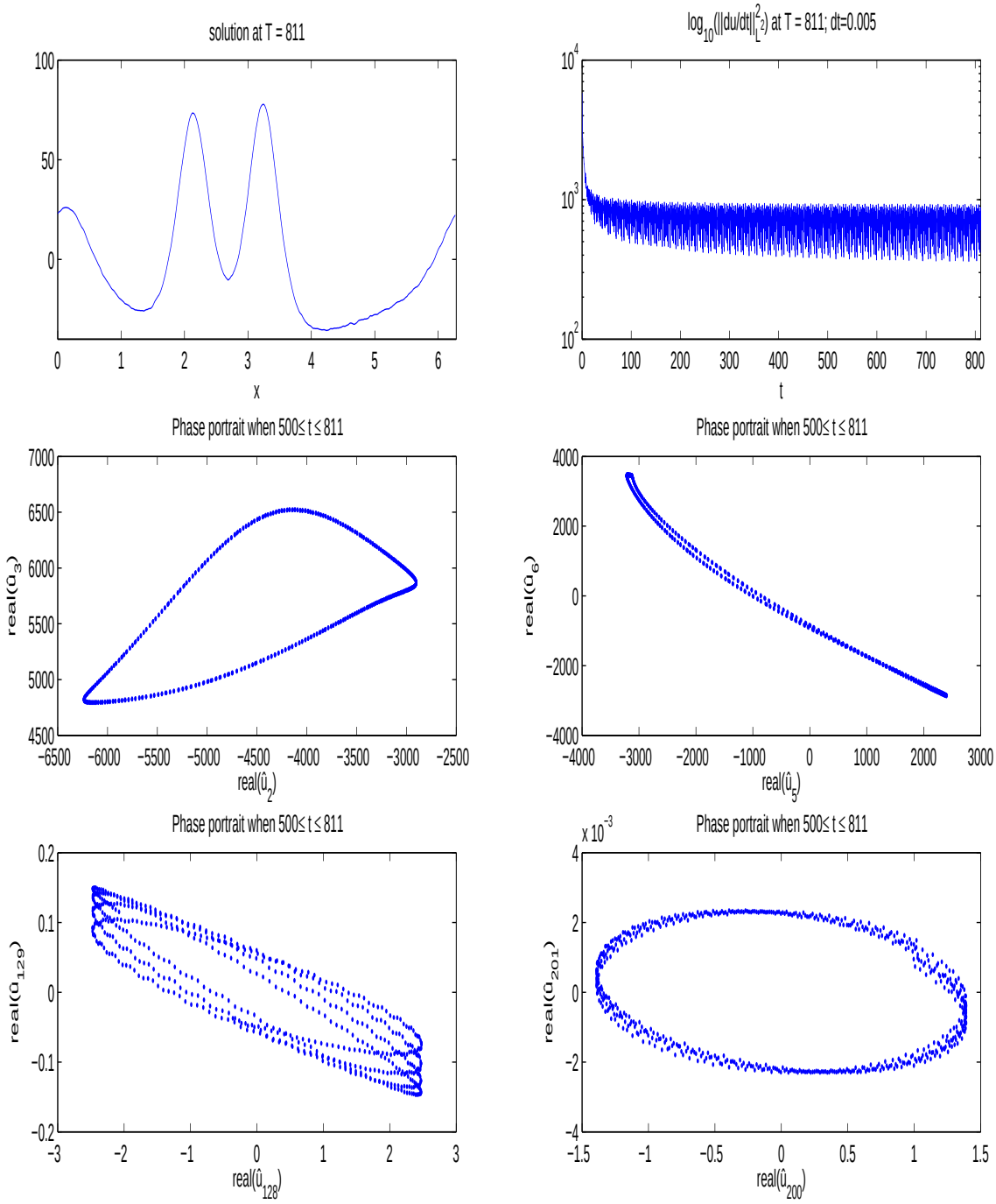

Figure 77: $u_0(x) = S4$,$\gamma_k = \dfrac{4.4}{(1+|k|)^{0.4}}$, $f(x) = \sin(2\pi x/L)$

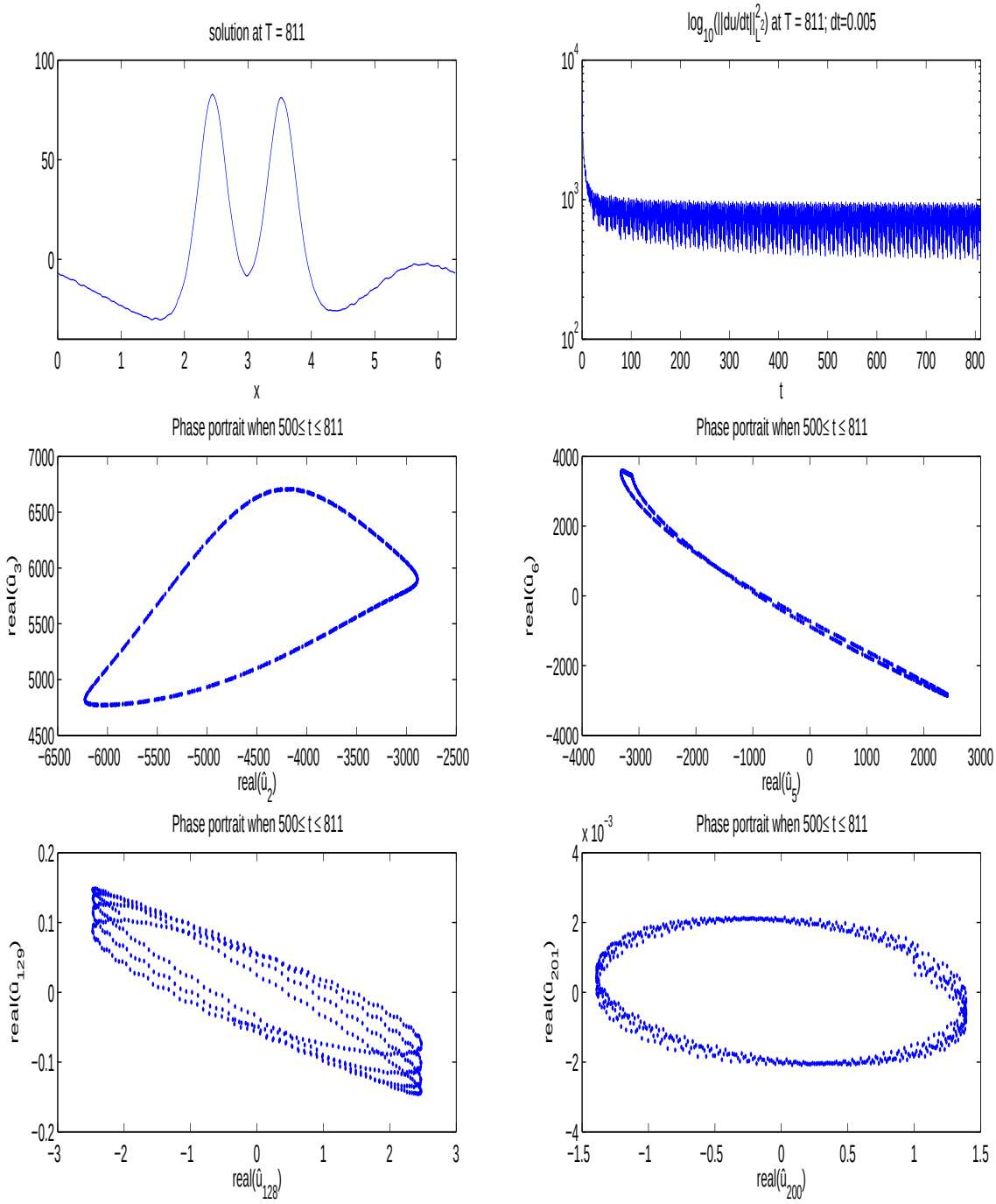

Figure 78: $u_0(x) = S4$,$\gamma_k = \dfrac{4.8}{(1+|k|)^{0.5}}$, $f(x) = \sin(2\pi x/L)$

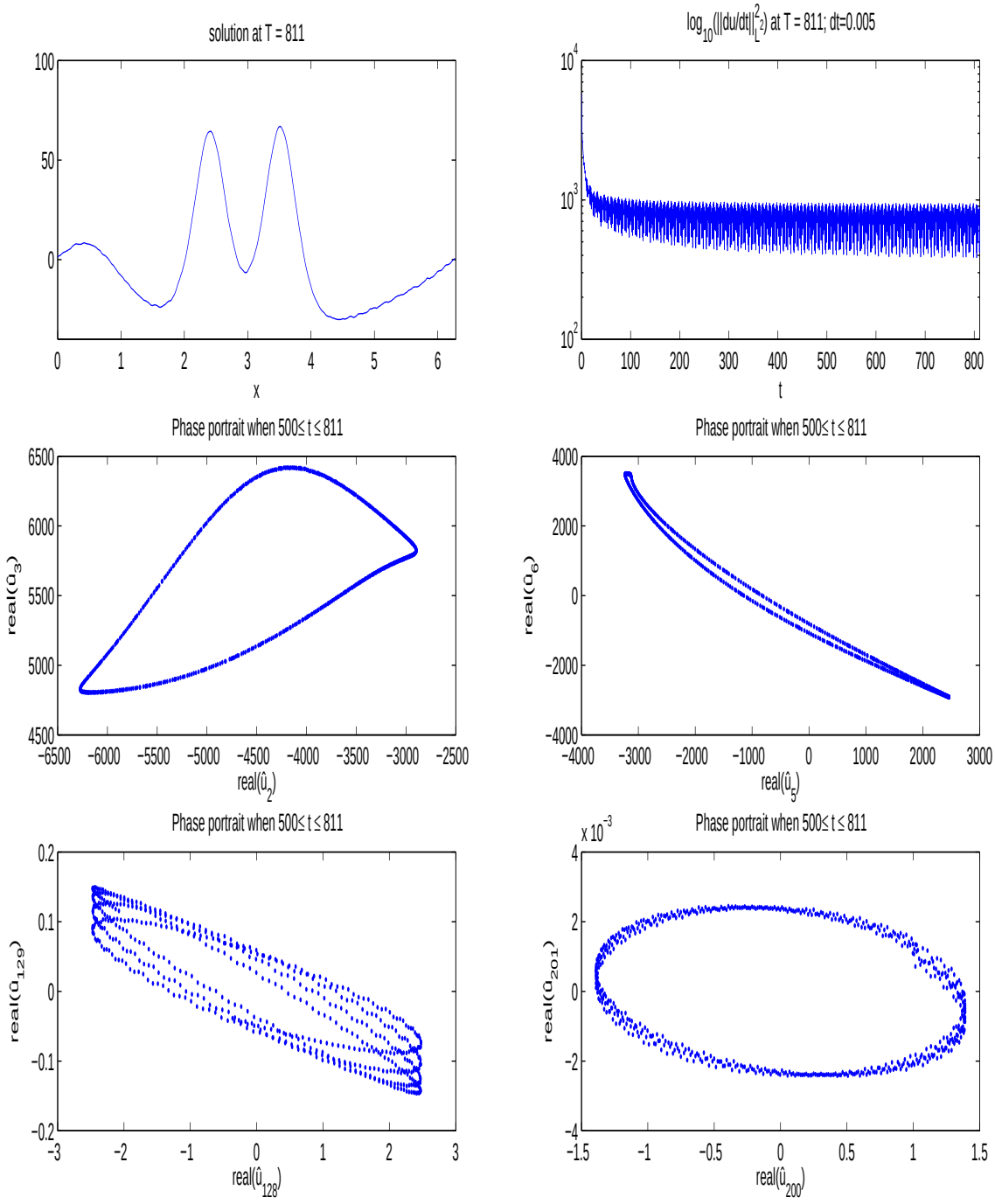

Figure 79: $u_0(x) = S4$,$\gamma_k = \dfrac{5.5}{(1+|k|)^{0.6}}$, $f(x) = \sin(2\pi x/L)$

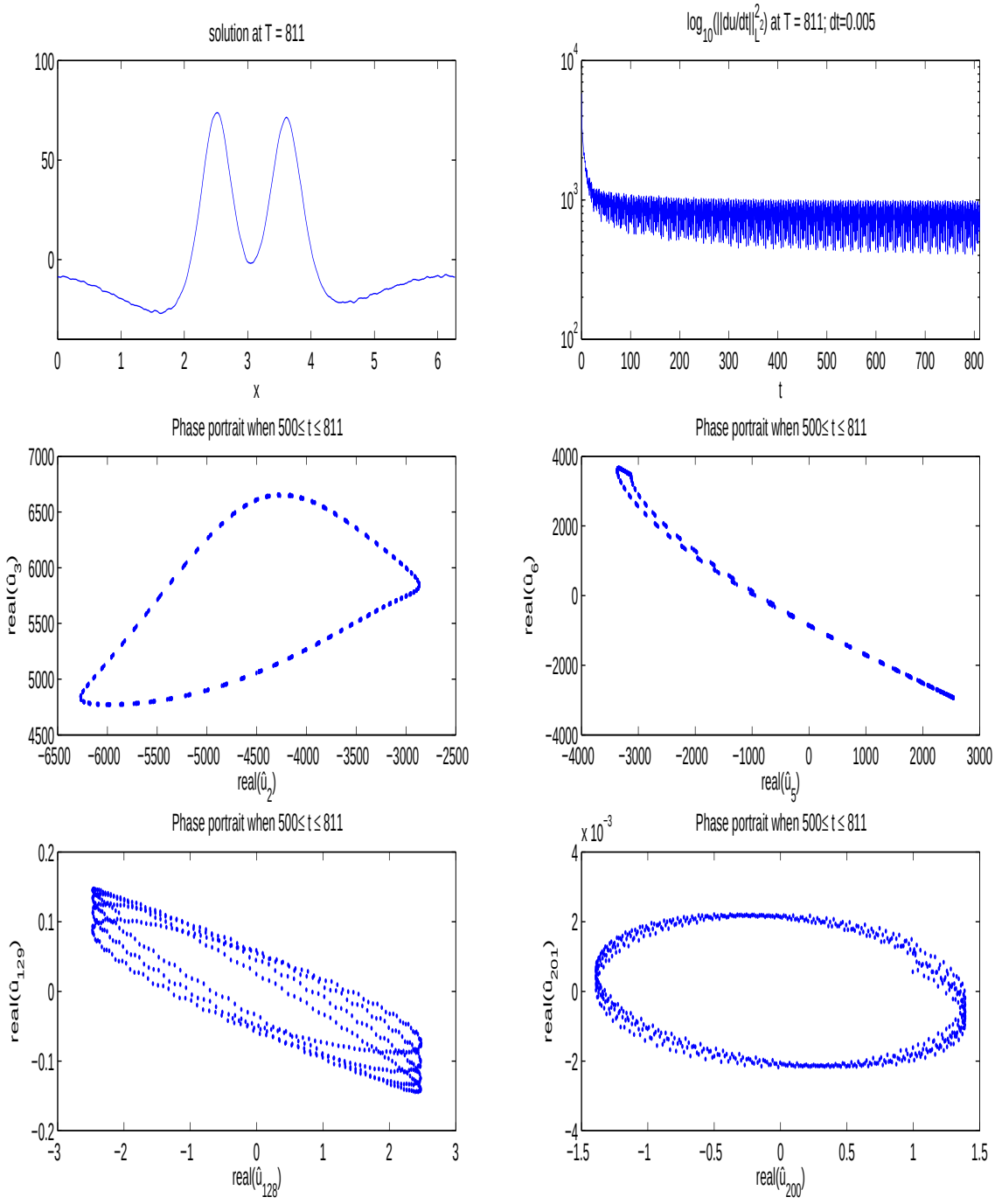

Figure 80: $u_0(x) = S4$,$\gamma_k = \dfrac{6.6}{(1+|k|)^{0.8}}$, $f(x) = \sin(2\pi x/L)$

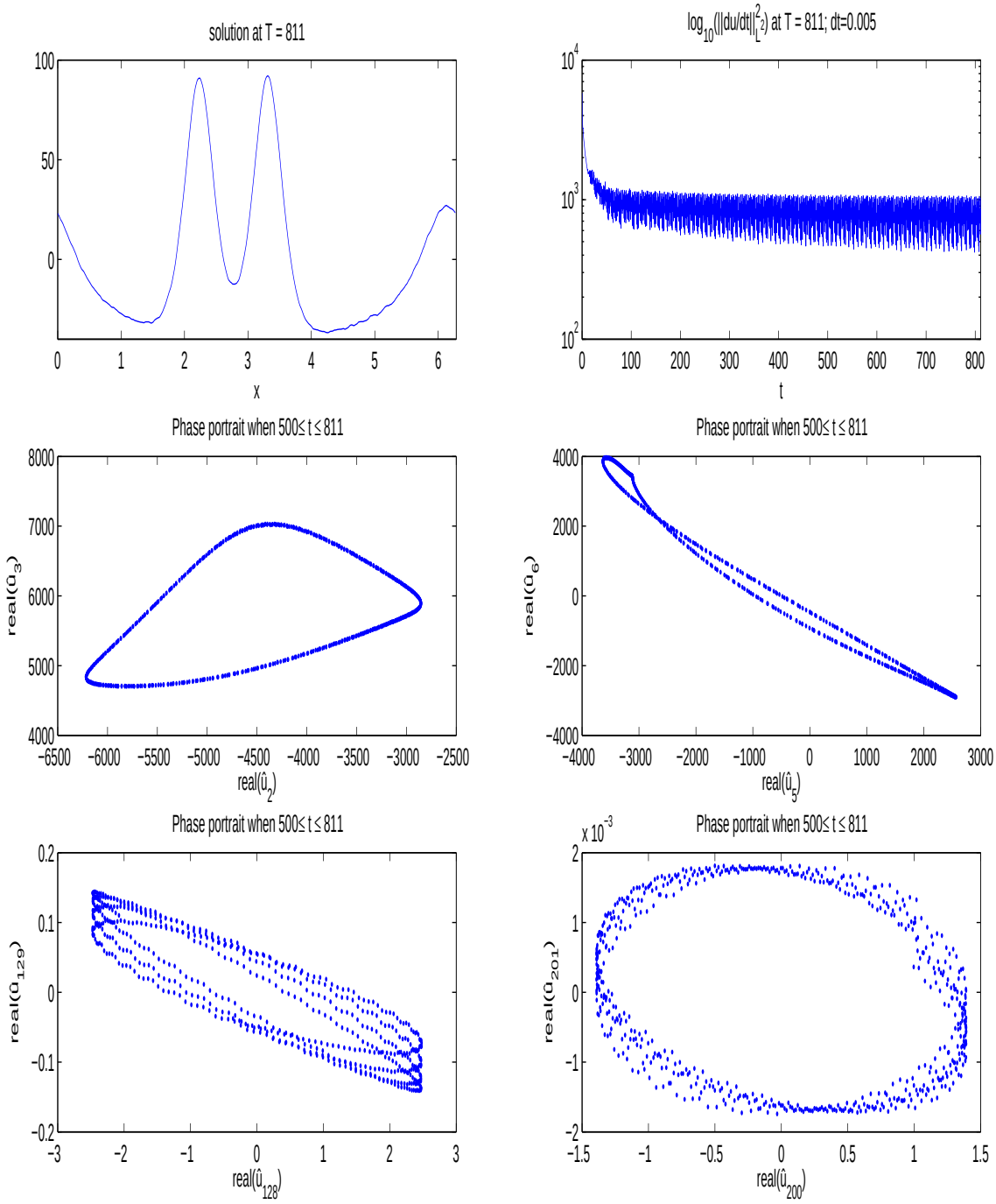

Figure 81: $u_0(x) = S4$,$\gamma_k = \dfrac{7.7}{(1+|k|)}$, $f(x) = \sin(2\pi x/L)$

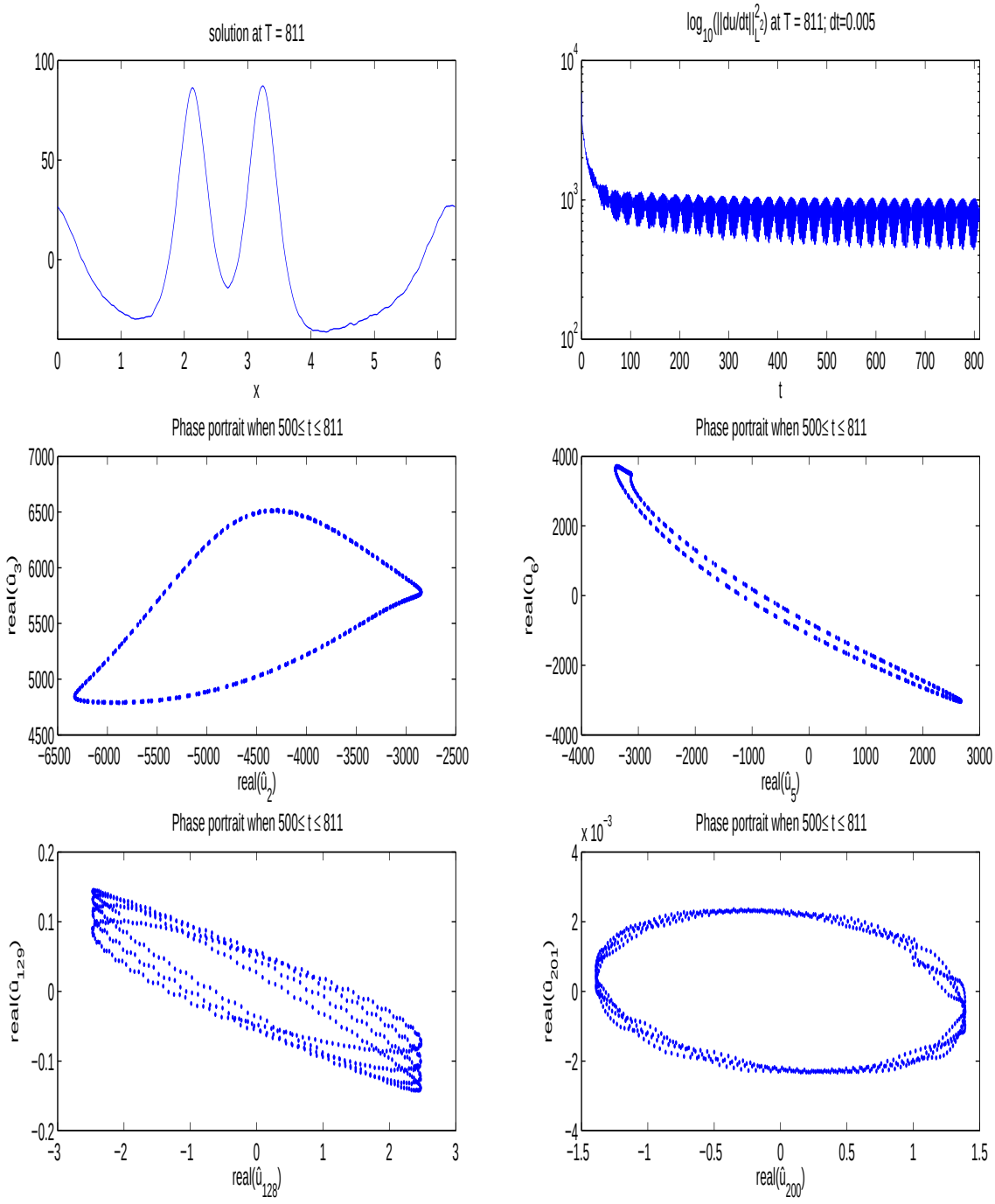

Figure 82: $u_0(x) = S4$,$\gamma_k = \dfrac{9.9}{(1+|k|)^{1.2}}$, $f(x) = \sin(2\pi x/L)$

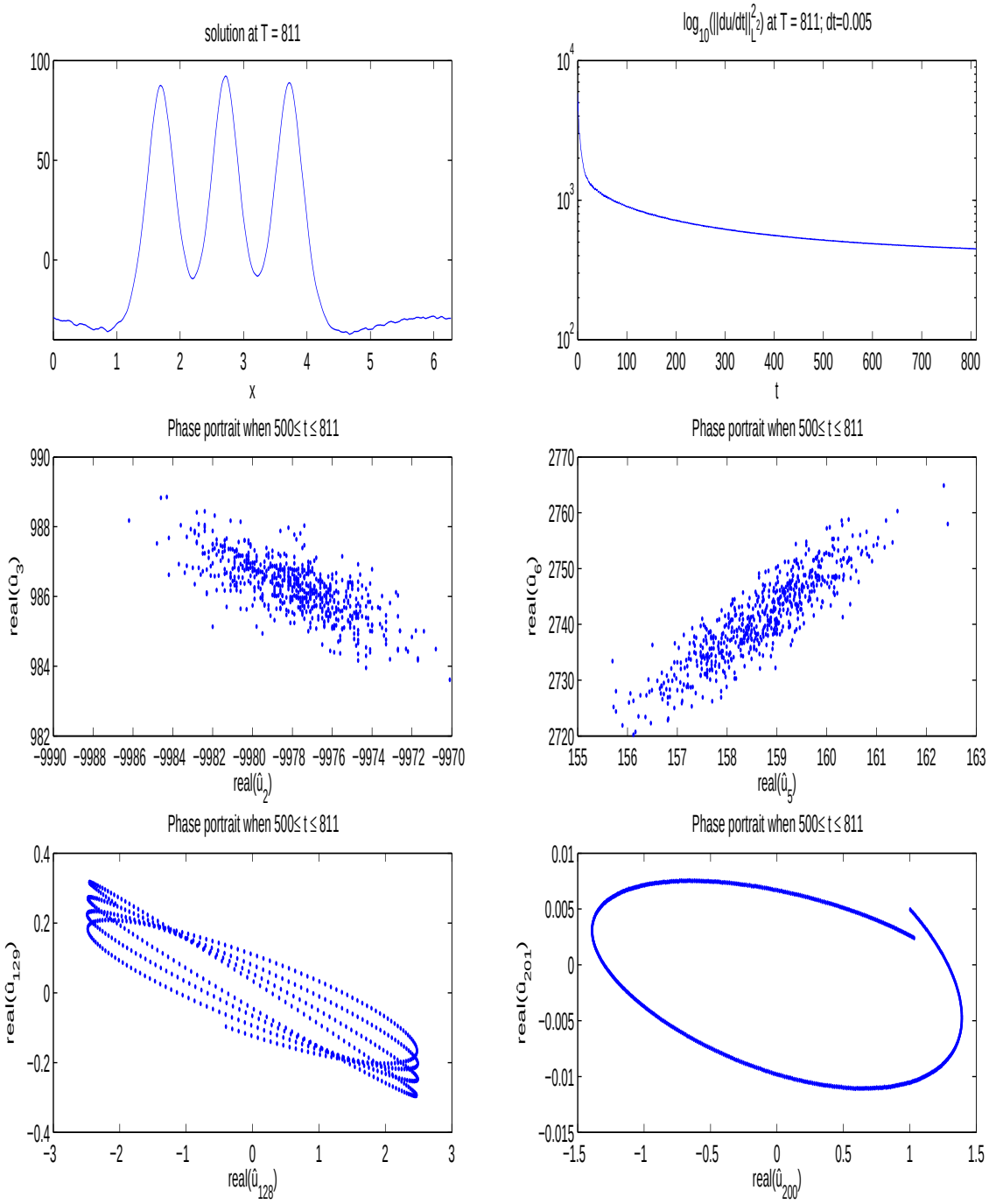

Figure 83: $u_0(x) = S4$,$\gamma_k = \dfrac{12}{(1+|k|)^{1.5}}$, $f(x) = \sin(2\pi x/L)$

5 Concluding remarks and perspectives

The family of weak damped KdV equation we have presented here allows to consider damping weaker than those studied in [12, 13, 14, 15] in the sense that, when $\gamma_k \to 0$ as $|k| \to +\infty$,

$$\exists c > 0 \text{ s.t. } |u|_\gamma \leq c|u|_{L^2} \forall u \in L^2 \text{ and } \nexists d > 0 \text{ s.t. } d|u|_\gamma \geq |u|_{L^2} \forall u \in L^2,$$

for which an asymptotic regularization property was proved. The numerical illustrations show that a damping is still present in energy norm, the main problem being that we do not have a uniform control on the rate of damping. Anyway, and as in the weak damping case considered by Cabral and Rosa ([4]) (see also [2]), we pointed out by numerical evidence, the existence of steady states and of time-periodic solutions, which means a nontrivial long time dynamics. As possible perspectives of the present work, we propose:

1. The rough mathematical analysis of the long time behavior of (5) still remain to be done; it presents technical difficulties due to the non embedding of H_γ in L^2 when $\lim_{k\to+\infty} \gamma_k = 0$, it is then helpful to produce first numerical evidences.

2. We can consider such damped KdV equations when the boundary conditions are not periodic. It suffices to expand the solution in a proper (Hilbert) orthogonal polynomial basis p_k with respect to a weighted L^2 scalar product $(.,.)_\omega$. We have then

   $$u(x,t) = \sum_{k=0}^{\infty} \hat{u}_k p_k(x),$$

   where $\hat{u}_k = \dfrac{(u,p_k)_\omega}{(p_k,p_k)_\omega}$ and we define the damping linear operator L_γ as

   $$L_\gamma(u) = \sum_{k=0}^{\infty} \gamma_k \hat{u}_k p_k(x).$$

   More widely, the study of the long time behavior of equations as

   $$\frac{\partial u}{\partial t} + L_\gamma u + F(u) = 0,$$

   with $Re(F(u),u)_\omega = 0$ and L_γ defined as above can be addressed following the same approach. For example damped Nonlinear Schrodinger equations as presented in [1] can be considered.

3. In a numerical point of view, the damping when treated implicitly in a numerical marching scheme, has a stabilization property. The Fourier expression of L_γ allows to study in a accurate way the effect of the damping by band of frequency: this can be a first step before building filtering operators for stabilizing numerical scheme without deteriorating the consistency, as done e.g. in [5] for nonlinear parabolic equations.

4. Another weak damping can be considered: it consists in a local damping in the physical space and reads as

   $$Lu = \chi_{[a,b]} u$$

   where $\chi_{[a,b]}$ is the characteristic function of $[a,b] \subset [O,L]$ as studied in the perspective of the stabilization of KdV equations, see [17, 25]; of course one can replace $\chi_{[a,b]}$ by a smooth function with compact support in $[a,b]$, see annex.

We hope to develop these topics in a near future.

Acknowledgements : This work is supported by the regional program "Appui à l'émergence" of the Region Picardie. The authors thank Benoît Merlet (CMAP, Ecole Polytechnique), Youcef Mammeri (LAMFA, Amiens) and Lionel Rosier (IECN, Univ. Nancy) for fruitful discussions and remarks.

References

[1] M. Abounouh, H. Al Moatassime, J-P. Chehab, S. Dumont, and O. Goubet. Discrete schrodinger equations and dissipative dynamical systems. *Communications on Pure and Applied Analysis*, 7(2):211–227, 2008.

[2] M. Abounouh, H. Al Moatassime, C. Calgaro, J-P. Chehab, A numerical scheme for the long time simulation of a forced damped KdV equation, in preparation

[3] J. Ball,*Global attractors for damped semilinear wave equations. Partial differential equations and applications*, Discrete Contin. Dyn. Syst. 10 (2004), no. 1-2, 31–52.

[4] M. Cabral, R. Rosa, Chaos for a damped and forced KdV equation, *Phys. D* , 192 (2004), no. 3-4, 265–278

[5] J.-P. Chehab, B. Costa, Time Explicit Schemes and Spatial Finite Differences Splittings, Journal of Scientific Computing, Vol. 20, No. 2, 159–189, 2004.

[6] M. Chen, S. Dumont, L. Dupaigne and O. Goubet, Decay of solutions to a water wave model with nonlocal viscous dispersive term, discrete and continuous dynamical systems, Volume 27, Number 4, August 2010 pp. 1473Đ1492

[7] T. A. Driscoll, A composite Runge-Kutta method for the spectral solution of semilinear PDEs. Journal of Computational physics 182, 357-367(2002).

[8] F. Dubois, *http://www.math.u-psud.fr/∼ fdubois/travaux/evolution/marrakech01/semidif4/ semidif4.juin01.f*

[9] F. Dubois, A. Galucio et N. Point, *Introduction à la dérivation fractionnaire ; théorie et applications*, Ref AF510, Techniques de l'ingénieur, april 2010.

[10] F. Dubois, A. Galucio et N. Point,The G^{α}-scheme for approximation of fractional derivatives: application to the dynamics of dissipative systems. (English summary) J. Vib. Control 14 (2008), no. 9-10, 1597–1605

[11] D. Dutykh, *Modélisation mathématique des Tsunamis*, Thèse de doctorat, ENS Cachan, 2007.

[12] J-M. Ghidaglia, *Weakly damped forced Korteweg-de Vries equations behave as a finite dimensional dynamical system in the long time*, J. Diff. Eq., 74, pp 369-390, (1988)

[13] J-M. Ghidaglia, *A note on the strong convergence towards attractors for damped forced KdV equations*, J. Diff. Eq. **110**, 356-359, (1994).

[14] O. Goubet, *Asymptotic smoothing effect for weakly damped forced Korteweg-de Vries equations*, Discrete Contin. Dynam. Systems **6** (2000), no. 3, 625–644.

[15] O. Goubet, R. Rosa *Asymptotic smoothing and the global attractor of a weakly damped KdV equation on the real line* , J. Differential Equations **185** (2002), no. 1, 25–53.

[16] D. J. Korteweg and G. de Vries, *On the change of form of long waves advancing in a rectangular canal, and on new type of long stationary waves,* Phil. Mag. (5), 39, p. 422, (1895)

[17] C. Laurent, L. Rosier, B-Y Zhang, COntrol stabilization of the Korterweg-De-Vries equation in a periodic domain, Comm. PDE, 35: 707-744, 2010.

[18] Lele, S. K. (1992). Compact finite difference schemes with spectral-like resolution. J. Comput. Phys. 103, 16-42.

[19] J.-L. Lions, *Quelques méthodes de résolution des problèmes aux limites non linéaires*, Dunod Gauthier-Vilars, Paris, 1969.

[20] S. Mallat, "A wavelet tour of signal processing", Academic press, (1998).

[21] A. Miranville and R. Temam, Mathematical Modeling in Continuum Mechanics, Cambridge University Press, 2005

[22] L. Molinet and S. Vento, preprint, 2010

[23] E. Ott and R.N. Sudan, Nonlinear theory of ion acoustic wave with Landau damping, The Physics of fluids, Vol 12, N 11, 1969.

[24] E. Ott and R.N. Sudan, Damping of solitary waves, The Physics of fluids, Vol 13, N 6, 1970.

[25] L. Rosier, B-Y Zhang, Control and stabilization of teh Korteweg-De-Vries equation: recent progresses, JrL Syst Sci & Complexity, (2009) 22: 647-682

[26] A. Duràn and J.M. Sanz-Serna. The numerical integration of a relative equilibrium solutions. the nonlinear schrodinger equation. IMA J. Num. Anal., 20:235-261, 2000.

[27] R. Temam, *Infinite Dimensional Dynamical Systems in Mechanics and Physics*, Springer- Verlag, Second Edition, (1997).

[28] V. Thomé and A. S. Vasudeva Murthy, A numerical method for Benjamin-Ono, equation, BIT, 1998, Vol. 38, No. 3, pp. 597-611.

[29] S. Vento, Global well-posedness for dissipative Korteweg-de Vries equations, preprint, 2008

[30] S. Vento, Asymptotic behavior for dissipative Korteweg-de Vrie equations, perprint, 2008

6 Annex

6.1 Non local time damped KdV

We consider the two problems

- NLTKdV1, see [6]

$$a_0u_t + a_1u_x + a_2u_{xxx} + \sqrt{\nu}\cdot\frac{1}{\sqrt{\pi}}\int_0^t \frac{u_t(s)}{\sqrt{t-s}}ds + a_3uu_x - a_4u_{xx} = 0,$$

- NLTKdV2, see [11]

$$a_0u_t + a_1u_x + a_2u_{xxx} - \sqrt{\frac{\nu g}{h}}\cdot\frac{1}{\sqrt{\pi}}\int_0^t \frac{u_x(s)}{\sqrt{t-s}}ds + a_3uu_x - a_4u_{xx} = 0,$$

where $a_1 = h\cdot\sqrt{\frac{g}{h}}$, $a_2 = \frac{h^3}{6}\cdot\sqrt{\frac{g}{h}}$, $a_3 = \frac{3}{2}\cdot\sqrt{\frac{g}{h}}$ and $a_4 = 2\nu$.

The time and space discretizations of these equations are presented below.

6.1.1 The problem NLTKDV1

We here describe the time and space discretization of the problem

$$a_0u_t + a_1u_x + a_2u_{xxx} + \sqrt{\nu}\cdot\frac{1}{\sqrt{\pi}}\int_0^t \frac{u_t(s)}{\sqrt{t-s}}ds + a_3uu_x - a_4u_{xx} = 0.$$

We set $G_t^{1/2}u(t) = \frac{1}{\sqrt{\pi}}\int_0^t \frac{u_t(s)}{\sqrt{t-s}}ds$.

Spatial discretization

According to Dubois [9], $(G_t^{1/2}u)^n = \sqrt{\frac{3}{2\Delta t}}\cdot\sum_{j=0}^{+\infty} g_{j+1}u^{n-j} = \sqrt{\frac{3}{2\Delta t}}\cdot\sum_{j=0}^{n} g_{n+1-j}u^j$ where g_j are the Gear coefficients computed in [8].
Taking the Fourier serie of each term we have

$$a_0\frac{d}{dt}\widehat{u}_k + \sqrt{\nu}\cdot G_t^{1/2}\widehat{u}_k + \underbrace{\left[a_1\cdot i\cdot\left(\frac{2\pi k}{L}\right) - a_2\cdot i\cdot\left(\frac{2\pi k}{L}\right)^3 + a_4\cdot\left(\frac{2\pi k}{L}\right)^2\right]}_{\text{TL}}\cdot\widehat{u}_k + \underbrace{a_3\cdot i\cdot\left(\frac{2\pi k}{L}\right)}_{\text{TNL}}\cdot\frac{\widehat{u^2}_k}{2} = 0.$$

We now set $C = \frac{2\pi k}{L}$, $\text{TL} = C\cdot(a_1\cdot i - a_2\cdot i\cdot C^2 + a_4\cdot C)$ and $\text{TNL} = a_3\cdot i\cdot C$.

The system to be solved is then:

$$\begin{cases} a_0\frac{d}{dt}\widehat{u}_k + \sqrt{\nu}\cdot G_t^{1/2}\widehat{u}_k + \text{TL}\cdot\widehat{u}_k + \text{TNL}\cdot\frac{\widehat{u^2}_k}{2} = 0, \\ \widehat{u}_k(x,0) = \widehat{u}_k(0). \end{cases}$$

We will set for the sequel $U(x,t) = u(x,t) - u_0(x)$, so

$$\begin{cases} a_0\frac{d}{dt}\widehat{U}_k + \sqrt{\nu}\cdot G_t^{1/2}\widehat{U}_k + \text{TL}\cdot\left(\widehat{U}_k + \widehat{u_0}\right) + \text{TNL}\cdot\frac{\widehat{(U+u_0)^2}_k}{2} = 0, \\ \widehat{U}_k(x,0) = 0. \end{cases}$$

Time discretization

For simplicity, we consider the following explicit scheme

$$\begin{cases} a_0\dfrac{\widehat{U}_k^{n+1}-\widehat{U}_k^n}{\Delta t}+\sqrt{\nu}\cdot G_t^{1/2}\widehat{U}_k^{n+1}+\mathrm{TL}\cdot\left(\widehat{U}_k^{n+1}+\widehat{u_0}\right)+\mathrm{TNL}\cdot\dfrac{\widehat{(U^{n+1})^2}_k}{2}=0 \\ \widehat{U}_k(x,0)=0 \end{cases}$$

We have $\sqrt{\nu}\cdot G_t^{1/2}\left(\widehat{U}_k^{n+1}\right)=\sqrt{\nu}\cdot\sqrt{\dfrac{3}{2\Delta t}}\cdot\sum_{j=0}^{n+1}g_{n+1-j}U^j=\sqrt{\nu}\cdot\sqrt{\dfrac{3}{2\Delta t}}\cdot\left(g_0\widehat{U}_k^{n+1}+\sum_{j=0}^{n}g_{n+1-j}U^j\right)$

Therefore, we obtain

$$\begin{cases} \widehat{U}_k^{n+1}=\left[-\sqrt{\dfrac{3\nu\Delta t}{2}}\cdot\sum_{j=0}^{n}g_{n+1-j}U^j+a_0\cdot\widehat{U}_k^n-\Delta t\cdot\left(\mathrm{TL}\cdot\widehat{u_0}+\mathrm{TNL}\cdot\dfrac{\widehat{(U^{n+1})^2}_k}{2}\right)\right]/M1 \\ \widehat{U}_k(x,0)=0 \end{cases}$$

where $M1=a_0+\Delta t\cdot\mathrm{TL}+\sqrt{\dfrac{3\nu\Delta t}{2}}\cdot g_0$

6.1.2 The problem NLTKDV2

We here describe the time and space discretization of the problem NLTKDV2 [11].

$$a_0u_t+a_1u_x+a_2u_{xxx}-\sqrt{\frac{\nu g}{h}}\cdot\frac{1}{\sqrt{\pi}}\int_0^t\frac{u_x(s)}{\sqrt{t-s}}ds+a_3uu_x-a_4u_{xx}=0,$$

where $a_1=h\cdot\sqrt{\dfrac{g}{h}}$, $a_2=\dfrac{h^3}{6}\cdot\sqrt{\dfrac{g}{h}}$, $a_3=\dfrac{3}{2}\cdot\sqrt{\dfrac{g}{h}}$ and $a_4=2\nu$.

Space discretization

Considering the Fourier serie of each term of the equation, we get

$$a_0\frac{d}{dt}\widehat{u}_k-i\frac{2\pi k}{L}\sqrt{\frac{\nu g}{h}}\underbrace{\frac{1}{\sqrt{\pi}}\int_0^t\frac{\widehat{u}_k(s)}{\sqrt{t-s}}ds}_{D_t^{1/2}\widehat{u}_k}+\underbrace{\left[a_1i\frac{2\pi k}{L}-a_2i\left(\frac{2\pi k}{L}\right)^3+a_4\left(\frac{2\pi k}{L}\right)^2\right]}_{\mathrm{TL}}\widehat{u}_k+\underbrace{a_3i\left(\frac{2\pi k}{L}\right)}_{\mathrm{TNL}}\frac{\widehat{u^2}_k}{2}=0.$$

We set $C=\dfrac{2\pi k}{L}$, $\mathrm{TL}=C\cdot\left(a_1\cdot i-a_2\cdot i\cdot C^2+a_4\cdot C\right)$ et $\mathrm{TNL}=a_3\cdot i\cdot C$.
The time scheme reads as

$$\begin{cases} a_0\dfrac{d}{dt}\widehat{u}_k-i\cdot C\cdot\sqrt{\dfrac{\nu g}{h}}\cdot D_t^{1/2}\widehat{u}_k+\mathrm{TL}\cdot\widehat{u}_k+\mathrm{TNL}\cdot\dfrac{\widehat{u^2}_k}{2}=0, \\ \widehat{u}_k(x,0)=\widehat{u}_k(0). \end{cases}$$

We have $D_t^{1/2}\widehat{u}_k=\dfrac{1}{\sqrt{\pi}}\displaystyle\int_0^t\frac{\widehat{u}_k(s)}{\sqrt{t-s}}ds\Rightarrow\frac{d}{dt}D_t^{1/2}\widehat{u}_k=\frac{1}{\sqrt{\pi t}}\cdot\widehat{u}_k(0)+\underbrace{\frac{1}{\sqrt{\pi}}\int_0^t\frac{d}{ds}\widehat{u}_k(s)\frac{ds}{\sqrt{t-s}}}_{G_t^{1/2}\widehat{u}_k}.$

From [9] $(G_t^{1/2}\widehat{u}_k)^n = \sqrt{\dfrac{3}{2\Delta t}} \cdot \sum_{j=0}^{+\infty} g_{j+1}\widehat{u}_k^{n-j} = \sqrt{\dfrac{3}{2\Delta t}} \cdot \sum_{j=0}^{n} g_{n+1-j}\widehat{u}_k^{j}$ where g_j are the Gear coefficients given in [8].

It follows that

$$D_t^{1/2}\widehat{u}_k^{n+1} = D_t^{1/2}\widehat{u}_k^{n} + \Delta t \left(\frac{1}{\sqrt{\pi t}} \cdot \widehat{u}_k(0) + \sqrt{\frac{3}{2\Delta t}} \cdot \sum_{j=0}^{n} g_{n+1-j}\widehat{u}_k^{j} \right) \text{ with } D_t^{1/2}\widehat{u}_k^{0} = 0.$$

Time discretization

$$\begin{cases} a_0 \dfrac{\widehat{u}_k^{n+1} - \widehat{u}_k^{n}}{\Delta t} + \left(-i \cdot C \cdot \sqrt{\dfrac{\nu g}{h}} \cdot D_t^{1/2} + \mathrm{TL} \right) \widehat{u}_k^{n+1} + \dfrac{\mathrm{TNL}}{2} \widehat{u^{n+1^2}}_k = 0, \\ \widehat{u}_k(x,0) = \widehat{u}_k(0). \end{cases}$$

$$\begin{cases} \widehat{u}_k^{n+1} &= \left[i\Delta t \cdot C \cdot \sqrt{\dfrac{\nu g}{h}} \cdot \left[D_t^{1/2}\widehat{u}_k^{n} + \Delta t \left(\dfrac{1}{\sqrt{\pi t}} \cdot \widehat{u}_k(0) + \sqrt{\dfrac{3}{2\Delta t}} \cdot \sum_{j=0}^{n} g_{n+1-j}\widehat{u}_k^{j} \right) \right] \right] + a_0\widehat{u}_k^{n} \\ & \quad -\Delta t \cdot \dfrac{\mathrm{TNL}}{2} \cdot \widehat{u^{n+1^2}}_k \Big] / M1 \\ \widehat{u}_k(x,0) &= \widehat{u}_k(0) \end{cases}$$

where $M1 = a_0 + \Delta t \cdot \mathrm{TL}$.

6.1.3 Numerical results for NLTKdV1

We hereafter represent the solution at different times when varying α and ν.

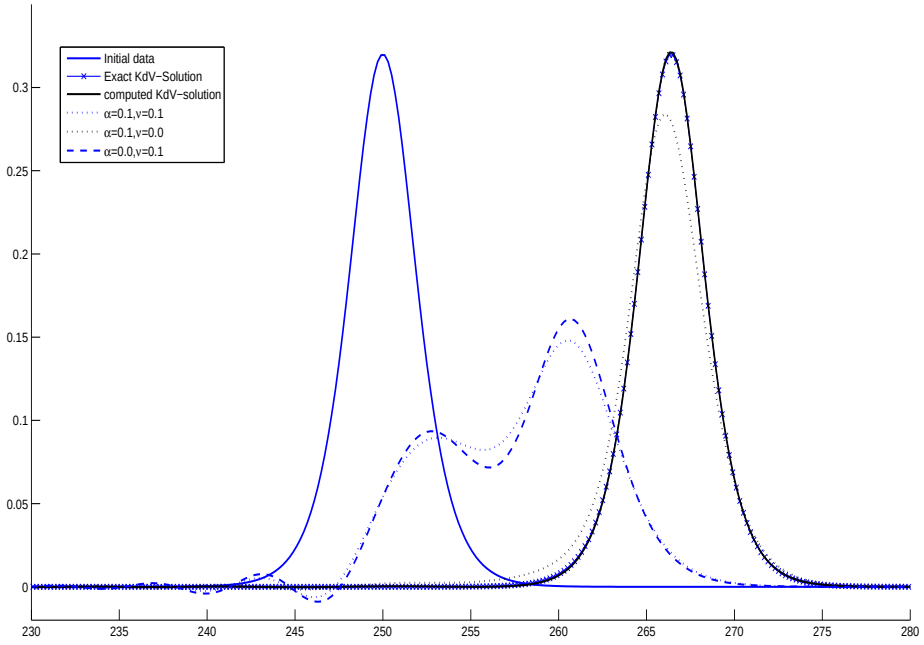

Figure 84: $T = 10, N = 2499, 0 < x < 500, a_0 = 1, a_1 = 1, a_2 = 1, a_3 = 6, a_4 = \alpha, f(x,t) = 0$

6.1.4 Numerical results for NLTKdV2

We here display on FIG.85 and FIG.86 the time evolution of the ratio $\frac{\|u(t)\|_{L^2}}{\|u_0\|_{L^2}}$

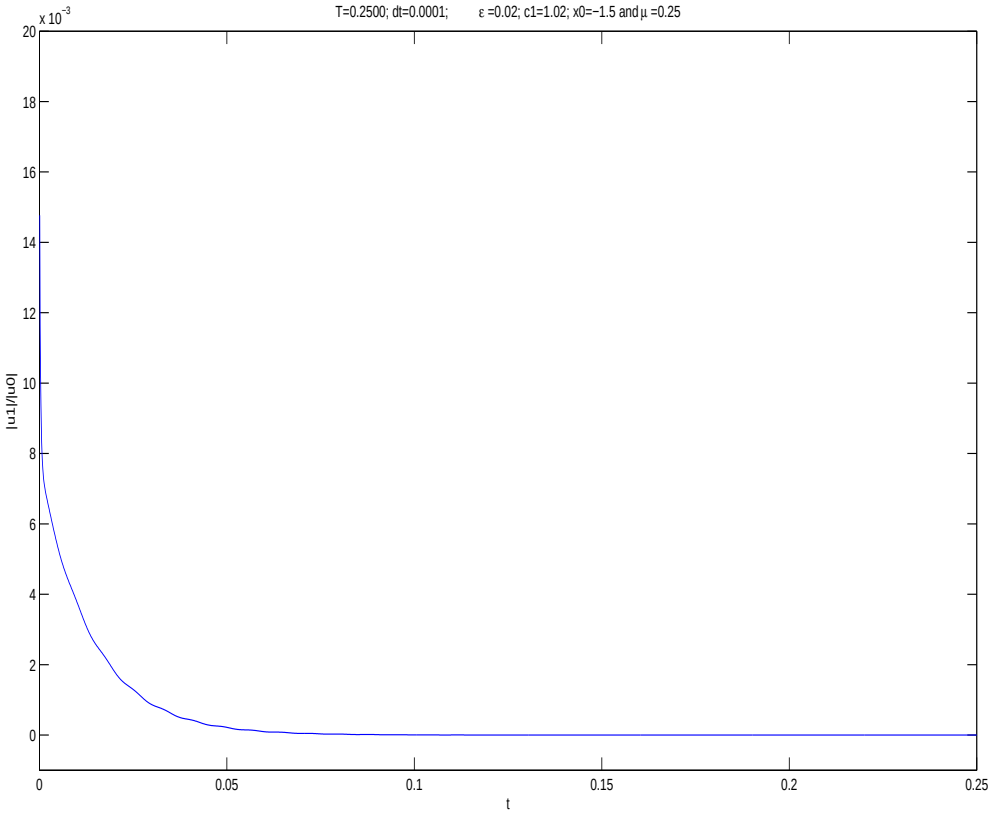

Figure 85: u is zero mean,$\|u(t)\|/\|u_0\|; u_0 = \frac{2(c1-1)}{\varepsilon}\left[sech\left(\frac{\sqrt{6(c1-1)}}{2\mu}(x+x0)\right)^2\right]$; Here: $N = 2499, 0 < x < 500, g = 9.8, h = 3600, \nu = 10^{-3}, f(x,t) = 0$

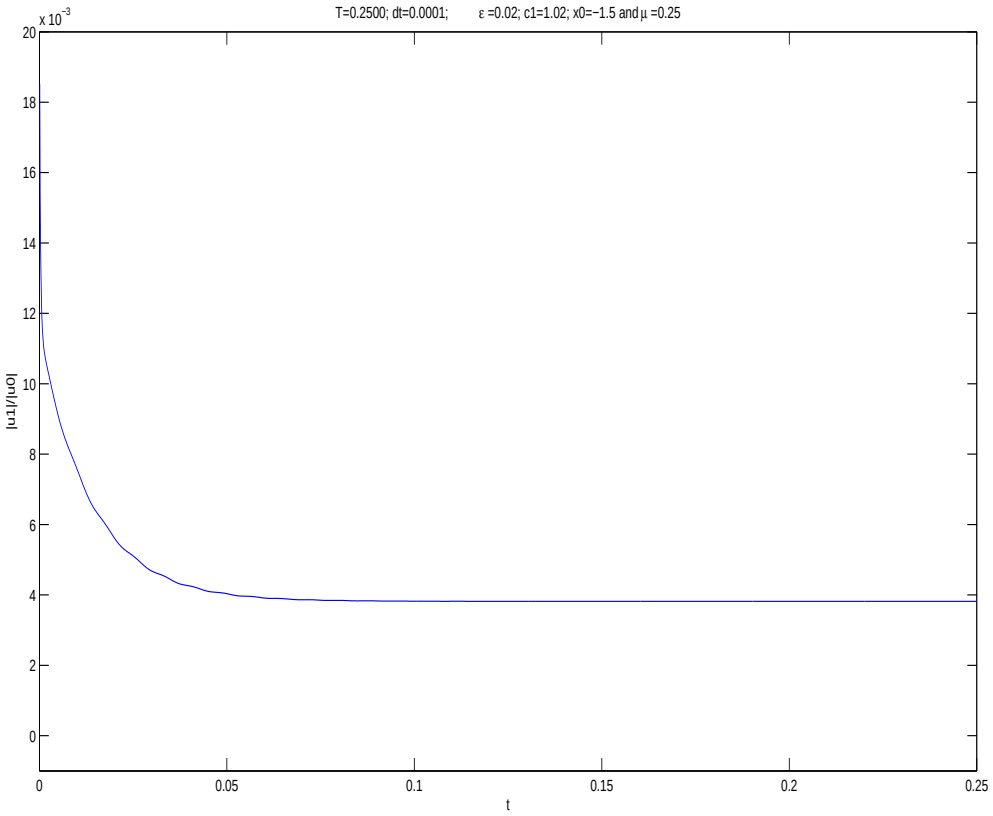

Figure 86: u is non zero mean,$\|u(t)\|/\|u_0\|; u_0 = \frac{2(c1-1)}{\varepsilon}\left[sech\left(\frac{\sqrt{6(c1-1)}}{2\mu}(x+x0)\right)^2\right]$; Here: $N = 2499, 0 < x < 500, g = 9.8, h = 3600, \nu = 10^{-3}, f(x,t) = 0$

6.2 KdV with local damping in the physical space

We give hereafter a first illustration. Such a damped equation will be studied more widely in a forthcoming work. We consider the damped KdV equation

$$u_t + \epsilon u_{xxx} + L[u] + uu_x = 0$$

where the (linear) damping is defined by

$$Lu = \chi_{[a,b]} u$$

We can say that this is a weak damping, in the sense that the term $< u, L[u] >$ is controlled by $|u|^2_{L^2}$. This was studied in the perspective of the stabilization of KdV equations, see [17, 25].

We take 8th order finite differences for the discretization in space as follows writing the finite differences discretization schemes for the 3 first derivatives in space with periodic boundary conditions with centered

stencils:

$$u_x(x_m) \simeq \sum_{\ell=1}^{p} \alpha_\ell \frac{u_{m+\ell} - u_{m-\ell}}{2\ell h},$$
$$u_{xx}(x_m) \simeq \sum_{\ell=1}^{p} \beta_\ell \frac{u_{m+\ell} - 2u_m + u_{m-\ell}}{(\ell h)^2},$$
$$u_{xxx}(x_m) \simeq \sum_{\ell=1}^{p} \theta_\ell \frac{-2(u_{m+\ell} - u_{m-\ell}) + (u_{m+2\ell} - u_{m-2\ell})}{(2\ell h)^3}.$$

Here u_m stands for $u(x_m)$ or an approximation of it. The non null coefficients $\alpha_\ell, \beta_\ell, \theta_\ell$ are computed such that these schemes are $2p$ order accurate and given below. As time scheme we have implemented

Op.	p=1	p=2	p=3	p=4
∂_x	$\alpha_1 = 1$	$\alpha_1 = \frac{4}{3}, \alpha_2 = -\frac{1}{3}$	$\alpha_1 = \frac{3}{2}, \alpha_2 = -\frac{3}{5}, \alpha_3 = \frac{1}{10}$	$\alpha_1 = \frac{8}{5}, \alpha_2 = -\frac{4}{5}, \alpha_3 = \frac{8}{35}, \alpha_3 = -\frac{1}{35}$
∂_{xx}	$\beta_1 = 1$	$\beta_1 = \frac{4}{3}, \beta_2 = -\frac{1}{3}$	$\beta_1 = \frac{3}{2}, \beta_2 = -\frac{3}{5}, \beta_3 = \frac{1}{10}$	$\beta_1 = \frac{8}{5}, \beta_2 = -\frac{4}{5}, \beta_3 = \frac{8}{35}, \beta_3 = -\frac{1}{35}$
∂_{xxx}	$\theta_1 = 1$	$\theta_1 = \frac{4}{3}, \theta_2 = -\frac{1}{3}$	$\theta_1 = \frac{3}{2}, \theta_2 = -\frac{3}{5}, \theta_3 = \frac{1}{10}$	$\theta_1 = \frac{8}{5}, \theta_2 = -\frac{4}{5}, \theta_3 = \frac{8}{35}, \theta_3 = -\frac{1}{35}$

Table 3: Coefficients of the finite difference schemes for the space derivatives

RK34, see [7]. To illustrate the damping, we hereafter display the evolution in time of the mean value, the L^2 and the L^∞ norms. Here $\Delta t = 0.005$, $N = 256$, $L = 1$ and we take as initial data the soliton

$$u = A(sech(B(x - x0))^2),$$

with $L = 1$, $A = 0.8$, $C = 2\frac{A^p}{6}$, $B = \frac{1}{2} \cdot \sqrt{\frac{C}{\epsilon}}$. We observe that after a transient time, the damping to zero is at an exponential rate (linear decreasing in log scale). In the figure (87), we see that the solution is damped uniformly. Does it mean that after a transient time, the solution is damped in a same way as a weak damping of type $\chi_{[0,L]}$ can do, say exponentially on the whole domain ?

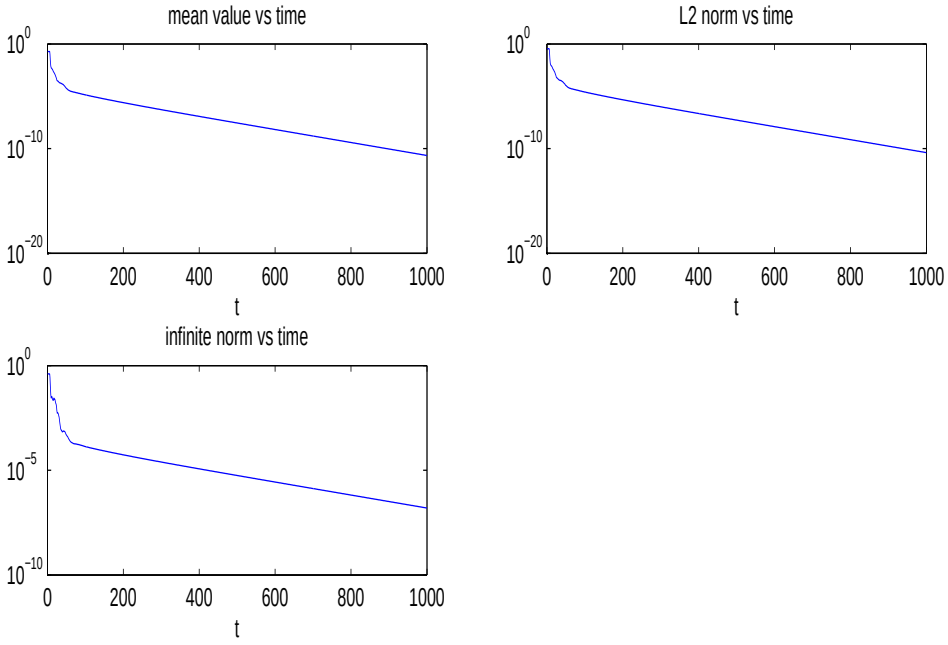

Figure 87: $[a, b] = [0.4L, 0.6L]$